Title
Abrogating the Protumorigenic Impact of Tumor-Infiltrating Myeloid Cells During Prostate Cancer Therapy

Author
Escamilla, Jemima

Publication Date
2013

Peer reviewed|Thesis/dissertation

UNIVERSITY OF CALIFORNIA

Los Angeles

Abrogating the Protumorigenic Impact of Tumor-Infiltrating Myeloid Cells During Prostate Cancer Therapy

A dissertation submitted in partial satisfaction of the requirements for the degree

Doctor of Philosophy in Molecular and Medical Pharmacology

by

Jemima Escamilla

2013

ABSTRACT OF THE DISSERTATION

Abrogating the Protumorigenic Impact of Tumor-Infiltrating Myeloid Cells During Prostate Cancer Therapy

by

Jemima Escamilla

Doctor of Philosophy in Molecular and Medical Pharmacology

University of California, Los Angeles, 2013

Professor Lily Wu, Chair

Despite recent advances in treatment modalities for advanced prostate cancer (PCa) and castration-resistant prostate cancer (CRPC), PCa continues to be a major cause of morbidity and mortality in American men. An improved understanding of the tumor microenvironment and immune surveillance has opened new avenues for targeted therapeutic strategies for the treatment of PCa. The primary cause of treatment failure is the development of cellular resistance to the cytotoxic effects of cancer therapeutics. Both cell intrinsic and extrinsic mechanisms can underlie this acquired therapeutic resistance. More recently, the tumor microenvironment, and more importantly tumor-related inflammation, have emerged as a crucial players in promoting cancer initiation and progression, invasion and metastasis, and resistance to both conventional and targeted therapies. In particular, there have been fundamental leaps in our understanding of the complex roles of tumor-infiltrating myeloid cells (TIMs). TIMs are a heterogeneous population of monocytic and granulocytic myeloid derived suppressor cells (MDSCs) and tumor-associated macrophages (TAMs) that have a profound impact on tumor development. TIMs have

been reported to promote tumor growth. In PCa, first-line radiotherapy (RT) and blockade of androgen signaling have potent anti-cancer effects, but PCa patients inevitably develop resistance mechanisms to evade therapy. Recently, elevated inflammation has been demonstrated after RT and androgen inhibition, yet the impact of this aberrant inflammation and the potential therapeutic options for preventing resistance in PCa have been largely unexplored. Therefore, we sought to further understand the impact of inflammation in acquired resistance to these two important therapeutic strategies, and whether combinatorial therapies may prevent resistance and improve therapeutic effectiveness. Our laboratory and others have shown a critical role for macrophage colony-stimulating factor-1 (M-CSF-1, CSF-1) signaling through its receptor, CSF1R, in the recruitment of TIMs to tumors, which promote cancer progression. Using murine models of prostate cancer, we found that RT resulted in pronounced increases in CSF-1 expression in PCa cells, which was transcriptionally regulated by the non-receptor tyrosine kinase, ABL1 (c-Abl), highly correlating with increased TIM recruitment. Importantly, utilizing a CSF1R inhibitor, PLX3397, in combination with RT resulted in significant depletion of TIMs and delayed RT tumor recurrence. In parallel, the potential impact of TIMs in therapeutic resistance to androgen blockade therapy (ABT) was also interrogated. Similarly to RT, we found that inhibiting androgen signaling using the novel androgen receptor inhibitor MDV3100 (Enzalutamide) resulted in increased expression anti-inflammatory cytokine IL-10 and Th2 cytokine IL-13 in PCa cells, as well as CSF-1 expression in PCa cells and in mice sera. Moreover, cellular interactions between macrophages and PCa cells treated with MDV3100 skewed macrophages to a protumorigenic “alternative” activation state. In addition, tumors grown in surgically castrated mice showed increased CSF-1 expression in serum and in whole tumors compared to sham surgery mice, resulting in a considerable increase in TAM infiltration.

More importantly, TAM blockade using PLX3397 in combination with castration resulted in a significant delay in the onset of CRPC. Lastly, we sought to further investigate potential mechanisms underlying TIM-mediated resistance to androgen depletion. Cytotoxic effects of androgen depletion are primarily due to induction of apoptosis after inhibition of androgen receptor (AR) signaling. Insulin-like growth factor 1 receptor (IGF1R) signaling is a well-established mode of CRPC development due to its anti-apoptotic and mitogenic functions. Furthermore, the Th2 cytokine IL-13, is known to induce IGF-1 expression in macrophages. Interestingly, we found that the increased IL-13 expression from MDV3100 treated Myc-CaP cells, correlated with increased macrophage IGF-1 expression. Subsequently, macrophage-derived IGF-1 levels correlated with increased p-IGF1R staining in tumors from castrated mice versus sham surgery controls. Additionally, tumors grown in castrated mice showed a significant increase in IGF-1 expression, and a subsequent reduction of IGF-1 levels upon macrophage depletion with PLX3397. Macrophage depletion also correlated with decreases in Ki67 proliferation index, as well as delayed onset of CPRC. Collectively, these data suggest that a strong interplay between TIMs and tumor cells generate a pro-tumor microenvironment that favors therapeutic resistance in PCa.

Overall, these studies increase our understanding of the complex role of TIMs in the prostatic microenvironment, and argue in favor of their contribution to PCa progression and therapeutic resistance to RT and therapies targeting androgen signaling. The rational targeted therapies pursued here and other combinatorial approaches hold promise to improve the long-term efficacy of new therapeutics and ultimately improve patient lives.

The dissertation of Jemima Escamilla is approved.

Steven J. Bensinger

Steven M. Dubinett

Benjamin Bonavida

Lily Wu, Committee Chair

University of California, Los Angeles

2013

DEDICATIONS

With great honor and appreciation, I would like to dedicate this dissertation to my family. To my abuelita and abuelito, Irene and Roque Ballote, who have both been an inspiration to me and outstanding role models throughout my life and instilled in me that hard work and determination was necessary to achieve anything worthwhile. To my mother, Maria Escamilla, who always fought for a better life for my siblings and I and for her unconditional love. To my father, Roque Escamilla, who has been the number one advocate for my education always giving me unconditional support and never doubting my abilities to achieve my goals. To my brother and sister in law Rene and Lola Escamilla, for their generosity and selflessness always doing what was necessary to help me succeed. To my little sister, Karen Gutierrez, for her love and support and for inspiring me to be a great role model. Lastly, to my neice and nephews Lola, Rene, Ethan and Elijah for always bringing a smile to face.

TABLE OF CONTENTS

LIST OF FIGURES AND TABLES

Chapter 1:

Chapter 2:

ACKNOWLEDGMENTS

I would like to first thank my mentor, Dr. Lily Wu for her continued support and encouragement throughout my graduate education. Thank you for being such a wonderful advisor and for creating a laboratory environment that was educationally challenging as well as warm and comfortable which I know is very unique to you because of your kind heart.

I would like to thank all the Wu lab members both past and present who have become more than just colleagues but also good friends. Thank you to my two mentors Dr. Breanne Karanikolas and Dr. Saul Priceman you both taught me invaluable lab and critical thinking skills that have been instrumental throughout my graduate studies and I am sure will carry on with me throughout my career. Dr. Steve Hyun thank you for being a great friend and mentor in my life and career. Dr. James Sung for always lending a helping hand and being so generous with your time. To the rest of the Wu lab members: Dr. Makoto Sato, Dr. Karen Jiang, Dr. Jingying Xu, Dr. Mai Johnson, Diana Moughon, and Shiruy Schokrpur, thank you all for your support and making lab feel like home.

I would like to thank my doctoral committee members and scientific mentors for their guidance and scientific support. Drs., Steven M. Dubinett, Paul Mischel, Benjamin Bonavida, Samson A. Chow, and Steven J. Bensinger. Dr. Chow thank you for giving me the opportunity to do research in your lab as an undergrad which inspired me to pursue a Ph.D. I would especially like to acknowledge Dr. Bensinger for the countless hours of mentoring he selflessly provided.

I would like to thank my amazing undergraduate assistant Connie Liu for all her time and devotion to our research. Her constant inquisitiveness, energy and passion for science was a huge motivator for me to carry on during the hard times of graduate school.

I want to thank the Molecular and Medical Pharmacology department: classmates, faculty, and administrative staff. To my classmates thank you for the all the infamous times at the pharmacology pubs and departmental retreats. Having shared this long voyage with you all has been a lot of fun and given me a lifetime memories.

I would like to thank my wonderful group of friends that I could not have gotten through graduate school without:

To Marisa Briones and Nereida Partosan, thank you for being amazing friends throughout my life. You are more than a friends you are family. I'm so grateful to have experienced what I consider some of the greatest times of my life with you guys.

Marisa, thank you for the countless hours of couch chatter and for your continued support through all the ups and downs that came with graduate school. It has been a blast to have shared so many of life's funny and mesmerizing moments (i.e. Michelangelo's David) with you. Having traveled the world with you has been an incredible adventure and I'm glad I got to share that with you.

Nereida, thank you for the long hours on the phone listening to my stresses about graduate school and life. You always brought a smile to my face and could make me laugh through some

of the hardest and some of the best times in life. I am so grateful to have shared so many experiences with you starting with our leap out to college through our travels all over Europe. It's been amazing to experience so many new things with you and building so many unforgettable memories.

To Glen Young, you are truly a great friend and support for me. You have always been there for me when I needed you and always so generously willing to lend a helping hand in any way possible. From being part of your beautiful wedding in Tuscany to camping on dirt and falling in the ocean with you it has all been a wonderful adventure. I can't wait to dig more holes with you.

To Karina Palomares, I can't imagine not having someone with whom to share and vent about all the graduate school frustrations we endured. Thank you for being a great friend and always being there when I needed you including the times I was feeling little sick and needed medicine.

Allison Banks, thank you for always sharing with me your very rational perspectives that turned out to be very useful in many aspects of my life. You are a dear friend thank you for your support and for always asking how my days were going even though you didn't really know what I was talking about most of the time.

Most importantly, I would like to thank my family, whom I owe everything to: thank you for the continued support throughout my long educational journey. Mom, thank you for always reminding me to take care of my health as well as my studies. For working so hard to provide me with anything I needed. Dad, thank you for always showing so much interest in my schoolwork and always being supportive of whatever choices I made in my life and career. Thank you for providing without question whatever was necessary for my success. Abuelita Irene, thank you for teaching me the value of always producing quality work and for sharing your wisdom with me and always supporting me in all my decisions. Abuelito Roque, thank you for showing me that hard work pays off and through hard work and dedication I could achieve anything. To my brother Rene, I'm so proud to see what a great father and husband you have become and grateful to have you as a role model. Thank you for your kindness and support you always showed so much enthusiasm for my education and I am very grateful for that. To my sister Karen, what can I say you are always going to be my little sister even now that you are grown you will always have a special place in my heart. To my sister in law, Lola I'm so grateful we have become great friends through the years thank you for all your support and everything you selflessly do for our family. To my niece and nephews, Lola, Rene, Ethan, and Elijah thank for entertaining me all theses years and always bringing me with so much joy.

Chapter 2 is a version of Xu, J., Escamilla J., and Wu L. Abrogating the Protumorigenic Influences of Tumor-infiltrating Myeloid Cells by CSF1R Signaling Blockade Improves the Efficacy of Radiotherapy in Prostate Cancer. doi: 10.1158/1535-7163.TARG-11-C226. *Cancer Research,* 2013.

Chapter 3 is a version of Escamilla J., Liu C., Mok S., David J., Priceman, S. J., West B., Bollag G., McBride W., Xu J., and Wu L. Augmenting the Durability of Androgen Blockade Therapy in Prostate Cancer by Disrupting the Paracrine Crosstalks between Tumor Cells and Macrophages through CSF1R Inhibition, *in preparation*.

VITA

2005-2006	Award Recipient Center for Academic and Research Excellence University of California, Los Angeles
2005-2006	Undergraduate Student Researcher Department of Molecular and Medical Pharmacology University of California, Los Angeles
2006	B.S. Molecular Cell and Developmental Biology University of California, Los Angeles Los Angeles, CA
2007-2013	Graduate Student Researcher Department of Molecular and Medical Pharmacology David Geffen School of Medicine University of California, Los Angeles Los Angeles, California
2007	Award Recipient National Science Foundation Alliance for Graduate Education and the Professoriate Grant University of California, Los Angeles
2007-2008	Award Recipient Eugene V. Cota-Robles Fellowship funded by the University of California Office of the President and the Graduate Division University of California, Los Angeles
2008	Teaching Assistant Department of Molecular Cell and Developmental Biology University of California, Los Angeles
2009	Teaching Assistant Department of Molecular Cell and Developmental Biology University of California, Los Angeles
2010-2011	Graduate Student Representative Service Award Department of Molecular and Medical Pharmacology University of California, Los Angeles
2010-2011	Seminar Organizing Committee Member Institute for Molecular Medicine Seminar Series University of California, Los Angeles

2010-2012	Award Recipient Research Supplement to Promote Diversity in Health-Related Research University of California, Los Angeles
2011	Travel Award American Association for Cancer Research Minority Scholar in Cancer Research, AACR-NCI-EORTC International Conference on Molecular Targets and Cancer Therapeutics San Francisco, California
2011-2013	Student Leadership Team Member Business of Science Center Department of Molecular Cell and Developmental Biology University of California, Los Angeles
2012	Co-Founder Advancing Women in Science and Engineering (AWISE) Business of Science Center Department of Molecular Cell and Developmental Biology University of California, Los Angeles
2012	UCLA-NIH Bridge Program Mentor University of California, Los Angeles
2012-2013	Award Recipient Eugene V. Cota-Robles Fellowship funded by the University of California Office of the President and the Graduate Division University of California, Los Angeles

PUBLICATIONS AND PRESENTATIONS

Escamilla J., Liu C., Priceman, S. J., Sung J. L., Jiang Z., Xu J., West B., Bollag G., Jung, E. M., and Wu L. Augmenting the Durability of Androgen Blockade Therapy in Prostate Cancer by Disrupting the Paracrine Crosstalk Between Tumor Cells and Macrophages Through CSF1R Inhibition. *(in preparation)*.

Sung J. L., Huang X., **Escamilla J.,** Burton J., and Wu L. The Role of CCR7 in Prostate Cancer Metastasis. *(in preparation)*.

Xu J., **Escamilla J.**, Mok S., David J, Priceman, S. J., West B., Bollag G., McBride W., and Wu L. Abrogating the Protumorigenic Influences of Tumor-Infiltrating Myeloid Cells by CSF1R Signaling Blockade Improves the Efficacy of Radiotherapy in Prostate Cancer. *Cancer Research,* 2013. PMC Journal - In Process.

Escamilla J., Priceman, S. J., Sung J. L. and Wu L. CSF1R Mediated Inhibition of Alternatively Activated Macrophages to Augment Androgen Receptor Blockade Therapy. *Department of Molecular and Medical Pharmacology Annual Retreat,* Huntington Beach, CA. Oral Presentation. 2012.

Escamilla J., Priceman, S. J., Sung J. L., Xu, J., and Wu L. CSF1R Mediated Inhibition of Alternatively Activated Macrophages to Augment Androgen Receptor Blockade Therapy. *AACR-NCI-EORTC International Conference on Molecular Targets and Cancer Therapeutics,* San Francisco, CA. Poster Presentation. 2011.

Escamilla J., Priceman, S. J., Sung J. L., Moughon D., Shaposhnik Z., and Wu L. CSF-1 Receptor Signaling Regulates the Tumor Recruitment of Distinct Myeloid Cells in Prostate Cancer. *Prostate Cancer Research Program IMPaCT Conference,* Orlando, FL. Poster Presentation. 2011.

Chapter 1:

Introduction

Prostate cancer (PCa) is the most common type of cancer in men and the second leading cause of cancer related death in American men. PCa accounts for approximately 200,000 new diagnoses and 30,000 deaths per year in the United States (1). The major modes of treatment for advanced PCa include surgical resection, radiation and hormonal therapy. Localized radiotherapy (RT) is the most common of the treatment options, and while efficacious, approximately 60% of patients will experience biochemical recurrence as measured by prostate specific antigen (PSA) levels and disease progression (2). Of the patients that receive hormonal therapy, 80-90% of them respond to treatment, but almost all patients eventually acquire castration-resistant prostate cancer (CRPC) (3). Because of the development of recurrence and resistance to these major modes of treatment, new treatment options are imperative to extend the survival of advanced PCa patients. To this end, immune modulating approaches have emerged as promising therapeutic options for use in combination with frontline treatments of prostate cancer patients.

In the 1940s, Huggins and colleagues highlighted the importance of the endocrine system in prostate cancer growth. More specifically, the impact of androgen deprivation via surgical castration on tumor burden (4). Since then, therapeutic inhibition of androgen signaling, either by dampening androgen synthesis or by direct androgen receptor (AR) blockade has emerged as a key pathway for targeted therapies for this disease, termed androgen deprivation therapy (ADT) or androgen blockade therapy (ABT). In recent years, novel drugs have been developed as hormonal therapy, in particular, Abiraterone (Zytiga) and MDV3100 (Enzalutamide). These drugs target different aspects of AR signaling; Abiraterone functions by inhibiting the androgen synthesis activity of the CYP17 enzymes, while MDV3100 functions via competitive inhibition of AR ligand (5). In CRPC patients with limited treatment options, these drugs were shown to prolong overall survival by 4-5 months. However, patients eventually develop resistance and

CRPC progresses (5, 6). Interestingly, retrospective studies assessing AR status in CRPC patients have found that AR is still functional and active. This finding suggests the persistence of PCa dependence on AR even when systemic androgen is reduced below levels indicative of chemical castration (7). There are multiple mechanisms utilized by PCa cells to bypass androgen deprivation and to continue growing. Some examples include AR gene mutations as well as alternative splice variants lacking ligand binding domains (8, 9), amplified AR gene copy number and expression (10), aberrant activation of AR by receptor tyrosine kinase (RTK) signaling pathways, and atypical activation of AR by co-activators including epidermal growth factor (EGF) and IL-6 via STAT3 activation (11-13).

First generation anti-androgen drugs, such as bicalutamide (Casodex), are efficacious in treating androgen-dependent PCa, but are presumed to lose their antagonistic properties and become agonists after long-term treatment due to aberrant recruitment of enhancers and co-activators (14). New, second-generation anti-androgen drugs, such as MDV3100, do not show an agonist conversion after long-term use in murine xenograft studies using the human PCa cell line, LNCaP (14). Additionally, MDV3100 shows a longer time to tumor progression compared to the commonly used bicalutamide, with a median time to tumor progression of 186 days with MDV3100 versus 35 days with bicalutamide (14). Although it demonstrates superior activity compared with other anti-androgen drugs, acquired resistance to MDV3100 still occurs (14).

Since the 1950s, RT has emerged as a key treatment option for localized or locally advanced PCa. The most common type of RT used today is external beam radiation therapy (EBRT). EBRT employs high energy x-rays delivered by a linear accelerator which can deliver precise radiation deep into a tissue to a target site such as a tumor (2). RT functions by generating free radicals, which lead to genotoxic DNA damage that activates cell stress

responses and lead to cell death (15). Although this type of treatment is intended to be curative, there is a high incidence of treatment failure and recurrence. Clinical studies using ADT as the preferred salvage therapy after RT failure found that 73% patients failed ADT salvage therapy, and these patients had worse overall survival rate (2). Because PCa is not very responsive to chemotherapies typically used for other cancers, there are little to no options for PCa patients that have failed both RT and ADT (16).

An emerging area of research is the involvement of the tumor microenvironment in the progression of cancer. Many reports have shown immune cell involvement in resistance to various anti-cancer agents (17, 18). The underlying hypothesis of these studies is that communication between tumor cells and the microenviroment modulates immune cell activity to promote cancer progression. Therefore, it is believed that co-targeting the tumor microenvironment and the cancer cells may improve treatment outcomes.

It is a well-known phenomenon that dying/necrotic tumors have an increased inflammatory response (19). Dying tumor cells secrete cytokines that stimulate the immune system to respond as they would in the case of a wound or an injury (20). Macrophages are one of the first responders to a wound and play a significant role in promoting the growth of new blood vessels, or angiogenesis, and tissue remodeling (20), a process that is utilized by tumor cells to drive cancer progression and impact overall responses to various anti-cancer therapies (21). In particular, the activity of tumor infiltrating myeloid cells (TIMs) have been shown to promote tumor development and resistance to various chemotherapeutic agents (20). In PCa murine models, studies looking at the effects of castration on the inflammatory response showed there was a significant increase in cytokine production and immune cell infiltrates one week after castration. Immune infiltrates included B-cells, NK cells and macrophages. The focus of the

study was on B-cell-derived lymphotoxin, a cytokine that was able to promote CRPC development. Although this study highlighted for the first time that inflammation due to castration induced cell death actually promoted PCa progression (22), it did not address the likely contribution of protumorigenic myeloid cells in CPRC development.

Tumor microenvironment

The tumor microenviroment is a complex milieu containing stromal cells, such as immune cells and fibroblasts, signaling molecules, such as cytokines and chemokines, and extracellular matrix. There is growing evidence that immune cells in the tumor microenvironment can be co-opted into helping the cancer grow by inducing tumor angiogenesis, suppressing anti-tumor immune responses, and promoting growth by secretion of various cytokines and growth factors (23). It is therefore extremely important to further understand the interplay between cancer cells and cells in the tumor microenvironment during cancer treatment.

Immune cells present in the tumor microenviroment include effectors of adaptive immunity (immunity guided by specific identification of pathogens), such as T-cells, dendritic cells, and to a lesser extent, B-cells, as well as cells of the innate immune system (non-specific identification of pathogens), such as macrophages and other myeloid derived cells, leukocytes, and rarely natural killer (NK) cells (24). Cytotoxic $CD8^+$ T-cells kill tumor cells by secreting cytotoxic substances such as perforin, granzymes, and granulysin. Their activity can be regulated by various cytokines or signals from $CD4^+$ helper T-cells or other cells in the tumor microenviroment (25). However, the majority of immune infiltrates in solid tumors demonstrate alternative phenotypes that are either defective in their anti-tumoricidal activity or potently promote tumor progression.

Myeloid Lineage in Solid Tumors

Bone marrow (BM) derived monocytes/myeloid cells circulate in the peripheral blood and home to tumor sites by various cytokines and chemokines secreted by tumor cells (26). Myeloid cells in the tumor microenviroment are a diverse population of bone marrow-derived myeloid cells including macrophages or tumor associated macrophages (TAMs), myeloid-derived suppressor cells (MDSCs), as well as neutrophils. Together, this population is referred to as TIMs (Figure 1.1) (27, 28).

MDSCs are a heterogeneous population of immature myeloid cells that originate in the bone marrow and are recruited to distant sites by various cytokines and recruitment factors (29, 30). MDSCs share many functions with TAMs, although their most noted function is a strong ability to suppress T-cell proliferation and activity via arginase (ARG-1) and nitric oxide (NO) production (27). MDSCs have also been shown to promote angiogenesis and metastasis via vascular endothelial growth factor (VEGF) and matrix metalloproteinase (MMP) production, increase T-regulatory (T-reg) cell pools, and inhibit NK cell activation. MDSC subtypes consist of polymorphonuclear (granulocytic) and monocytic cells (PMN and MO-MDSC, respectively). These cell types are characterized by cell surface marker expression profiles, where $CD11b^{+}Gr\text{-}1^{hi}Ly6C^{lo}$ cells are PMN-MDSCs, and $CD11b^{+}Gr\text{-}1^{lo}Ly6C^{hi}$ cells are MO-MDSCs (27, 28). Based on the pro-tumorigenic properties of MDSCs, they present novel targets for anti-cancer therapies. Pre-clinical studies in mouse models suggest that blockade of MDSC recruitment to tumors in combination with chemotherapies, such as paclitaxel, and anti-angiogenic treatments delays the onset of resistance to therapy (31, 32).

TAMs, generally characterized by the cell surface marker expression profile $CD11b^{+}F4/80^{+}$ in mice, can exist in various activation states depending on the cues they receive

from their environment. These activation states include "classically activated" M1 macrophages, which are typically anti-tumorigenic and pro-inflammatory, and "alternatively activated" M2 macrophages, which are pro-tumorigenic and anti-inflammatory (33). Signaling from cytokines such as GM-CSF, TNF-α, IFN-γ, or microbial stimuli, including LPS, can promote an M1 response. M1 macrophages are said to be cytotoxic, secreting reactive oxygen species (ROS), thus damaging tissue, and promoting inflammation by secreting pro-inflammatory cytokines such as IL-12. M2 activation is said to occur through signaling from cytokines such as IL-4, IL-13 and IL-10 (34). M2-TAMs have been shown to promote tumor progression by various mechanisms (34). They can suppress the adaptive immune response against cancer cells through secretion of anti-inflammatory cytokines such as IL-10 and downregulation of major histocompatibility complex II (MHCII) expression, and thus are poor antigen presenters (35). Furthermore, in mouse tumor studies, M2-TAMs secrete ARG-1 to deplete levels of L-arginine necessary for T-cell activation and proliferation (36). Additionally, they can promote matrix remodeling and angiogenesis via secretion of MMPs and VEGFs. Furthermore they are known to promote cancer progression by producing growth factors such as PDGF, HGF, IGF-1 (37). Cell surface marker and cytokine expression profiles can be used to distinguish the two TAM polarization states. Amongst all $CD11b^{+}$ and $F4/80^{+}$ macrophages in a tumor, $MHCII^{Hi}IL\text{-}10^{lo}IL\text{-}12^{hi}$ would represent M1-TAMs and $MHCII^{Lo}IL\text{-}10^{hi}IL\text{-}12^{lo}$ would denote M2-TAMs (38).

TIM Recruitment Factors and Inflammatory Mediators

Tumor homing of TIMs is carried out by cytokines and chemokines. The most noted recruitment factors include monocyte chemotactic protein (MCP-1 or CCL2), stromal derived factor (SDF-1), RANTES (CCL5), and macrophage colony stimulating factor 1 (M-CSF-1 or

CSF-1) (29, 30, 39). CCL2 expression in breast, colorectal, and PCa has been associated with increased metastasis, blockade of apoptosis and an overall poor prognosis (30, 40). Perhaps one of the most important cytokines for TIM recruitment and function is CSF-1. CSF-1 signaling plays a key role in macrophage growth, differentiation, and proliferation, and potently regulates myeloid development in the BM (41). The CSF-1 receptor, CSF1R, is a receptor tyrosine kinase found primarily on myeloid populations, but is expressed at low levels in B-cells, fibroblasts, epithelial cells, and neurons (41). Chemotactic signaling by CSF-1 is known to be critical for monocyte/myeloid recruitment to tumor sites. Once at the tumor site, long-term stimulation by CSF-1 can differentiate monocytes into macrophages. In tumors, continuous CSF-1 signaling is also believed to promote an M2 phenotype (41, 42). Analyses of clinical samples indicate that increases in CSF-1 and CSF1R expression, correlate with tumor progression and a negative outcome in prostate (43, 44) and breast cancer patients (30). Paracrine signaling of CSF-1 in breast cancer was found to promote metastasis (45). Using a CSF-1 knock out mouse (op/op), Dr. Pollard and colleagues showed that CSF-1 was important for breast cancer metastasis, highlighting the significance of this axis in tumor progression (30). In PCa, increased CSF-1 serum levels were found to correlate with increased metastasis (46). Interestingly, usage of a small molecule CSF1R kinase inhibitor, GW2580, showed TIM blockade correlating with decreases in MMP-9, VEGF-A, ARG-1 expression and blood vasculature in several solid tumor models (42).

The first PCa immunotherapeutic, Sipuleucel-T, was approved in 2012. Sipuleucel-T utilizes a patient's own antigen presenting dendritic cells primed against PCa prostatic acid phosphatase (PAP) antigen to activate anti-tumoral T-cell responses (47). Although this treatment results in increased overall survival of CRPC patients, the effects are not durable (48).

It is plausible that the suppressive activity of innate immune cells, such as TIMs, may dampen the anti-tumor adaptive immune activity, but studies directly investigating this mechanism have yet to be explored. Further studies are necessary to better understand the interplay of tumor cells and the microenvironment, as well as how to better fine-tune the tumor microenvironment against cancer, in order to develop improved therapeutic intervention for PCa and other cancers.

Overall, preclinical and clinical studies indicate the tumor microenvironment is a highly important aspect of cancer progression and resistance to cancer therapies. However, these studies also underscore that much remains to be learned. Further studies are necessary to better understand the interplay of tumor cells and the microenvironment, in order to develop improved therapeutic interventions for PCa and other cancers, as well as how to better fine-tune the molecular processes controlling the tumor microenvironment against cancer**.**

Specific Aims of Dissertation

The goals of these studies were to gain a better understanding of the involvement of TIMs in two major modes of PCa treatment: RT and androgen signaling blockade. The first aim was to determine the specific molecular changes that occur in PCa cells after RT that increase TIM recruitment and modulate their activity. Extending from these studies we sought to investigate the contribution of TIMs on RT recurrence by blocking their recruitment, and thus their activity, using therapeutic CSF1R inhibition in combination with RT in murine models. Analogous to the first aim the second aim was to determine the particular molecular changes in PCa post-androgen deprivation and androgen blockade therapy that may induce TIM subset recruitment and modulate their pro-tumorigenic phenotype. We built upon these studies to further evaluate the therapeutic impact of TIMs on CRPC development by inhibiting their

recruitment and activity by CSF1R blockade. The third aim of this dissertation was to identify specific mechanisms mediated by TIMs in promoting CPRC development by examining changes in growth factor expression in TIMs that may lead to alternative proliferation pathways in PCa.

Figures

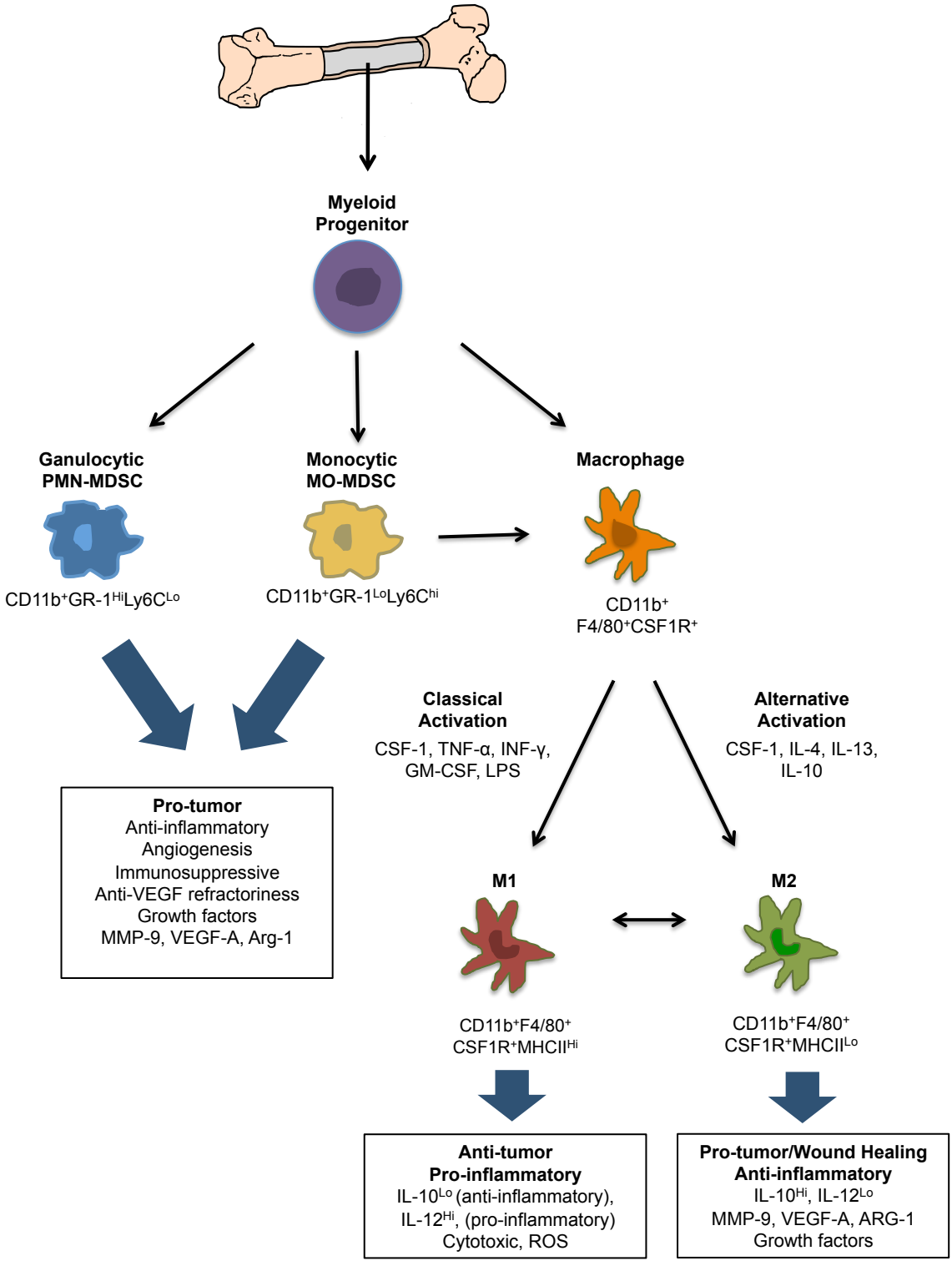
Myeloid Progenitor
Ganulocytic PMN-MDSC
Monocytic MO-MDSC
Macrophage
CD11b+GR-1HiLy6CLo
CD11b+GR-1LoLy6Chi
CD11b+ F4/80+CSF1R+
Classical Activation
CSF-1, TNF-α, INF-γ, GM-CSF, LPS
Alternative Activation
CSF-1, IL-4, IL-13, IL-10
Pro-tumor
Anti-inflammatory
Angiogenesis
Immunosuppressive
Anti-VEGF refractoriness
Growth factors
MMP-9, VEGF-A, Arg-1
M1
M2
CD11b+F4/80+ CSF1R+MHCIIHi
CD11b+F4/80+ CSF1R+MHCIILo
Anti-tumor
Pro-inflammatory
IL-10Lo (anti-inflammatory),
IL-12Hi, (pro-inflammatory)
Cytotoxic, ROS
Pro-tumor/Wound Healing
Anti-inflammatory
IL-10Hi, IL-12Lo
MMP-9, VEGF-A, ARG-1
Growth factors

Figure 1.1: Tumor infiltrating myeloid cell subsets and their tumor promoting properties. Tumor infiltrating myeloid cells (TIMs) are a heterogeneous population originating from the bone marrow consisting of macrophages, monocytic (MO) and granulocytic/polymorphonuclear (PMN) myeloid derived suppressor cells (MDSC). TIMs are recruited out of the bone marrow into the peripheral blood and eventually to tumor sites. Macrophage factors secreted by tumor cells can skew macrophages to an anti-tumor M1 phenotype or a pro-tumor M2 phenotype. M2 macrophages and MDSCs exert their pro-tumorigenic properties by suppressing the anti-tumor immune response, promoting angiogenesis and matrix remodeling, and producing growth factors.

References

1. Siegel, R., D. Naishadham, and A. Jemal, *Cancer statistics, 2013*. CA Cancer J Clin. 63(1): p. 11-30.
2. Agarwal, P.K., et al., *Treatment failure after primary and salvage therapy for prostate cancer: likelihood, patterns of care, and outcomes*. Cancer, 2008. 112(2): p. 307-14.
3. Niu, Y., et al., *Differential androgen receptor signals in different cells explain why androgen-deprivation therapy of prostate cancer fails*. Oncogene. 29(25): p. 3593-604.
4. Huggins C, S.J.R., Hodges CV, *The effect of castration on advanced carcinoma of the prostate gland*. 1941.
5. Omlin, A. and J.S. de Bono, *Therapeutic options for advanced prostate cancer: 2011 update*. Curr Urol Rep. 13(2): p. 170-8.
6. Attard, G., J. Richards, and J.S. de Bono, *New Strategies in Metastatic Prostate Cancer: Targeting the Androgen Receptor Signaling Pathway*. Clin Cancer Res.
7. Harris, W.P., et al., *Androgen deprivation therapy: progress in understanding mechanisms of resistance and optimizing androgen depletion*. Nat Clin Pract Urol, 2009. 6(2): p. 76-85.
8. Watson, P.A., et al., *Constitutively active androgen receptor splice variants expressed in castration-resistant prostate cancer require full-length androgen receptor*. Proc Natl Acad Sci U S A. 107(39): p. 16759-65.
9. Li, Y., et al., *Androgen receptor splice variants mediate enzalutamide resistance in castration-resistant prostate cancer cell lines*. 2012.
10. Tapio Visakorpi, E.H., Pasi Koivisto1, Minna Tanner1, Riitta Keinänen1, Christian Palmberg3, Aarno Palotie4, Teuvo Tammela3, Jorma Isola1 & Olli-P. Kallioniemi1, *In*

vivo amplification of the androgen receptor gene and progression of human prostate cancer. Nature Genetics 1995. 9, 401 - 406.

11. Kung, H.J., *Targeting tyrosine kinases and autophagy in prostate cancer*. Horm Cancer. 2(1): p. 38-46.

12. *Progressive growth of prostate cancer*. Available from: http://www.erasmusmc.nl/47463/51019/100415/trapfig3.

13. Hobisch, A., et al., *Interleukin-6 regulates prostate-specific protein expression in prostate carcinoma cells by activation of the androgen receptor*. Cancer Res, 1998. 58(20): p. 4640-5.

14. Tran, C., et al., *Development of a second-generation antiandrogen for treatment of advanced prostate cancer*. Science, 2009. 324(5928): p. 787-90.

15. Shiao, S.L. and L.M. Coussens, *The tumor-immune microenvironment and response to radiation therapy*. J Mammary Gland Biol Neoplasia. 15(4): p. 411-21.

16. Gerritsen, W.R., *The evolving role of immunotherapy in prostate cancer*. Ann Oncol. 23 Suppl 8: p. viii22-7.

17. DeNardo, D.G., et al., *Leukocyte complexity predicts breast cancer survival and functionally regulates response to chemotherapy*. Cancer Discov. 1(1): p. 54-67.

18. Loges, S., T. Schmidt, and P. Carmeliet, *Mechanisms of resistance to anti-angiogenic therapy and development of third-generation anti-angiogenic drug candidates*. Genes Cancer. 1(1): p. 12-25.

19. Hanahan, D. and R.A. Weinberg, *Hallmarks of cancer: the next generation*. Cell. 144(5): p. 646-74.

20. Van Ginderachter, J.A., *The wound healing chronicles*. Blood. 120(3): p. 499-500.

21. Mantovani, A., et al., *Macrophage plasticity and polarization in tissue repair and remodelling*. J Pathol, 2013. 229(2): p. 176-85.

22. Ammirante, M., et al., *B-cell-derived lymphotoxin promotes castration-resistant prostate cancer*. Nature. 464(7286): p. 302-5.

23. Gabrilovich, D.I., S. Ostrand-Rosenberg, and V. Bronte, *Coordinated regulation of myeloid cells by tumours*. Nat Rev Immunol. 12(4): p. 253-68.

24. Whiteside, T.L., *The tumor microenvironment and its role in promoting tumor growth*. Oncogene, 2008. 27(45): p. 5904-12.

25. Topfer, K., et al., *Tumor evasion from T cell surveillance*. J Biomed Biotechnol. 2011: p. 918471.

26. Yamashiro, S., et al., *Tumor-derived monocyte chemoattractant protein-1 induces intratumoral infiltration of monocyte-derived macrophage subpopulation in transplanted rat tumors*. Am J Pathol, 1994. 145(4): p. 856-67.

27. Gabrilovich, D.I. and S. Nagaraj, *Myeloid-derived suppressor cells as regulators of the immune system*. Nat Rev Immunol, 2009. 9(3): p. 162-74.

28. Umemura, N., et al., *Tumor-infiltrating myeloid-derived suppressor cells are pleiotropic-inflamed monocytes/macrophages that bear M1- and M2-type characteristics*. J Leukoc Biol, 2008. 83(5): p. 1136-44.

29. Sawanobori, Y., et al., *Chemokine-mediated rapid turnover of myeloid-derived suppressor cells in tumor-bearing mice*. Blood, 2008. 111(12): p. 5457-66.

30. Lin, E.Y., et al., *Colony-stimulating factor 1 promotes progression of mammary tumors to malignancy*. J Exp Med, 2001. 193(6): p. 727-40.

31. DeNardo, D., et al., *Leukocyte complexity predicts breast cancer survival and functionally regulates response to chemotherapy*. Cancer Discovery, 2011. 1: p. 52-65.

32. Schmid, M.C. and J.A. Varner, *Myeloid cells in the tumor microenvironment: modulation of tumor angiogenesis and tumor inflammation*. J Oncol. 2010: p. 201026.

33. Gordon, S., *Alternative activation of macrophages*. Nat Rev Immunol, 2003. 3(1): p. 23-35.

34. Shih, J.-Y., *Tumor-Associated Macrophage: Its Role in Cancer Invasion and Metastasis*. Journal fo Cancer Molecules, 2006. 2(3): p. 101-106.

35. Benfan Wang, Q.L., Li Qin1, Siting Zhao1, Jinyan Wang1,4* and Xiaoping Chen1,2*, *Transition of tumor-associated macrophages from MHC class IIhi to MHC class IIlow mediates tumor progression in mice*. BMC Immunology 2011. 12:43.

36. Talmadge, J.E., *Pathways mediating the expansion and immunosuppressive activity of myeloid-derived suppressor cells and their relevance to cancer therapy*. Clin Cancer Res, 2007. 13(18 Pt 1): p. 5243-8.

37. Pollard, J.W., *Tumour-educated macrophages promote tumour progression and metastasis*. Nat Rev Cancer, 2004. 4(1): p. 71-8.

38. Sica, A., et al., *Tumour-associated macrophages are a distinct M2 polarised population promoting tumour progression: potential targets of anti-cancer therapy*. Eur J Cancer, 2006. 42(6): p. 717-27.

39. Mantovani, A., et al., *Role of tumor-associated macrophages in tumor progression and invasion*. Cancer Metastasis Rev, 2006. 25(3): p. 315-22.

40. Fujimoto, H., et al., *Stromal MCP-1 in mammary tumors induces tumor-associated macrophage infiltration and contributes to tumor progression*. Int J Cancer, 2009. 125(6): p. 1276-84.

41. Hamilton, J.A., *Colony-stimulating factors in inflammation and autoimmunity*. Nat Rev Immunol, 2008. 8(7): p. 533-44.

42. Priceman, S.J., et al., *Targeting distinct tumor-infiltrating myeloid cells by inhibiting CSF-1 receptor: combating tumor evasion of antiangiogenic therapy*. Blood. 115(7): p. 1461-71.

43. Ide, H., et al., *Expression of colony-stimulating factor 1 receptor during prostate development and prostate cancer progression*. Proc Natl Acad Sci U S A, 2002. 99(22): p. 14404-9.

44. Richardsen, E., et al., *The prognostic impact of M-CSF, CSF-1 receptor, CD68 and CD3 in prostatic carcinoma*. Histopathology, 2008. 53(1): p. 30-8.

45. Patsialou, A., et al., *Invasion of human breast cancer cells in vivo requires both paracrine and autocrine loops involving the colony-stimulating factor-1 receptor*. Cancer Res, 2009. 69(24): p. 9498-506.

46. Ide, H., et al., *Serum level of macrophage colony-stimulating factor is increased in prostate cancer patients with bone metastasis*. Hum Cell, 2008. 21(1): p. 1-6.

47. Miller, A.M. and P. Pisa, *Tumor escape mechanisms in prostate cancer*. Cancer Immunol Immunother, 2007. 56(1): p. 81-7.

48. Lu, C., et al., *Immunotherapy for metastatic prostate cancer: where are we at with sipuleucel-T?* Expert Opin Biol Ther. 11(1): p. 99-108.

Chapter 2:

Abrogating the Protumorigenic Influences of Tumor-Infiltrating Myeloid Cells by CSF1R Signaling Blockade Improves the Efficacy of Radiotherapy in Prostate Cancer

Abstract

Radiotherapy is used to treat many types of cancer, but many treated patients relapse with local tumor recurrence. Tumor-infiltrating myeloid cells (TIMs), including CD11b (ITGAM)$^{+}$F4/80 (EMR1)$^{+}$ tumor-associated macrophages (TAMs) and CD11b^{+}Gr-1 (LY6G)$^{+}$ myeloid-derived suppressor cells (MDSCs), respond to cancer-related stresses and play critical roles in promoting tumor angiogenesis, tissue remodeling and immunosuppression. In this report, we employed a prostate cancer (PCa) model to investigate the effects of irradiation on TAMs and MDSCs in tumor-bearing animals. Unexpectedly, when primary tumor sites were irradiated we observed a systemic increase of MDSCs in spleen, lung, lymph nodes and peripheral blood. Cytokine analysis showed that the macrophage colony-stimulating factor, CSF1, increased by 2-fold in irradiated tumors. Enhanced macrophage migration induced by conditioned media from irradiated tumor cells was completely blocked by a selective inhibitor of CSF1R. These findings were confirmed in PCa patients, where serum levels of CSF1 increased after radiotherapy. Mechanistic investigations revealed the recruitment of the DNA damage-induced kinase, ABL1, into cell nuclei where it bound the *Csf1* gene promoter and enhanced *Csf1* gene transcription. When added to radiotherapy, a selective inhibitor of CSF1R suppressed tumor growth more effectively than radiation alone. Our results highlight the importance of CSF1/CSF1R signaling in the recruitment of TIMs which can limit the efficacy of radiotherapy. Further, they suggest that CSF1R inhibitors should be evaluated in clinical trials in combination with radiotherapy as a strategy to improve outcomes.

Introduction

Radiotherapy (RT) is one of the primary treatments for prostate cancer (PCa). Approximately 50% of patients are treated with radiotherapy either alone or in combination with other therapies (1). Data from Cancer of the Prostate Strategic Urologic Research Endeavor (CaPSURE) identified that 63% of patients experienced biochemical PSA recurrence after RT (2). In fact, D'Amico et al determined that a high rate of PSA velocity pretreatment is significantly associated with a shorter time to both PSA recurrence and PCa-specific mortality after RT (3), with most of the recurrence at the local site (4). Several studies have addressed the importance of hypoxia and the SDF-1/CXCR4 axis in promoting tumor regrowth after RT in brain tumor and breast cancer (5, 6). However, a better understanding of the mechanisms of tumor regrowth is needed to achieve increased local control by RT in PCa and improve the cure rate of this disease.

Solid tumors contain a significant population of tumor-infiltrating myeloid cells (TIMs) (7). TIMs are now recognized as important mediators of not only tumor progression and metastasis (8), but also therapeutic resistance (9, 10), through promoting angiogenesis and suppressing antitumor immune responses (11, 12). The pro-tumorigenic role of “alternatively” activated macrophages has been well-established (12). Recently, another specific subtype of TIMs, namely myeloid-derived suppressor cells (MDSCs), is receiving great attention in cancer research. MDSCs comprise a heterogeneous population of immature myeloid cells that originate in the bone marrow and are recruited to the tumor by a diverse array of cytokine and chemokine signals. Similar to tumor-associated macrophages (TAMs) (8), MDSCs have been shown to generate an environment favorable for tumors by heightening immunosuppression, angiogenesis and invasion (13-15). Various cell surface markers are used to identify TIM subsets: TAMs can

be identified by CD11b and F4/80, and MDSCs by CD11b and Gr-1 co-expression in murine models (11, 16). Macrophage colony-stimulating factor (M-CSF or CSF1) is a potent growth factor that promotes the differentiation, proliferation, and migration of monocytes/macrophages via signaling through its receptor tyrosine kinase CSF1R (cFMS) (17, 18). We recently showed that TAMs and MDSCs form a spectrum of bone marrow-derived myeloid cells dependent on CSF1/CSF1R signaling for recruitment into the tumor and that they play critical roles in tumor growth (15). DeNardo *et al*. also highlighted the importance of CSF1/CSF1R signaling in the recruitment of TAMs in breast cancer and further showed that CSF1R blockade can inhibit TAMs in chemotherapy and improve treatment outcome (19).

ABL1 (c-Abl) is a ubiquitously expressed non-receptor tyrosine kinase that has been implicated in many cellular processes including cell migration, differentiation, apoptosis and gene regulation (20-22). ABL1 has also been implicated in the proliferation and metastasis of melanoma and breast cancer cells (23-25). In the present study, we show that the infiltration of TIMs is significantly enhanced by local irradiation of PCa. In addition, CSF1 mRNA and CSF1 secretion is increased following radiotherapy through an ABL1-dependent mechanism. We further demonstrated that blockade of CSF1/CSF1R signaling effectively reduces TIMs infiltration to tumors, thereby achieving more effective tumor growth suppression after irradiation. The rational combination therapy reported here may provide a more effective and durable treatment strategy for PCa patients.

Materials and Methods

Cell Culture

Murine macrophage RAW264.7 cells (ATCC), ras+myc-transformed RM-1 and RM-9 prostate tumor cells, human glioblastoma cell lines U87 and U251 (a kind gift from Dr. Paul Mischel), human breast cancer cell line MDA-MB-283, and mouse malignant peripheral nerve sheath tumor cells (MMPNST, a kind gift from Dr. Hong Wu) were cultured in Dulbecco modified eagle medium (DMEM) containing 10% fetal bovine serum (FBS), 100 U/mL penicillin, and 15 mM HEPES at 37°C with 5% CO_2. Human PCa cell lines, CWR and LNCaP, and the human carcinoma cell line A549 were cultured in RPMI-1640 medium containing 10% FBS, 100 U/mL penicillin, and 15 mM HEPES at 37°C with 5% CO_2. Cell lines were periodically authenticated by morphologic inspection and tested negative for mycoplasm contamination by PCR tests.

Chromatin Precipitation (ChIP)

Treated Myc-CaP cells were cross-linked with 1% formaldehyde at room temperature for 15 minutes. The cells were then washed with phosphate-buffered saline (PBS) and processed by the manufacturers instruction using Pierce® Agarose ChIP Kit (Thermo Scientific). c-Abl antibody K-12 (Santa Cruz) and RNA polymerase II (Santa Cruz) were used for immunoprecipitation. The following primers were used for detecting CSF1 promoter sequences: Forward: 5'ATGTGTCA GTGCCTGTGAGTGTGT3', Reverse: 5'GCCAGGGTGATTTCCCATAAACCA 3'; CSF1 control sequences: Forward, 5'TGCAAGAAGCACCCATGAAATGGC3', Reverse: 5'ATGCCAAAGCCTGCAGTTAAACCC3'.

Human Serum Assessment

Sera from human PCa patients before and after radiotherapy was obtained from by the Department of Radiation Oncology, UCLA Medical Center Hospital, with informed consent according to US federal law and are exempt from consideration by the UCLA Administrative Panel on Human Subjects in Medical Research. Analysis of CSF1 was done by Eve Technologies using human CSF1 multiplex kit (Biorad).

In vivo Tumor Models

C57BL6 male mice (4-8 weeks old) were purchased from Jackson Laboratory (Bar Harbor). RM-1 (2.5×10^5 cells), RM-9 (2.5×10^5 cells) or Myc-CaP (2×10^6 cells) were implanted subcutaneously in the thigh, and treatment was initiated when tumors reached 4 mm in diameter. All animal experiments were approved by the UCLA IACUC and conformed to all local and national animal care guidelines and regulations. Tumor size was measured by digital calipers daily or every two days depending on the model. Mice were sacrificed and tissues were analyzed at the ethical tumor size limit of 1.5 cm in diameter. For GW2580 treatment, mice were treated with control diluent (0.5% hydroxypropyl methylcellulose, Sigma-Aldrich; 0.1% Tween20 in distilled H_2O) or GW2580 (160 mg/kg) by oral gavage beginning on the same day irradiation treatment started. PLX3397 was provided in food chow together with daily food consumption.

In vitro Migration Assay

RAW264.7 (1.5×10^5 cells) were seeded in cell culture inserts (8 μm pore size; BD Falcon) in DMEM containing 0.1% FBS with or without 1000 nM GW2580. Inserts were placed

in 24-well plates with tumor-conditioned media collected 48 hrs after irradiation treatment (3Gy). After 6 hrs, migrated cells were immediately fixed in 3% formaldehyde and stained with 4,6-diamidino-2-phenylindole (DAPI). Nine fields/well at 4x magnification were quantified using ImageJ Version 1.34s (National Institute of Health).

Immunohistochemistry

Tissues were harvested and fixed in 3% paraformaldehyde overnight. Sections (5 μm) were stained with the following antibodies: anti-F4/80 (1:500; Serotec), anti-Gr-1 (1:100; eBioscience), or anti-CD31 (1:300; BD Biosciences) antibodies. Histology was performed, processed, and quantified as previously described (15). The samples were analyzed using an Olympus BX41 fluorescent microscope fitted with a Q-Imaging QICAM FAST 1394 camera. Images were captured at 4x, 10x, or 20x magnification using QCapture Pro Version 5.1 (Media Cybernetics), and quantified using ImageJ Version 1.34s (NIH).

Immunofluorescence Microscopy

Cells seeded on cover slips were fixed with 3% formaldehyde and incubated with c-Abl antibody (K-12, 1:100, Santa Cruz) followed by AlexaFluor 488 rabbit anti-mouse (Invitrogen) and then AlexaFluor 568 phalloidin and DAPI (Invitrogen). Mounting medium (Pro-Long Gold Antifade Reagent; Invitrogen) was applied and coverslips were sealed with clear nail polish. Fluorescent images were acquired at room temperature on a confocal microscope, LSM710 (Carl Zeiss).

Flow Cytometry Analysis

To prepare single-cell suspensions for flow cytometry, harvested tissues (tumors, lungs) were dissected into approximately 1- to 3-mm^3 fragments and digested with 80 U/mL collagenase (Invitrogen) in DMEM containing 10% FBS for 1.5 hrs at 37°C while shaking. Spleens and lymph nodes were gently dissociated between 2 glass slides for single-cell isolation. Peripheral blood was isolated directly into BD Vacutainer K2 EDTA tubes (BD Biosciences). After red blood cell (RBC) lysis (Sigma-Aldrich), single-cell suspensions were filtered and incubated for 30 min on ice with the following: APC, PerCP-Cy5.5, PE, APC-e780-conjugated antibodies (CD11b, Gr-1, CSF1R and F4/80) were purchased from eBioscience (1:200). Ly6C (1:200) was purchased from BD Bioscience. DAPI was purchased from Invitrogen. Cells were washed twice before analysis on the BD LSR-II flow cytometer (Beckman Coulter). Data was analyzed with FlowJo software (TreeStar).

Local Irradiation

Irradiation was performed using a Gulmay X-ray machine (300kV, 10mA) with a dose rate of 1.84 Gy/min. When tumors reach 4-5 mm in diameter, mice were anesthetized and irradiated with a daily dose of 3Gy for 5 days to the tumor area with the rest of body shielded.

Real-time RT-PCR Analysis

Total cellular RNA was extracted from cells using Tri Reagent (Sigma Aldrich). RNA was isolated according to the TRIzol procedure. RNA was quantified and assessed for purity by UV spectrophotometry and gel electrophoresis. RNA (1 μg) was reverse-transcribed using iScript cDNA synthesis kit (Biorad) according to manufacturer's instructions. For each sample, 1

μl cDNA (~ 20 ng) was amplified using Syber green 2× master mix (Bioline) and 10 μM primers (Primer sequences are listed in Table 1). The reaction was run on My IQ single color iCycler real time PCR machine (Biorad). Samples were amplified using the following cycling conditions: 40 cycles of 95°C/15 sec, 60°C/30 sec and 72°C/30 sec. Gene expression was determined by delta Ct method and normalized to β-actin expression.

SDS-PAGE

For experiments using concentrated media, cells were plated in 150mm tissue culture dish in 0% FBS DMEM overnight. 20 ml of media was collected 48 hrs after irradiation and subjected to media concentration using a protein concentrator (Pierce Biotechnology) at the speed of 4500 xg for 30 min. Total volume was normalized between samples and 40 μl was loaded onto 4-12% continuous gradient Tris-glycine gel (Invitrogen). For ABL1 cleavage experiments, cells were plated in 6-well plates overnight and collected after irradiation at the time indicated. Cells were lysed in RIPA buffer (Upstate) containing proteinase inhibitor cocktail (Sigma), sonicated briefly, and centrifuged 10 min at 12,000 xg. 20 μg of cell lysates were resolved on a 4-12% continuous gradient Tris–glycine gel (Invitrogen). The gels were then transferred to PVDF membrane (Millipore) and incubated with primary antibodies: anti-ABL1 (K-12, rabbit polyclonal, Santa Cruz), dilution 1:1000; anti-CSF1 (H-300, rabbit polyclonal, dilution (1:20,000) Santa Cruz), dilution 1:1000; anti-GAPDH (A-3, mouse monoclonal, Santa Cruz).

Statistical Analysis

Data are presented as mean plus or minus SEM. Statistical comparisons between groups were performed using the Student *t* test.

Results

Local irradiation enhances myeloid cell infiltration to tumors. Abundant evidence points to the infiltrating myeloid cells exerting significant influences on tumor cell aggression and the immunological environment. Hence, we studied irradiation-induced TIMs recruitment in two immunocompetent murine PCa models, namely RM-1 and Myc-CaP syngeneic in the C57/BL6 and FVB strain, respectively. These models provide distinct host genetic background, tumor growth rate, degree of myeloid cells infiltration and response to irradiation to broaden the perspectives on this issue. We first examined the recruitment of TIMs to tumors after irradiation in the RM-1, a Ras- and Myc-transformed murine prostatic cancer model (26), with moderate level of TIMs infiltration. As shown in Figure 2.1, irradiation effectively delayed the tumor growth by approximately 7 days (Figure 2.1a). Control tumors and irradiated tumors were collected when they reached similar sizes (day 13 for control tumors and day 19 for irradiated tumors) and processed to assess their content of TIMs. Irradiation significantly induced the infiltration of $F4/80^{+}CD11b^{+}$ TAMs (Figure 2.1b) and $Gr\text{-}1^{+}CD11b^{+}$ MDSCs (Figure 2.1c) to the tumors. Immunohistochemistry staining further confirmed this increase of TIMs in the tumors (Figure 2.1d). Recent reports further distinguished the myeloid subsets within MDSCs as consisting of MO-MDSC ($CD11b^{hi}ly6C^{lo}$) and PMN-MDSC ($CD11b^{lo}ly6C^{hi}$) with different functional characteristics (27). We found that both MO-MDSCs and PMN-MDSCs were significantly induced by irradiation, with MO-MDSCs showing a larger increase (Figure 2.1e). Likewise, the irradiation-induced TIMs recruitment was also observed in RM-9 tumor, a C57BL6 compatible model derived in the same manner as RM-1, and Myc-CaP tumor, a c-Myc oncogene-driven model implantable in FVB host (Figure 2.2-2.3). Taken together, these data

demonstrated that local irradiation enhances recruitment of both TAMs and MDSCs to tumors in several murine PCa models.

Local irradiation enhances systemic myeloid cell expansion. To better characterize the potential systemic impact of local tumor irradiation, we examined the infiltration of MDSCs and TAMs in peripheral tissues at different time points after irradiation, providing insights on the dynamics and kinetics of the myeloid cell recruitment process. The level of $CD11b^+F4/80^+$ macrophages were low in lungs, spleens, lymph nodes, and blood, thus we focused on $CD11b^+Gr\text{-}1^+$ MDSCs in the systemic sites and analyzed the content of $CD11b^+F4/80^+$ macrophages only in the tumor (Figure 2.4b). As shown in Figure 2.4, prior to irradiation, the baseline levels of MDSCs in tumors, blood and spleens were 1.5 ± 0.9%, 30.1 ± 1.3%, and 3.4 ± 1.1%, respectively and the levels in the lungs and lymph nodes were negligible. In untreated mice, MDSC levels stay the same or only mildly increases over time (Figure 2.4). In irradiated mice, within two days after irradiation, MDSCs in the peripheral blood doubled to 69.0 ± 6.8% (Figure 2.4c), while MDSCs stayed relatively stable in spleens, lymph nodes and lungs (Figure 2.4d-2.4f). In the irradiated tumor, there was a sustained low level of tumoral MDSCs throughout and beyond the duration of irradiation while they increased nearly 4 fold (1.5 ± 0.9% to 6.5 ± 1.9%) in non-irradiated tumors. On day 12, 2 days after cessation of tumor irradiation, MDSC levels reached their nadir in the tumors, but had begun to rise in the other organs. By day 15, a dramatic increase in the MDSC population was observed in the tumor, spleen, and lymph node, with levels reaching a peak of ~15% in all 3 sites (Figure 2.4a, d, f) before falling on day 17. In the blood and lung, the trend of MDSC elevation continued from day 15 on, reaching a remarkable level of 80.0 ± 5.3% and 30.7 ± 14.6%, respectively, on day 17. Collectively, these

data suggest that local tumor irradiation induces the expansion of MDSCs and their subsequent influx into different organs in a time-dependent manner.

Irradiation induces macrophage migration and expression of protumorigenic genes. We next used an *in vitro* culture system to aid in dissecting the complex cross-signaling between different cellular components in the tumor microenvironment after irradiation. We first examined the effects of conditioned media from irradiated tumor cells on the migration ability of macrophages. RAW264.7 murine macrophages were analyzed in a transwell migration assay with conditioned media from irradiated or non-irradiated murine PCa cells (RM-1 and Myc-CaP) as the migration stimulus. Conditioned media from irradiated tumor cells induced a nearly two-fold greater number of RAW264.7 cells to migrate across the transwell filter compared to non-irradiated controls (Figure 2.5a and data not shown for Myc-CaP).

A large volume of work points to the plasticity of tissue macrophages that are educated by tumor environmental cues to promote tumor growth (8). Hence, we interrogated whether irradiation could skew bone marrow-derived macrophages (BMDM) towards the gene expression profiles of pro-tumorigenic macrophages. Direct irradiation with 3 Gy (Figure 2.5b) and indirect effects transmitted through co-culturing BMDM with irradiated tumor-conditioned media (Figure 2.5c) both polarized BMDM towards a pro-tumorigenic phenotype, as we observed increased expression of *Arg1*, *Fizz1*, *Il-1β, Il-10*, *Mmp-9*, *Vegf-a*, *Cd206* and *Csf1*, and decreased expression of inflammatory genes such as *iNos* and *Il-12*. As a reflection of their immunosuppressive roles in tumors, protumorigenic macrophages also typically exhibit lower MHCII expression (28). By flow cytometry analysis, all (100%) of the $CD11b^{+}F4/80^{+}$ macrophages from irradiated tumors displayed low MHCII expression, while only 50% of the

macrophages in non-irradiated tumors were MHCII^{low} (Figure 2.5d). These data suggest that both direct and indirect effects of irradiation can have profound effects on macrophages by skewing them towards a protumorigenic subtype with enhanced migration ability and gene expression profile that favor tumor growth.

CSF1 expression is increased by irradiation. Next, we examined whether tumor cell irradiation can alter the expression of cytokines known to participate in myeloid cell recruitment (6, 29). The mRNA expression of CSF1, CCL2, CCL5 and SDF-1 was examined in Myc-CaP cells 24 hrs after 3Gy of irradiation. Among these cytokines examined, CSF1 showed the highest expression and the most significant increase in irradiated over untreated tumor cells (Figure 2.6a). We further evaluated secreted levels of CSF1 protein, which was elevated in conditioned media from irradiated tumor cells (Figure 2.6b). IL-34 is a recently discovered second CSF1R ligand that functions similarly to CSF1 (30). However the expression of IL-34 was 100 fold lower than CSF1 in our two PCa systems (RM-1 and Myc-CaP model, data not shown), and thus, we did not pursue IL-34 further. The ability of irradiation to augment CSF1 expression appeared to be a general phenomenon. In total, we tested 9 murine and human cancer cell lines, 8 out of 9 showed an increase in CSF1 after irradiation (Figure 2.6a, e, and Figure 2.7). Consistent with results from cell culture experiments, irradiated tumors (the same cohort as Figure 2.1a) showed a significant increase in *Csf1* gene expression compared to untreated tumors (Figure 2.6c). Importantly, an increase in CSF1 was also observed in the serum of PCa patients after radiotherapy (Figure 2.6d), supporting the clinical relevance of CSF1 increase seen in our murine models.

To explore the issue of crosstalk between tumor cells and macrophages on the CSF1 axis, we co-cultured RAW264.7 macrophages or bone marrow derived macrophages (BMDM) with RM-1 tumor cells and observed an increase in the magnitude of CSF1 expression above that in either cell grown alone, especially in the irradiation setting (Figure 2.6e and f). Furthermore, the addition of a highly selective CSF1R kinase inhibitor GW2850 (31) resulted in a complete negation of increased macrophage migration towards irradiated tumor-conditioned media (Figure 2.6g). Collectively, these data demonstrate that irradiation increases CSF1 expression in tumors, which is amplified by tumor-macrophage interactions. The heightened CSF1 production induced by irradiation in turn drives macrophage migration and recruitment into irradiated tumors.

Irradiation enhances CSF1 production through an ABL1-dependent mechanism. Given our findings shown above that irradiation boosts tumoral CSF1 expression, we sought to interrogate a signal transduction pathway implicated in irradiation-induced transcriptional regulation of CSF1. ABL1, a non-receptor tyrosine kinase, is known for mediating apoptosis and cycle arrest after irradiation (32). It has been reported that ABL1 can also be recruited to the promoter region of CSF1 and regulates *Csf1* gene expression in concert with AP-1 (33). Thus, we examined in detail the kinetics of irradiation-induced CSF1 expression and ABL1 activation in our system. First, detailed analysis of irradiation-induced gene expression of *Csf1* in Myc-CaP cells showed the increase in CSF1 RNA initiated at 4 hrs post irradiation (Figure 2.8a). Next we profiled the activation of ABL1 protein in response to irradiation. We observed that two ABL1 cleavage products, 75 kDa and 60 kDa product, emerged 2hr post irradiation (Figure 2.8b). Further examination of the subcellular localization of ABL1 by confocal microscopy revealed that prior to the radiation insult, ABL1 was predominantly located in the cytoplasm with very

little ABL1 immunocytochemical signal registered in the nucleus (Figure 2.8c, left). As early as 1 hr after irradiation a noticeable portion but not all of the ABL1 protein has translocated to the nucleus (Figure 2.8c, middle), and this is maintained at 4 hrs (Figure 2.8c, right). To further substantiate the functional impact of ABL1 on the *Csf1* gene expression, we analyzed the binding of ABL1 to the CSF1 promoter by a chromatin immunoprecipitation assay (ChIP). An increase in ABL1 binding to the CSF1 promoter was observed as early as 1 hr after irradiation and peaked at 2 hrs before slowly declining (Figure 2.8d). When looking into the kinetics of RNA polymerase II binding to the CSF1 promoter, it first showed a significant decrease at 1hr and an increase starting 2 hrs post irradiation (Figure 2.8e). This bell shape kinetics of RNA polymerase activity could be attributed to the radiation-induced DNA damage causing an initial inhibition on transcription (34). The timing of ABL1 nuclear translocation, its binding to the CSF1 promoter, and the binding of RNA polymerase II to the CSF1 promoter preceded the changes in CSF1 mRNA level. These findings support the involvement of ABL1 in the regulation of CSF1 expression in response to irradiation.

Next, we used an ABL1-targeted siRNA and small molecular inhibitor to further confirm its regulatory role on CSF1 in our system. The irradiation induced CSF1 expression in MycCaP cells was significantly inhibited by the addition of the ABL1 kinase inhibitor, STI-571 (5 μM, Figure 2.8f). A similar result was also observed in the human PCa cell line CWR22Rv1 (Figure 2.9a). Using a migration assay, we found that STI-571-treated conditioned media displayed decreased ability to promote macrophage migration (Figure 2.8g). Furthermore, the addition of GW2580 to macrophages (top chamber) did not further retard macrophage migration over STI treatment of tumor cells (Figure 2.8g), suggesting STI-571 and GW2580 may be targeting the same pathway to regulate migration. Like most of the pharmacologic protein kinase inhibitors,

STI-571 is not completely specific. STI-571 also inhibits c-Kit, platelet-derived growth factor receptor (PDGFR) and CSF1R (35). Thus, we employed siRNA-mediated knockdown of ABL1 to examine its effect on CSF1. Due to the low efficiency of transfecting murine PCa cells, we used the human CWR22Rv1 cell line for this experiment. The ABL1 siRNA was able to decrease ABL1 mRNA expression to 30% of the normal level in the CWR22Rv1 cells (Figure 2.8h, right panel). As expected, ABL1 siRNA effectively blocked the CSF1 mRNA induction by irradiation (Figure 2.8h, left panel). These data suggest that upon irradiation, ABL1 is activated, translocates to the nucleus, binds to the promoter region of CSF1 and promotes its expression.

Blockade of CSF1/CSF1R signaling retards tumor regrowth after local irradiation. CSF1 is a potent cytokine well-known to promote myeloid cell proliferation, differentiation and migration. In a recent study, we demonstrated that blockade of CSF1/CSF1R signaling can effectively inhibit TIM function and recruitment to tumors (15). Thus, in this study we investigated whether blocking CSF1R can also reduce TIMs recruitment and diminish their pro-tumorigenic influences in the RT setting. The combined irradiation and CSF1R blockade treatment was first tested with the selective CSF1R inhibitor, GW2580. Significant reductions in TIM populations in RM-1 tumors were observed with GW2580 treatment (160 mg/kg/day), which augmented the efficacy of irradiation by achieving more effective suppression of tumor growth than irradiation alone (Figure 2.8a-e, and data not shown). To further substantiate this rational combination strategy, we employed a recently described small molecule, CSF1R kinase inhibitor PLX3397. This inhibitor was shown to be a highly potent inhibitor of CSF1R (cFMS) with IC_{50} of 20 nM and it is under active clinical investigation for several types of cancers (19). Here, RM-1 prostate tumor bearing mice were treated with control (chow), local irradiation (3Gy

x 5 days), PLX3397 (drug chow) or the combination. As shown in Figure 2.10a, PLX3397 alone has little effect on tumor growth compared with the control group. Irradiation reduced tumor size by 43% at day 10, 1 day after cessation of irradiation ($p<0.001$). The irradiated tumor sizes were stabilized for a short duration, and subsequently resumed an aggressive tumor growth rate, whereas the combined irradiation and PLX3397 treated group maintained a much slower growth rate (Figure 2.10a). Both flow cytometry and histological analyses of tumors revealed a significant reduction of $CD11b^{+}Gr\text{-}1^{+}$ MDSCs and $CD11b^{+}F4/80^{+}$ macrophages in tumors, as well as in spleens of both PLX3397-treated groups, with more pronounced effects observed in the combination treatment (Figure 2.10b-e, and g). Interestingly, both subsets of MDSCs, monocytic and polymorphonuclear, were reduced by PLX3397 (Figure 2.10f), a result that differed from our previous findings with GW2580 treatment in 3LL tumors where only the monocytic subtype of MDSCs was inhibited (15). At the molecular level, CSF1R blockade significantly reduced RT-induced CSF1, MMP-9 and Arg1 (Figure 2.10h-j). The latter 2 genes are known to be involved in cancer progression and metastasis by promoting tissue remodeling, angiogenesis, and immunosuppression (15). Similar reductions in the expression of CSF1 and Arg1 were also observed in irradiated tumors treated with GW2580, along with a significant reduction in the macrophage chemotactic factor, CCL2 (Figure 2.11d-e). In summary, we observed that prostate tumor-directed irradiation can potently induce the influx of TIMs, which in turn can thwart treatment efficacy. The addition of potent CSF1R inhibitors such as PLX3397 and GW2580 can prevent the influx of TIMs and halt their pro-tumorigenic functions leading to more effective and durable tumor growth control.

Discussion

In the present study, we demonstrate that the recruitment of TIMs to prostate tumors is highly induced by local irradiation in several immunocompetent mouse models. We find elevated expression of CSF1, an important cytokine for macrophage survival, migration and differentiation, in tumor cells after irradiation, which was also observed in the serum of post-radiotherapy PCa patients. Increased CSF1 expression was mediated, at least partially, by the ABL1 tyrosine kinase. Upon irradiation, ABL1 was activated and translocated to the nucleus, where it bound to the promoter region of CSF1 to up-regulate its expression. We further showed that blockade of CSF1R with selective small molecule kinase inhibitors, such as GW2580and PLX3397, greatly inhibit TIMs infiltration and significantly delay tumor re-growth after irradiation. These results suggest that disrupting the pro-tumorigenic contributions of host innate immune cells, namely MDSCs and macrophages, through blockade of the CSF1/CSF1R axis can be a promising approach for developing rational and more effective combination cancer therapies. A schema of irradiation induced expression of CSF1 and recruitment of TIMs and the impact of CSF1R inhibition on TIMs' modulation of tumor regrowth is shown in Figure 2.12.

The use of immunocompetent murine prostate tumor models in this study allowed us to directly assess the contributions of host immune cells, in particular the distinct myeloid subpopulations, to tumor progression after therapy. Our results demonstrated that the major impact of CSF1R blockade is directed at the tumor microenvironment, namely TIMs. Interestingly, CSF1R has been shown to be expressed and can contribute to the oncogenesis of several types of cancer, including PCa (36, 37). Hence, the blockade of the CSF1/CSF1R axis could potentially have a direct suppressive impact on tumor cells, albeit unlikely as the the RM-1 and Myc-CaP tumors used here express negligible levels of CSF1R based on sensitive RT-PCR

analyses (data not shown). We also believe IL-34, a newly identified ligand for CSF1R having similar functions in stimulating macrophage proliferation and migration (30, 38), is unlikely to play a significant role as its expression level is 100-fold lower than CSF1 in our models (data not shown). Recent findings from Dr. Hong Wu's group using the PTEN-knockout transgenic prostatic carcinoma model revealed that intratumoral MDSCs expansion contributes to tumor progression and that CSF1R blockade was an effective means to suppress the infiltration and function of MDSCs in this spontaneous murine PCa model (data not shown).

It is promising that our initial exploratory study on 10 consecutive PCa patients, who recently underwent RT, also yielded data supportive of CSF1 axis being involved. Although our data suggests that serum CSF1 could potentially be a biomarker of TIMs recruitment, there are several considerations that caution against this premature conclusion. First, a wide range of serum CSF1 level was detected in patients (Figure 2.6d). This issue could likely be attributed to the different infection or inflammation status of the patients. Second, the timing of patient specimen procurement after RT was not uniform between patients in the small cohort tested. We did observe an increase in a MDSC population ($CD11b^{+}CD15^{+}$) in the peripheral blood of a few patients whose serum CSF1 increased from pre- to post-RT (data not shown). Due to the heterogeneity issues, data from a much larger cohort of patients will be needed to fully validate the concept put forth here. We are actively pursuing these studies with more and standardized time points of peripheral blood collection in PCa patients undergoing RT.

Our findings are consistent with CSF1 being an important stimulus for the influx of TIMs to tumors especially in response to irradiation. However, our study does not exclude other pathways that may also be involved in this complex inflammatory cascade. For instance, several recent papers highlighted the role of the SDF-1/CXCR4 axis in local irradiation-induced influx

of TIMs to tumors (5, 6). The authors demonstrated that irradiation-induced hypoxia though destruction of endothelial cells and the microvasculature, and the resultant increased expression of HIF-1α in turn induced the expression of CXCR4 and SDF-1, which then mediated the recruitment of TIMs to tumors. Likewise, CCL2 has also been implicated in the recruitment of bone marrow-derived myeloid cells into tumors and this axis can also modulate PCa growth and metastasis to bone (39, 40). However, we observed negligible SDF-1 and CCL2 expression with or without irradiation in our tumor cells (Figure 2.6a). The migration/recruitment of TIMs is a complex process that is likely regulated by several pathways, especially in the context of different tumor types, host genetic background and stimulus induced by different therapeutic settings or progression status. Of interest, we consistently observed a decrease in CCL2 level with GW2580 or PLX3397 treatment (data not shown and data Figure 2.8f). This finding is also in accordance with a recent study which showed the removal of CSF1 significantly decreases CCL2 (41). An intriguing possibility could be that CSF1 is an upstream regulator of other cytokines like CCL2. Clearly the influence of CSF1/CSF1R axis and its cross-talk with other cytokine/chemokine pathways in the recruitment of TIMs deserves further investigation.

A unique aspect of this study is the finding that the ABL1 pathway mediates the heightened CSF1 transcription induced by irradiation. Several factors have been implicated in the regulation of CSF1 gene expression, including PDGF (42), ABL1 (33), INF-γ (43) and AP-1, CTF/NF-1, SP1, SP3 (44) and nuclear actin (45) in different cell types and contexts. Among these, ABL1 is known to respond to irradiation or DNA damage via DNA-PK, ATM and p53 pathway (46-48). ABL1 contains a catalytic domain as well as a nuclear export sequence (NES) and three nuclear localization signal (NLS) motifs. Several groups reported that ABL1 localizes to both nucleus and cytoplasm and can shuttle between these two compartments (49). In our

study, we observed that a portion of cytoplasmic ABL1 is activated and translocated to the nucleus as early as 1hr after irradiation (Figure 2.8b). The ABL1 DNA-binding domain is critical for its biological function (50), yet no classical DNA-binding motifs have been identified so far. The few ABL1 transcriptional targets identified include p21 and CSF1 (33, 51). Here we demonstrated that ABL1 binds to the promoter region of CSF1 and activates CSF1 gene transcription. A previous study suggested that ABL1 forms a complex with AP-1, a transcription factor composed of c-jun and c-fos, in the regulation of CSF1 (33). Based on this finding, a potential feedback loop in CSF1R-dependent cells is that the blockade of CSF1R signaling inhibits c-fos, which further downregulates CSF1 expression. This mechanism might explain why we observed a decrease in CSF1 expression in tumors after PLX3397 treatment (Figure 2.10h).

In summary, the data presented in this study demonstrate that irradiation induces CSF1 through an ABL1-dependent mechanism in PCa. The heightened CSF1 serves a critical role in the systemic recruitment of pro-tumorigenic myeloid cells to irradiated tumors. Hence, the blockade of TIMs in combination with local irradiation of prostate tumors displays an augmented and more durable response than irradiation alone in preclinical models. We believe that co-targeting the CSF1/CSF1R pathway with local irradiation of prostate tumors will be a promising strategy for clinical translation.

Figures

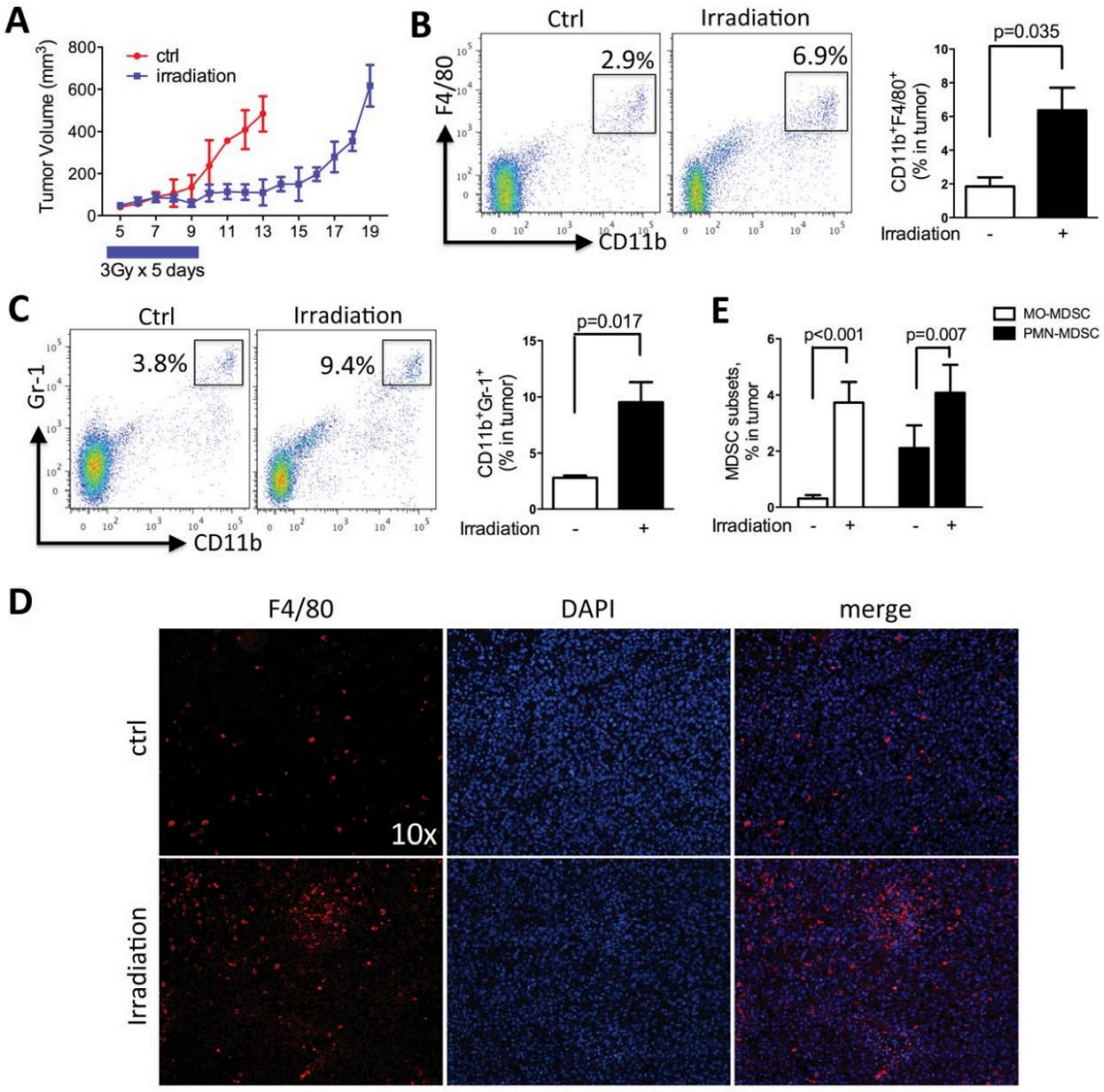

Figure 2.1: Local irradiation enhances myeloid infiltration into tumors. Subcutaneous RM-1 tumors were collected, processed to single cell suspension and assayed by flow cytometry and immunohistochemistry for $CD11b^{+}Gr\text{-}1^{+}$ MDSCs and $CD11b^{+}F4/80^{+}$ TAMs. A) Growth curve of RM-1 tumors with or without irradiation. B) Flow cytometry plots and quantification of TAMs

in tumor. C) Flow cytometry plots and quantification for MDSCs in tumor. D) Representative F4/80 staining of RM-1 tumors from control and irradiation-treated mice. E) Effect of irradiation on the two subsets of MDSCs: MO-MDSC and PMN-MDSC. n=4 for each group.

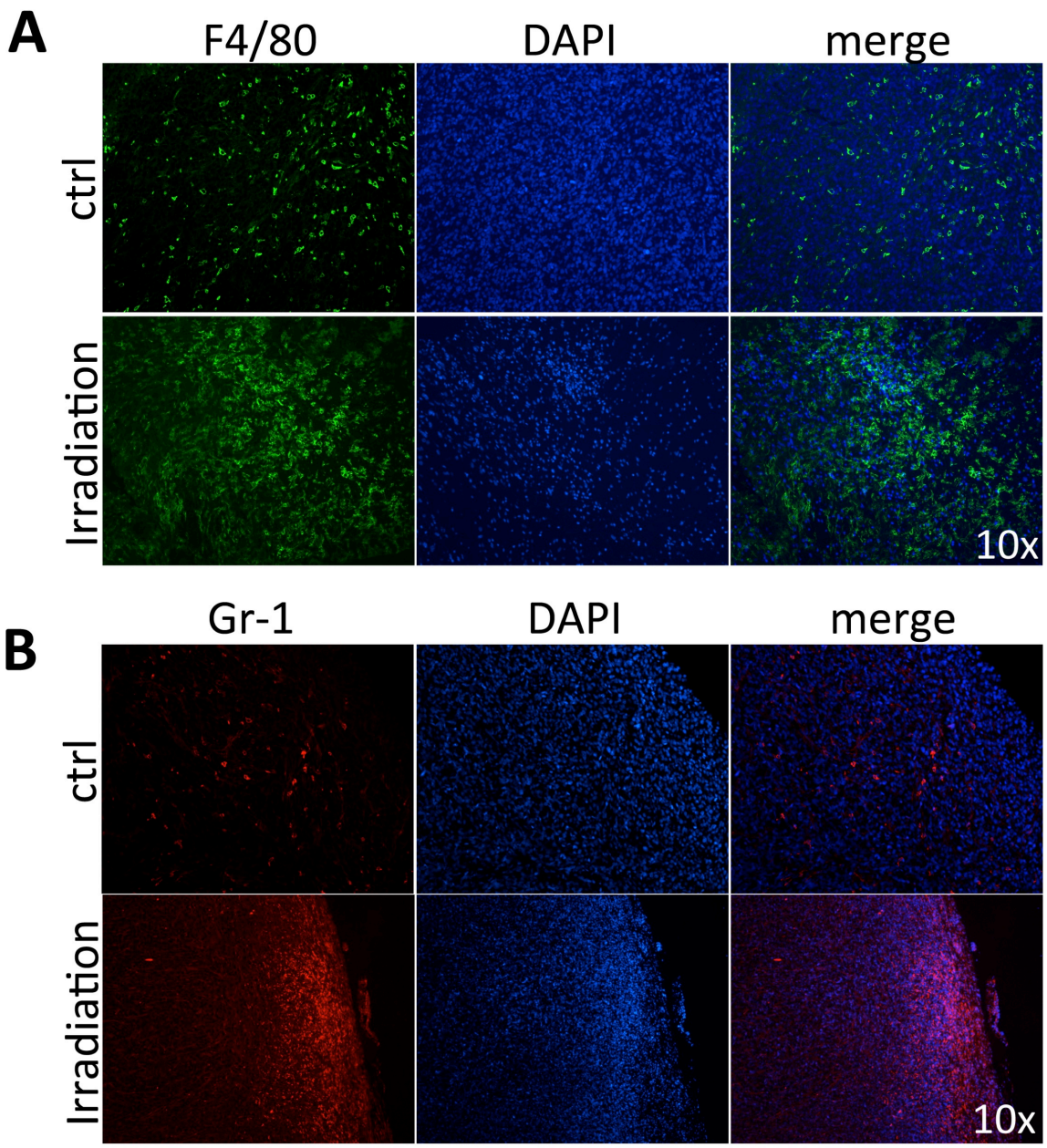

Figure 2.2: Local irradiation enhances recruitment of TAMs and MDSCs to tumors in RM-9 model. Subcutaneous RM-9 tumors were irradiated with 3Gy for 5 days after tumors reach 4 mm in diameter. Tumors were measured by caliper daily. Control mice and treated mice were sacrificed at day 13 when control tumors reached 1.5 cm in diameter. Tumors were collected, processed to single cell suspension and assayed by flow cytometry for $CD11b^{+}Gr\text{-}1^{+}$ MDSCs and

$CD11b^{+}F4/80^{+}$ TAMs. A) Immunohistochemistry staining for F4/80. B) Immunohistochemistry staining for Gr-1.

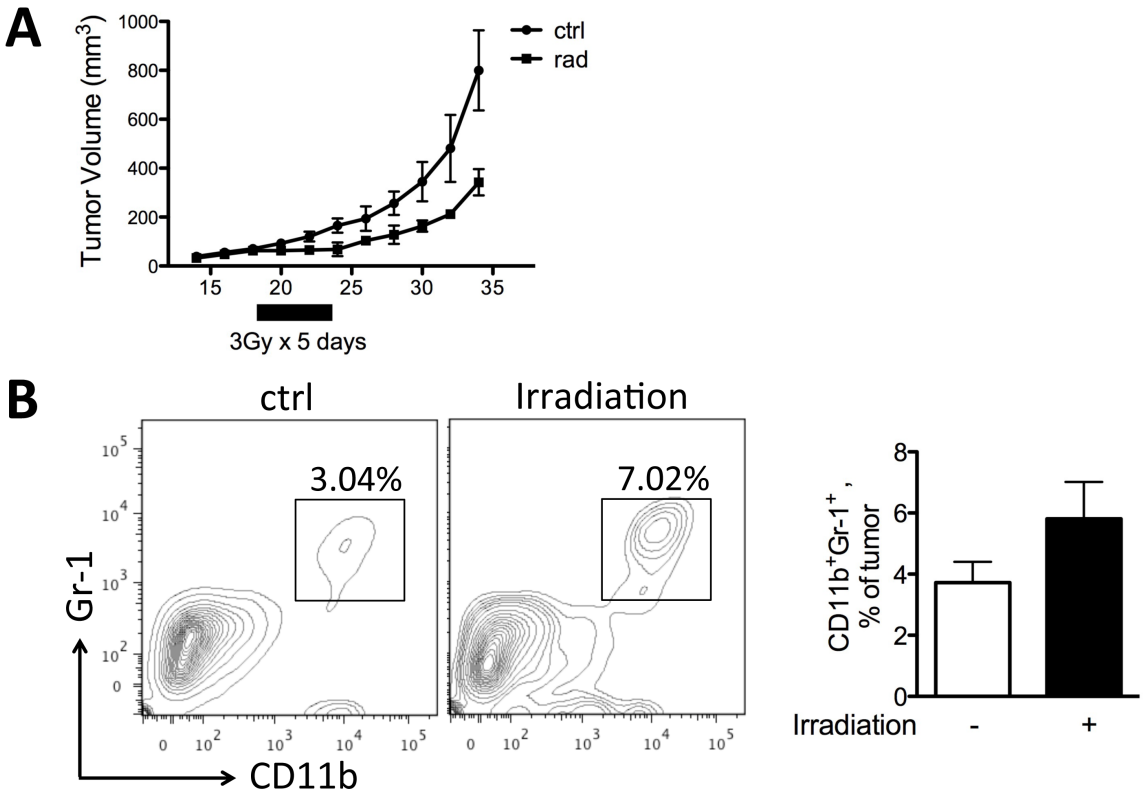

Figure 2.3: Local irradiation enhances recruitment of TAMs to tumors in Myc-CaP model. A) Growth curve of Myc-CaP tumors with 3Gy for 5 days after tumors reach 4 mm in diameter by day 14. Tumors were measured by caliper every other day. Mice were sacrificed at day 34 when control tumors reached 1.5 cm in diameter. Tumors were collected, processed to single cell suspension and assayed by flow cytometry for $CD11b^{+}F4/80^{+}$ TAMs. A) Growth curve of Myc-CaP tumors with or without irradiation. B) Flow cytometry plots and quantification for TAMs in the tumors.

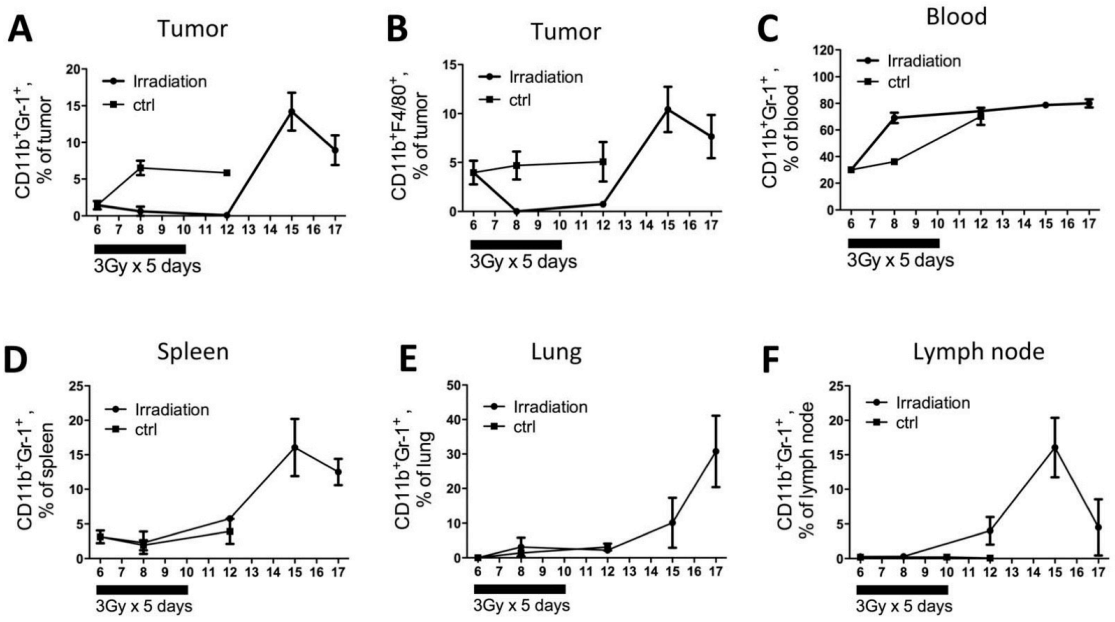

Figure 2.4: Local irradiation enhances systemic myeloid cell expansion. Control mice were sacrificed on day 6, 8 and 12. Irradiated mice were sacrificed on day 6, 8, 12, 15 and 17. Tumors, blood, spleens, lungs and lymph nodes were collected for flow cytometry analysis for MDSC and TAM population. (n = 4 for each time point).

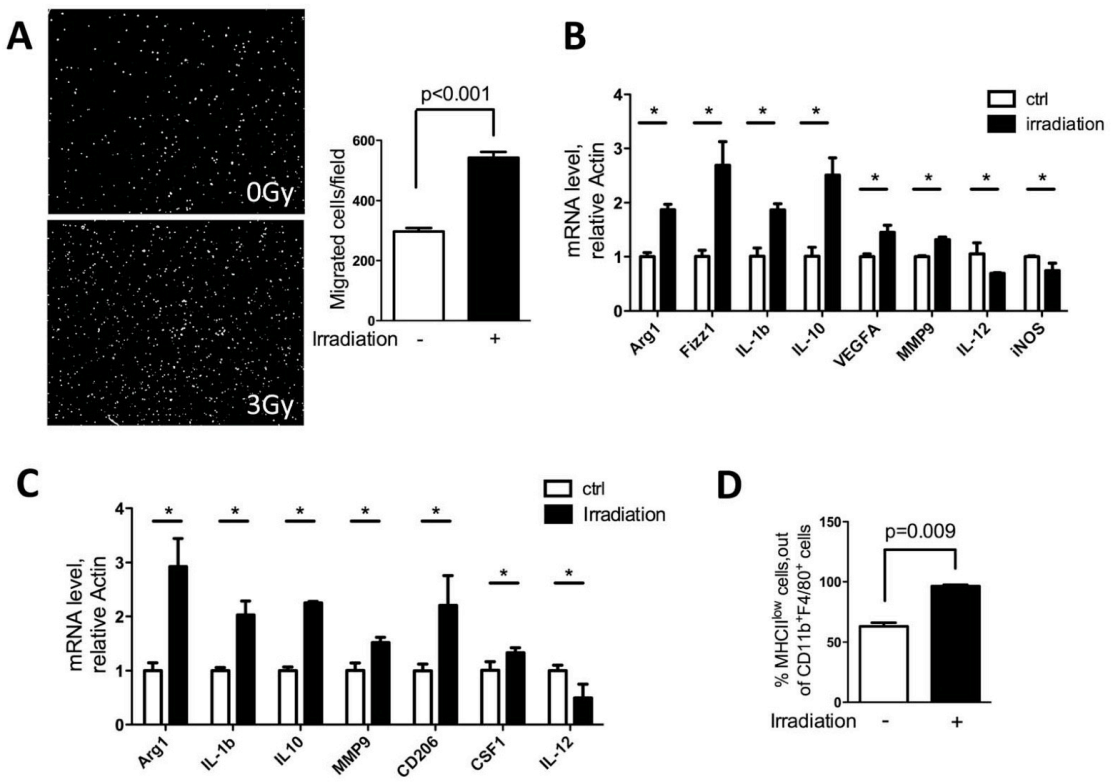

Figure 2.5: Irradiation increases cell migration and induces protumorigenic genes in macrophages. A) RAW264.7 macrophages were seeded in 8 μm transwell inserts, and tumor conditioned media (collected 48 hrs after 3Gy irradiation) was placed in the bottom. Cells were allowed to migrate toward bottom for 6 hrs. Then cells were fixed and stained with DAPI. Representative images of migrated cells are shown and they were quantified using ImageJ software (n = 3). B) Effect of irradiation on bone marrow derived macrophages (BMDM). Bone marrows were collected and induced to macrophages by CSF1 (10 ng/ml) for 6 days. Cells were counted, seeded and subjected to 3Gy irradiation. Cells were collected 24 hrs later, and RT-PCR was performed to detect RNA for the protumorigenic and inflammatory genes noted. C) BMDMs as prepared above were cultured in 50% tumor conditioned media + 50% complete DMEM for

24 hrs. Cells were collected and assayed by RT-PCR for the genetic markers noted. D) Tumors collected as shown in Figure 2.1a were analyzed by flow cytometry for MHCII expression on $CD11b^{+}F480^{+}$ macrophages. An increase in MHCII low-expressing macrophage population was observed. (*indicates significant changes with $P < 0.05$).

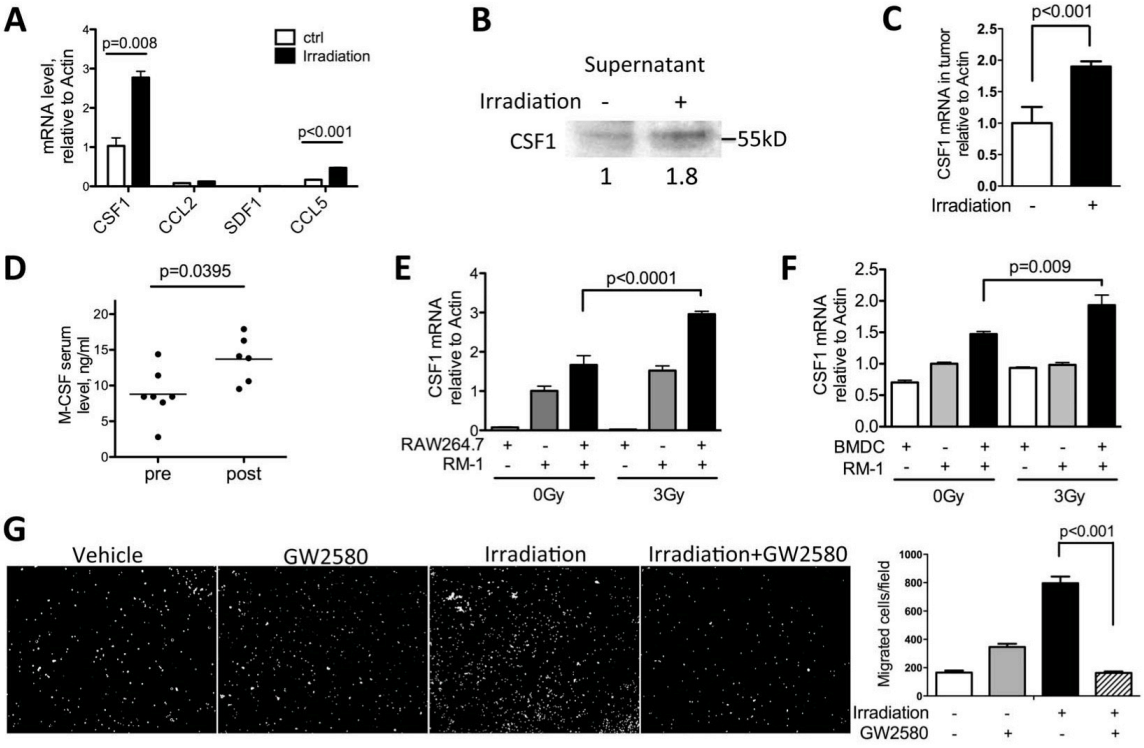

Figure 2.6: CSF1 expression is increased by irradiation. A) MycCaP cells were plated overnight and irradiated with 3Gy. Cells were collected 24 hrs after, and assayed by RT-PCR for factors known to recruit myeloid cells: CSF1, CCL2, SDF1 and CCL5. CSF1 is shown to have the highest expression and most significant increase. B) Conditioned media from Myc-CaP cells 48 hrs after irradiation were collected, concentrated by centrifugation, normalized and analyzed by SDS-PAGE. Secreted CSF1 was detected at 50 kDa. Relative expression level quantified by ImageJ was shown below the blot. C) Tumors collected as shown in Figure 2.1a were assayed by RT-PCR for CSF1 mRNA expression. D) Serum samples from PCa patients pre- and post-radiotherapy were analyzed by ELISA for CSF1. E) RM-1 cells and macrophage cell line RAW264.7 were co-cultured overnight and irradiated with 3Gy. Cells were collected 24 hrs and analyzed by RT-PCR for CSF1 mRNA. F) RM-1 cells and BMDM were co-cultured for 4 hrs

and irradiated with 3Gy. Cells were collected 24 hrs and analyzed by RT-PCR for CSF1 mRNA. G) RAW264.7 macrophage migration assay was performed by using conditioned media in lower chamber, collected as in panel B. GW2580 (1 μM) was added to the top chamber. Quantification of 9 fields was summarized in panel F. Representative images of migrated cells were shown in G.

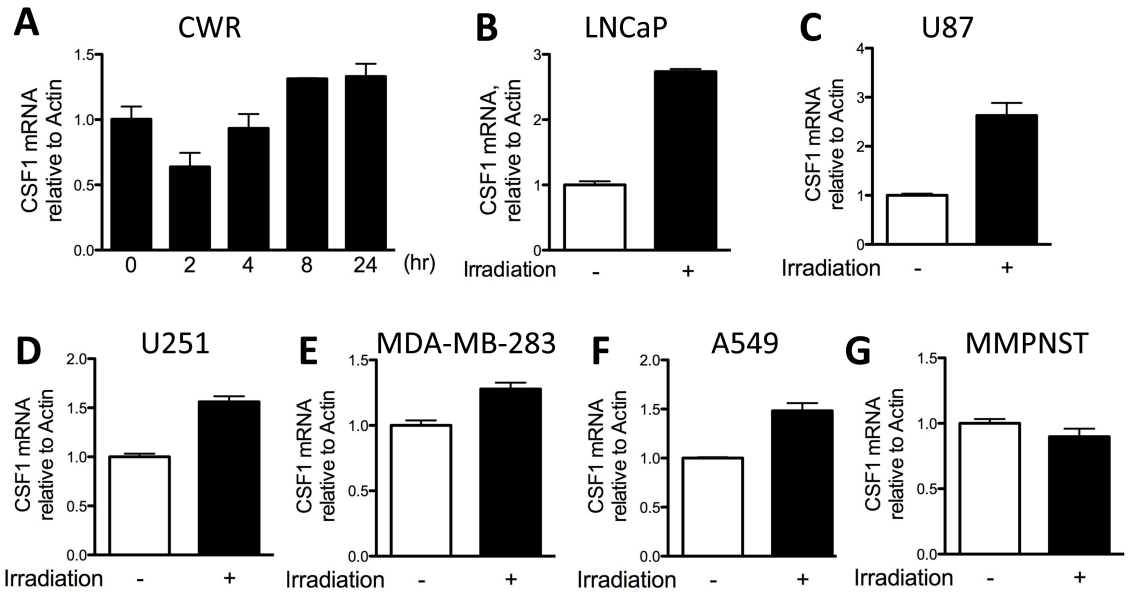

Figure 2.7: Irradiation increases CSF1 expression in other human and murine cancer cell lines. A) CSF1 expression from CWR cells collected 2, 4, 8, and 24 hrs after radiation. B-H) Cells were seeded in 6-well overnight, and collected 24 hrs after irradiation (3Gy). CSF1 expression was analyzed by RT-PCR.

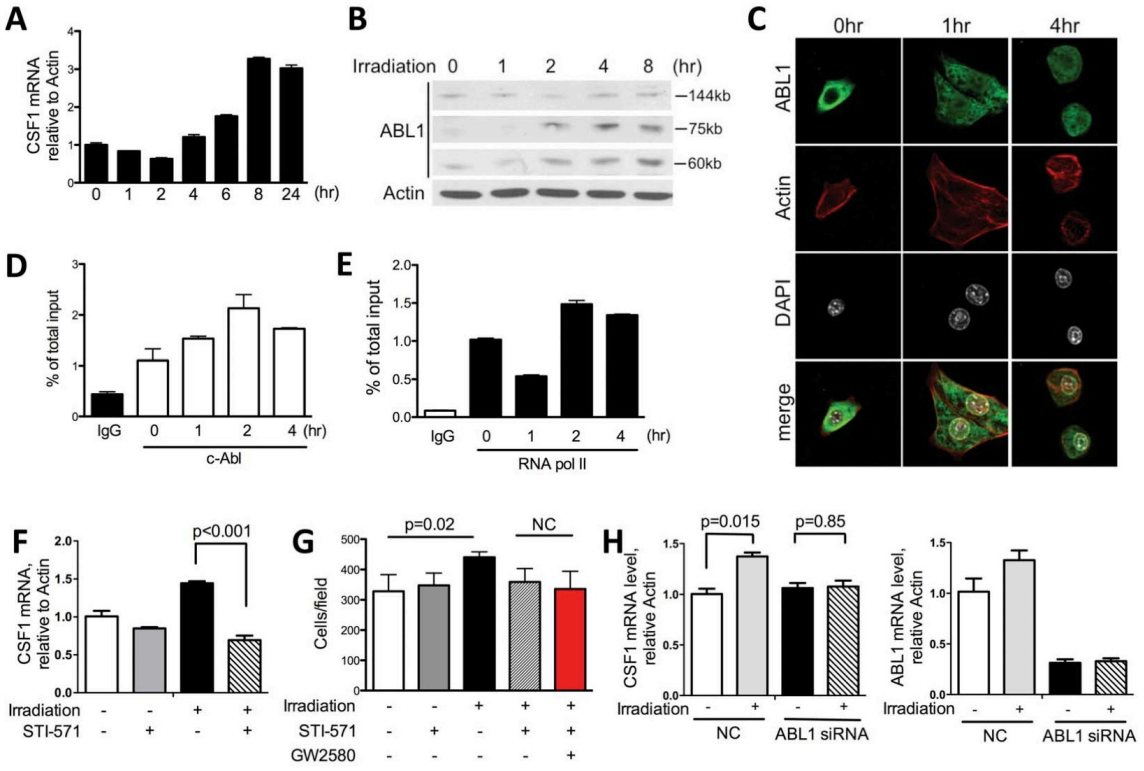

Figure 2.8: Irradiation induces CSF1 production through an ABL1-dependent mechanism. A) CSF1 mRNA expression in Myc-CaP cells 0, 1, 2, 4, 6, 8, and 24 hrs after irradiation (3Gy). B) ABL1 is cleaved by irradiation *in vitro*. $4x10^5$ Myc-CaP cells were plated in 6-well plate overnight and irradiated with 3Gy the next day. Cells were collected at 1, 2, 4, and 8 hrs after irradiation. Cells lysates were normalized and assayed by SDS-PAGE. Western blot was probed with ABL1 (K-12) antibody for both full length and cleaved ABL1. Two cleavage products, 60 kDa and 75 kDa, were detected. C) Confocal images of Myc-CaP cells at 1 and 4 hrs after irradiation. Green: ABL1; red: actin; white: nucleus (DAPI). D-E) Myc-CaP cells 0, 1, 2, 4 hrs after irradiation were fixed in 3% PFA and processed for ChIP assay using c-Abl antibody (D) and RNA polymerase II antibody (E) as described in Material and Methods section. Rabbit IgG was used as negative control. F) Myc-CaP cells were irradiated with 3Gy and STI-571 (5 μM)

was added right after. Cells were collected 24 hrs later and analyzed by RT-PCR for CSF1 mRNA expression. G) Migration assay using conditioned media collected as in panel F. GW2580 was added to the top chamber to examine the additive effects between STI-571 and GW2580. H) CSF1-mRNA in human PCa cells after ABL1 directed RNAi. CWR22Rv1 cells were transfected with ABL1 siRNA and negative control (NC: non-specific siRNA). Cells were irradiated 30 hrs after siRNA treatment and collected 24 hrs after irradiation. Expression level of ABL1 was reduced to 30% of control after specific siRNA treatment (right panel). CSF1 mRNA was analyzed by RT-PCR with and without irradiation.

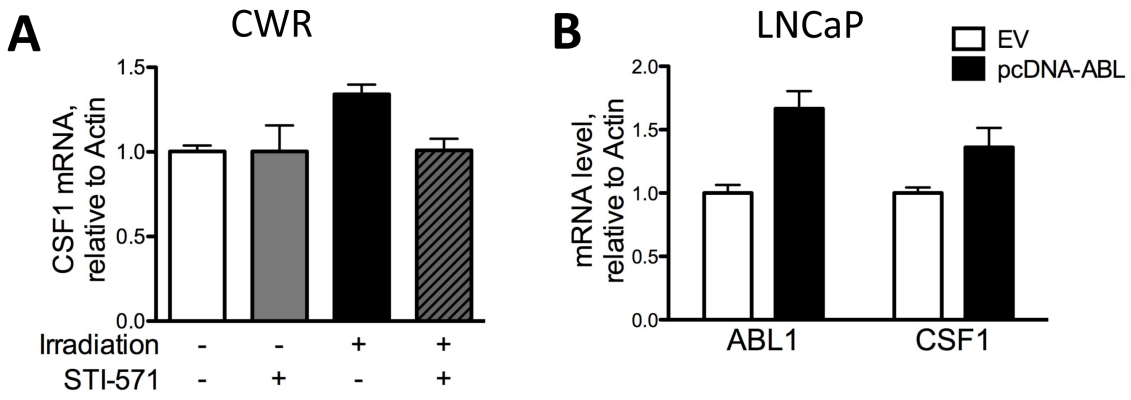

Figure 2.9: ABL1 mediates CSF1 expression in other human PCa cell lines. A) Human PCa cells CWR were treated with irradiation and STI-571 (5 μM) as indicated. Cells were collected 24 hrs after and analyzed by RT-PCR for CSF1 expression. B) Human PCa LNCaP cells was transfected with empty vector control (EV, pcDNA) or pcDNA-Abl (wild-type), and cells were collected 24 hrs after transfection for RT-PCR analysis.

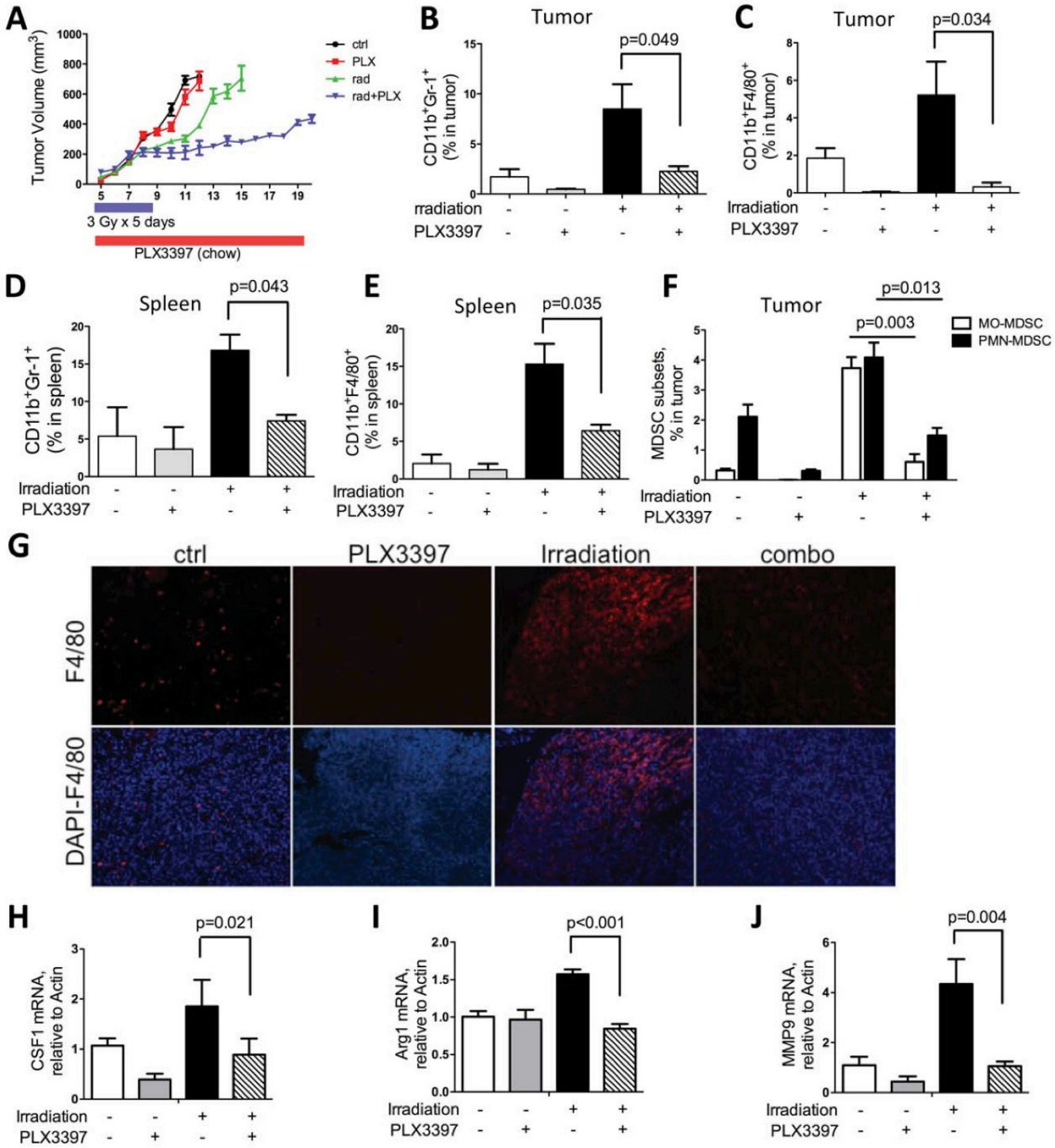

Figure 2.10: CSF1/CSF1R blockade inhibits tumor growth after irradiation. A) Growth curve of subcutaneous RM-1 tumors treated with RT (3Gy x 5 days), PLX3397 (in food chow) or combination as indicated. Tumors were measured daily by caliper. B-C) Flow cytometry analysis of $CD11b^{+}F4/80^{+}$ macrophages and $CD11b^{+}Gr\text{-}1^{+}$ MDSCs in tumor, collected at end points (tumor n = 6/cohort). D-E) Flow cytometry analysis of $CD11b^{+}F4/80^{+}$ macrophages and

$CD11b^{+}Gr\text{-}1^{+}$ MDSCs in spleen, at the same termination time as above. F) Flow cytometry analysis for MDSC subsets, MO-MDSC and PMN-MDSC with single or combination treatment. G) Representative immunohistochemsitry staining for F4/80 on tumor sections with single or combination treatment. H-J) RT-PCR analysis of mRNA extracted from tumors for CSF1, MMP-9 and Arg1.

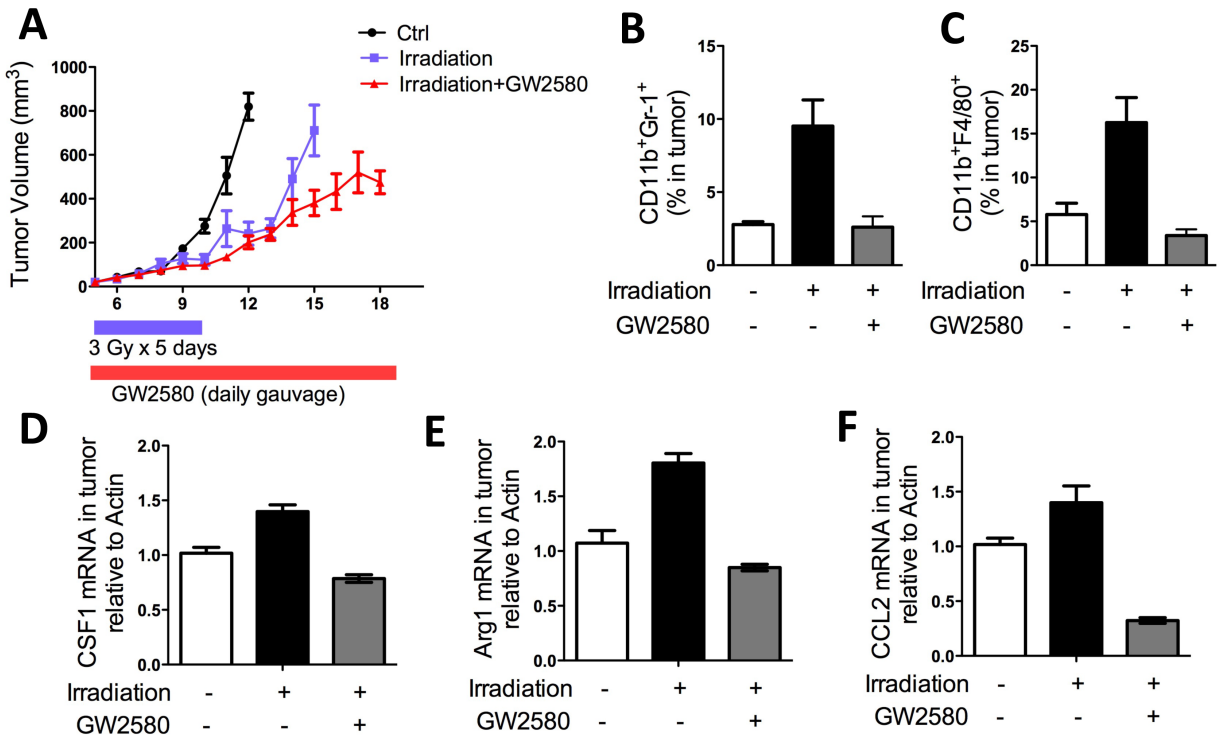

Figure 2.11: CSF1/CSF1R blockade by GW2580 inhibits tumor growth after irradiation. A) Growth curve of subcutaneous RM-1 tumors treated with irradiation (3Gy x 5 days) or GW2580 (160 mg/kg) in combined with irradiation. Tumors were measured daily by caliper. B-C) Flow cytometry analysis of TAMs and MDSCs in tumor. D-F) mRNA expression of CSF1, Arg1 and CCL2 in tumor collected at end point and assayed by RT-PCR.

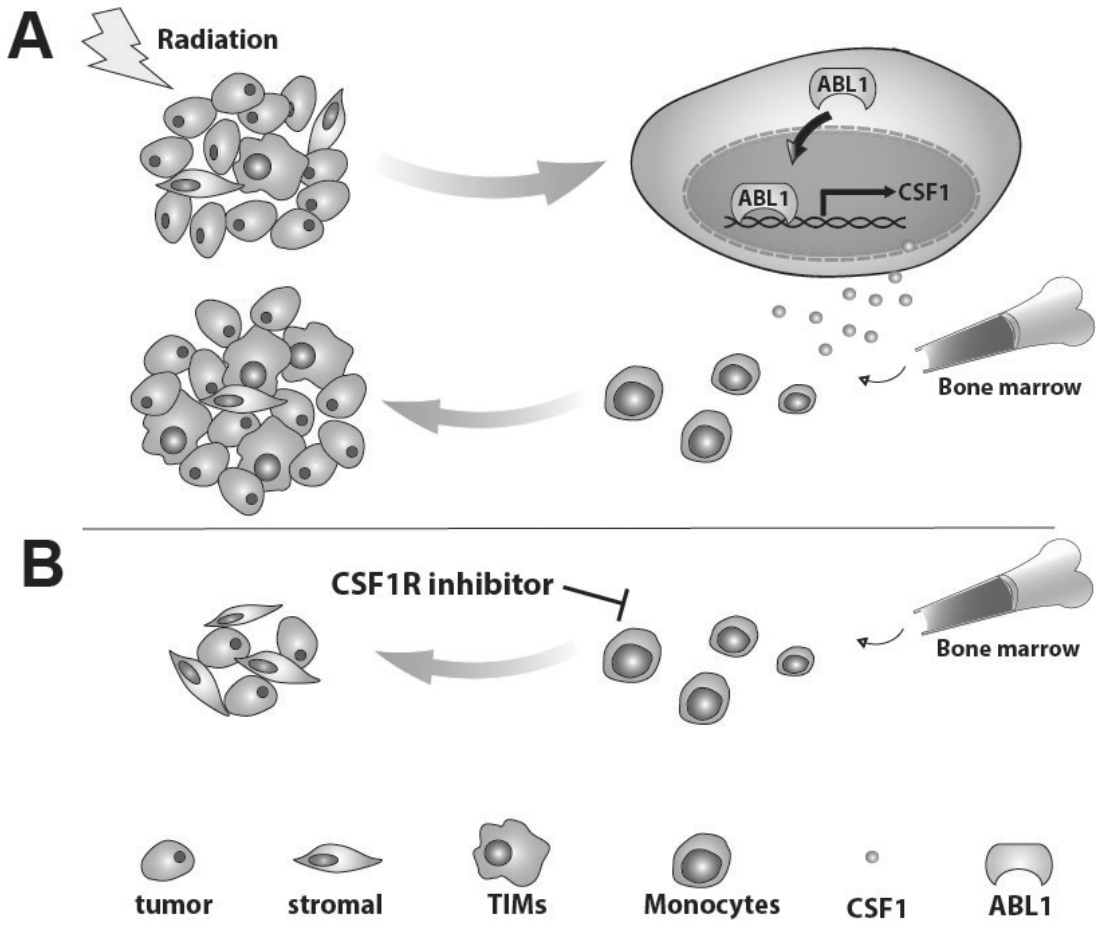

Figure 2.12: Model of CSF1 expression induced by irradiation, promoting TIMs recruitment and tumor regrowth. A) Tumor irradiation activates ABL1, which translocates to the nucleus, binding to the promoter region of CSF1 and up-regulates its gene expression. Additional TIMs are recruited to tumor sites due to the increase in CSF1 and they can thus promote tumor growth. B) When tumor-bearing mice were treated with a small molecule CSF1R kinase inhibitor, CSF1/CSF1R signaling is inhibited resulting in decreased infiltration of TIMs, reducing their tumor growth promoting influences.

	Forward primer	Reverse primer
mActin	TCAAGATCATTGCTCCTCCTGAGC	TACTCCTGCTTGCTGATCCACATC
mArg1	ACCTGGCCTTTGTTGATGTCCCTA	AGAGATGATGCTTCCAACTGCCAGACT
mCCL2	GGGCCTGCTGTTCACAGTT	GGGATCATCTTGCTGGTGAA
mCCL5	TACACCAGCAGCAAGTGCTCCAAT	TTCTTCTCTGGGTTGGCACACACT
mCD206	GGCAGGATCTTGGCAACCTAGTA	CCTTTCTTCCGACTCTTCACCC
mCSF1	GGCGCTGCCCTTCTTCGACATG	GATCAACTGCTGCAGGACCTTCAGG
mCSF1R	GTGTGAGCAATGGCAGTGTGGAAT	AGTGGGCCGGATCTTTGACATACA
mFizz	CTTGTGGCTTTGCCTGTGGATCTT	TGGTCCAGTCAACGAGTAAGCACA
mIL6	ATCCAGTTGCCTTCTTGGGACTGA	TAAGCCGACTTGTGAAGTGGT
mIL10	GGGTTGCCAAGCCTTATCGGAAAT	TCTTCAGCTTCTCACCCAGGGAAT
mIL12	GAGGAGGGGTGTAACCAGAAAGG	GCATCCTAGGATCGGACCCTG
miNOS	GAGATGGTCAGGGTCCCCT	GCTGGAAGCCACTGACACTTC
mMMP9	TGAGCTGGACAGCCAGACACTAAA	TCGCGGCAAGTCTTCAGAGTAGTT
mSDF1	CTGGCCGCGCTCTGCATCAGTG	GATGCTTGACGTTGGCTCTGGCG
mVEGFA	TGTACCTCCACCATGCCAAGT	CGCTGGTAGACGTCCATGAA

Table 2.1: RTPCR primers.

References

1. Delaney, G., et al., *The role of radiotherapy in cancer treatment: estimating optimal utilization from a review of evidence-based clinical guidelines*. Cancer, 2005. 104(6): p. 1129-37.
2. Agarwal, P.K., et al., *Treatment failure after primary and salvage therapy for prostate cancer: likelihood, patterns of care, and outcomes*. Cancer, 2008. 112(2): p. 307-14.
3. D'Amico, A.V., et al., *Pretreatment PSA velocity and risk of death from prostate cancer following external beam radiation therapy*. JAMA : the journal of the American Medical Association, 2005. 294(4): p. 440-7.
4. Bianco, F.J., Jr., et al., *Long-term oncologic results of salvage radical prostatectomy for locally recurrent prostate cancer after radiotherapy*. International journal of radiation oncology, biology, physics, 2005. 62(2): p. 448-53.
5. Kozin, S.V., et al., *Recruitment of myeloid but not endothelial precursor cells facilitates tumor regrowth after local irradiation*. Cancer Res, 2010. 70(14): p. 5679-85.
6. Kioi, M., et al., *Inhibition of vasculogenesis, but not angiogenesis, prevents the recurrence of glioblastoma after irradiation in mice*. J Clin Invest, 2010. 120(3): p. 694-705.
7. Hanahan, D. and L.M. Coussens, *Accessories to the crime: functions of cells recruited to the tumor microenvironment*. Cancer Cell, 2012. 21(3): p. 309-22.
8. Qian, B.Z. and J.W. Pollard, *Macrophage diversity enhances tumor progression and metastasis*. Cell, 2010. 141(1): p. 39-51.
9. Shojaei, F., et al., *Tumor refractoriness to anti-VEGF treatment is mediated by CD11b+Gr1+ myeloid cells*. Nat Biotechnol, 2007. 25(8): p. 911-20.

10. Muthana, M., et al., *Macrophage Delivery of an Oncolytic Virus Abolishes Tumor Regrowth and Metastasis After Chemotherapy or Irradiation*. Cancer Res, 2012.

11. Murdoch, C., et al., *The role of myeloid cells in the promotion of tumour angiogenesis*. Nat Rev Cancer, 2008. 8(8): p. 618-31.

12. Lewis, C.E. and J.W. Pollard, *Distinct role of macrophages in different tumor microenvironments*. Cancer research, 2006. 66(2): p. 605-12.

13. Ostrand-Rosenberg, S. and P. Sinha, *Myeloid-derived suppressor cells: linking inflammation and cancer*. J Immunol, 2009. 182(8): p. 4499-506.

14. Gabrilovich, D.I. and S. Nagaraj, *Myeloid-derived suppressor cells as regulators of the immune system*. Nat Rev Immunol, 2009. 9(3): p. 162-74.

15. Priceman, S.J., et al., *Targeting distinct tumor-infiltrating myeloid cells by inhibiting CSF-1 receptor: combating tumor evasion of antiangiogenic therapy*. Blood, 2010. 115(7): p. 1461-71.

16. Yang, L., et al., *Expansion of myeloid immune suppressor Gr+CD11b+ cells in tumor-bearing host directly promotes tumor angiogenesis*. Cancer Cell, 2004. 6(4): p. 409-21.

17. Hamilton, J.A., *Colony-stimulating factors in inflammation and autoimmunity*. Nat Rev Immunol, 2008. 8(7): p. 533-44.

18. Chitu, V. and E.R. Stanley, *Colony-stimulating factor-1 in immunity and inflammation*. Curr Opin Immunol, 2006. 18(1): p. 39-48.

19. DeNardo, D., et al., *Leukocyte complexity predicts breast cancer survival and functionally regulates response to chemotherapy*. Cancer Discovery, 2011. 1: p. 52-65.

20. Wang, J.Y., *Nucleo-cytoplasmic communication in apoptotic response to genotoxic and inflammatory stress*. Cell research, 2005. 15(1): p. 43-8.

21. Ren, X., et al., *c-Abl is an upstream regulator of acid sphingomyelinase in apoptosis induced by inhibition of integrins alphavbeta3 and alphavbeta5*. PloS one, 2012. 7(8): p. e42291.

22. Xu, J., et al., *c-Abl mediates endothelial apoptosis induced by inhibition of integrins alphavbeta3 and alphavbeta5 and by disruption of actin*. Blood, 2010. 115(13): p. 2709-18.

23. Ogawa, Y., et al., *Improving chemotherapeutic drug penetration in melanoma by imatinib mesylate*. Journal of dermatological science, 2008. 51(3): p. 190-9.

24. Ganguly, S.S., et al., *c-Abl and Arg are activated in human primary melanomas, promote melanoma cell invasion via distinct pathways, and drive metastatic progression*. Oncogene, 2011.

25. Srinivasan, D., J.T. Sims, and R. Plattner, *Aggressive breast cancer cells are dependent on activated Abl kinases for proliferation, anchorage-independent growth and survival*. Oncogene, 2008. 27(8): p. 1095-105.

26. Baley, P.A., et al., *Progression to androgen insensitivity in a novel in vitro mouse model for prostate cancer*. The Journal of steroid biochemistry and molecular biology, 1995. 52(5): p. 403-13.

27. Youn, J.I., et al., *Subsets of myeloid-derived suppressor cells in tumor-bearing mice*. Journal of immunology, 2008. 181(8): p. 5791-802.

28. Gordon, S., *Alternative activation of macrophages*. Nature reviews. Immunology, 2003. 3(1): p. 23-35.

29. Murdoch, C., A. Giannoudis, and C.E. Lewis, *Mechanisms regulating the recruitment of macrophages into hypoxic areas of tumors and other ischemic tissues*. Blood, 2004. 104(8): p. 2224-34.

30. Lin, H., et al., *Discovery of a cytokine and its receptor by functional screening of the extracellular proteome*. Science, 2008. 320(5877): p. 807-11.

31. Conway, J.G., et al., *Inhibition of colony-stimulating-factor-1 signaling in vivo with the orally bioavailable cFMS kinase inhibitor GW2580*. Proc Natl Acad Sci U S A, 2005. 102(44): p. 16078-83.

32. Yuan, Z.M., et al., *Regulation of DNA damage-induced apoptosis by the c-Abl tyrosine kinase*. Proceedings of the National Academy of Sciences of the United States of America, 1997. 94(4): p. 1437-40.

33. Chen, C., et al., *L-selectin ligation-induced CSF-1 gene transcription is regulated by AP-1 in a c-Abl kinase-dependent manner*. Hum Immunol, 2008. 69(8): p. 501-9.

34. Rockx, D.A., et al., *UV-induced inhibition of transcription involves repression of transcription initiation and phosphorylation of RNA polymerase II*. Proceedings of the National Academy of Sciences of the United States of America, 2000. 97(19): p. 10503-8.

35. Dewar, A.L., et al., *Macrophage colony-stimulating factor receptor c-fms is a novel target of imatinib*. Blood, 2005. 105(8): p. 3127-32.

36. Ide, H., et al., *Expression of colony-stimulating factor 1 receptor during prostate development and prostate cancer progression*. Proceedings of the National Academy of Sciences of the United States of America, 2002. 99(22): p. 14404-9.

37. Wrobel, C.N., et al., *Autocrine CSF-1R activation promotes Src-dependent disruption of mammary epithelial architecture*. The Journal of cell biology, 2004. 165(2): p. 263-73.

38. Wei, S., et al., *Functional overlap but differential expression of CSF-1 and IL-34 in their CSF-1 receptor-mediated regulation of myeloid cells*. J Leukoc Biol, 2010. 88(3): p. 495-505.

39. Li, X., et al., *A destructive cascade mediated by CCL2 facilitates prostate cancer growth in bone*. Cancer research, 2009. 69(4): p. 1685-92.

40. Sawanobori, Y., et al., *Chemokine-mediated rapid turnover of myeloid-derived suppressor cells in tumor-bearing mice*. Blood, 2008. 111(12): p. 5457-66.

41. El Chartouni, C., et al., *Transcriptional effects of colony-stimulating factor-1 in mouse macrophages*. Immunobiology, 2010. 215(6): p. 466-74.

42. Wittrant, Y., et al., *PDGF up-regulates CSF-1 gene transcription in ameloblast-like cells*. J Dent Res, 2008. 87(1): p. 33-8.

43. Tsuchimoto, D., A. Tojo, and S. Asano, *A mechanism of transcriptional regulation of the CSF-1 gene by interferon-gamma*. Immunol Invest, 2004. 33(4): p. 397-405.

44. Harrington, M., et al., *Transcriptional regulation of the mouse CSF-1 gene*. Mol Reprod Dev, 1997. 46(1): p. 39-44; discussion 44-5.

45. Song, Z., et al., *Nuclear actin is involved in the regulation of CSF1 gene transcription in a chromatin required, BRG1 independent manner*. Journal of cellular biochemistry, 2007. 102(2): p. 403-11.

46. Hamer, G., et al., *Role for c-Abl and p73 in the radiation response of male germ cells*. Oncogene, 2001. 20(32): p. 4298-304.

47. Kharbanda, S., et al., *The stress response to ionizing radiation involoves c-Abl-dependent phosphorylation of SHPTP1*. Proceedings of the National Academy of Sciences of the United States of America, 1996. 93(14): p. 6898-901.

48. Baskaran, R., et al., *Ataxia telangiectasia mutant protein activates c-Abl tyrosine kinase in response to ionizing radiation*. Nature, 1997. 387(6632): p. 516-9.

49. Lewis, J.M., et al., *Integrin regulation of c-Abl tyrosine kinase activity and cytoplasmic-nuclear transport*. Proceedings of the National Academy of Sciences of the United States of America, 1996. 93(26): p. 15174-9.

50. Kipreos, E.T. and J.Y. Wang, *Cell cycle-regulated binding of c-Abl tyrosine kinase to DNA*. Science, 1992. 256(5055): p. 382-5.

51. Jing, Y., et al., *c-Abl tyrosine kinase activates p21 transcription via interaction with p53*. Journal of biochemistry, 2007. 141(5): p. 621-6.

Chapter 3:

Augmenting the Durability of Androgen Blockade Therapy in Prostate Cancer by Disrupting the Paracrine Crosstalks Between Tumor Cells and Macrophages Through CSF1R Inhibition

Abstract

Tissue macrophages play key roles in wound healing. In oncology, growing evidence suggests that tumor-associated macrophages (TAMs) promote cancer progression and therapeutic resistance. Furthermore, TAMs promote disease recurrence by enhancing angiogenesis, matrix-remodeling and immunosuppression. In this study, the specific role of TAMs in the context of androgen blockade therapy (ABT) for prostate cancer (PCa) was investigated. ABT, particularly in light of the plethora of newly approved agents, is and will remain the mainstay of therapy for advanced PCa. Here, we have demonstrated that TAMs contribute to PCa disease recurrence after ABT through paracrine signaling processes. ABT induced the tumor cells to express macrophage colony-stimulating factor-1 (M-CSF-1 or CSF-1) and other cytokines that recruit and modulate the functions of macrophages. Consequently, upon ABT, a significant increase in TAM infiltration was observed. As the recruitment and protumorigenic functions of TAMs are dependent on the CSF-1/CSF1R signaling axis, CSF1R inhibitors were tested in combination with ABT. This strategy effectively blocked TAM influx and disrupted their tumor promoting influences. Collectively, it was demonstrated that the incorporation of a CSF1R inhibiting regimen into traditional ABT treatment constitutes a rational combination strategy. When used together, these treatments may improve the long term-efficacy of proven and new androgen blockade therapeutics for PCa patients.

Introduction

Androgen blockade therapy (ABT) for treatment of prostate cancer (PCa) was conceptualized by Drs. Huggins and Hodges over 80 years ago, and is a principle that has withstood the test of time. Their work demonstrated that PCa growth was dependent on androgens. Consequently, surgical castration was prescribed to deplete androgens as a treatment option for this disease (1, 2). Over the years, pharmacological interventions that disrupt either androgen biosynthesis or its functional receptor, namely the androgen receptor (AR), have been developed to treat PCa. Two new drugs approved by the FDA in 2012, Abiraterone (Zitiga) and MDV3100 (Enzalutamide or Xtandi) that effectively block the androgen synthesis enzyme CYP17 and AR ligand binding, respectively, have energized the ABT field (3). Their expedited approval was fueled by the ability of both agents to prolong the overall survival of patients with castration resistant prostate cancer (CRPC), a patient population that is recalcitrant to pre-existing treatments. However, the great level of enthusiasm for these new agents is tempered by emerging data and prior experience of acquired resistance. Several tumor-intrinsic mechanisms can bypass ABT. Examples of these include amplified AR expression, aberrant activation of AR by tyrosine kinase signaling, atypical activation of AR co-activators, and AR splice variants (4, 5).

A less studied, but likely important, aspect of therapeutic resistance is the influence of the tumor microenvironment on ABT resistance (6). Tumor-associated macrophages (TAMs) often constitute a significant inflammatory component in the tumor, and have been shown to promote tumor progression and resistance to various chemotherapeutic agents (7, 8). The recruitment and functional evolution of macrophages from systemic sites to the tumor environment is a complex process that is dictated by various cytokines, tissue factors, and conditions (9). A prominent

cytokine known to regulate myeloid development, macrophage differentiation, and proliferation is the macrophage colony stimulating factor (M-CSF or CSF-1) (10). TAMs have been described to exist in different activation states, ranging from classically activated M1 macrophages, which are proposed to be anti-tumorigenic, to alternatively activated M2 macrophages, which are reported to be pro-tumorigenic (9). Reported mechanisms by which M2-TAMs can promote tumor progression include suppressing the adaptive immune response against cancer cells, promoting tumor growth through angiogenesis, or secreting tumorigenic growth factors (11-13). CSF-1-mediated signaling has been shown to be critical for the recruitment of TAMs to tumors (10), and also to modulate them towards the M2 phenotype (14, 15).

The role of TAMs in PCa progression, and more specifically in the context of ABT, is not well understood. It was reported that surgical castration of mice bearing murine Myc-CaP tumors resulted in increased cytokine expression and influx of inflammatory cells, including B-cells, natural killer (NK) cells, and macrophages (16). This study focused on B-cells and suggested they could be important contributors to the emergence of CRPC (16). In another study, biopsy samples taken from patients who had received ABT showed a positive correlation between time to tumor progression and TAM infiltration, based on histological analysis of $CD68^{+}$ macrophages (17). To gain a better understanding of the role of TAMs in the context of anti-androgen therapy in PCa, the androgen-dependent and immunocompetent Myc-CaP murine prostate cancer model was used. It was found that ABT, either by castration or MDV3100 treatment, induced cytokine expression in tumor cells, which, in turn, promoted a pro-tumorigenic M2 phenotype in TAMs. These findings suggest that the incorporation of a TAM inhibition regimen, such as CSF1R blockade, could improve the efficacy and durability of ABT for PCa (13).

Materials and Methods

Cell Culture

The murine macrophage RAW264.7 (RAW) cells (ATCC), Myc-CaP cells (a kind gift from Dr. Charles Sawyers, Memorial Sloan Kettering New York), and RM-9 cells (a kind gift from Dr. Timothy C. Thompson, Baylor College of Medicine) were cultured in Dulbecco's modified Eagle medium (DMEM), LNCAP and LNCaP-C4-2 (ATCC) cells were cultured in Roswell Park Memorial Institute medium (RPMI), containing 10% fetal bovine serum (FBS), 100 U/mL penicillin and 100 μg/mL streptomycin (P/S) (complete media) at 37°C with 5% CO_2. For experiments using charcoal stripped serum (CSS), FBS charcoal dextran treated (Omega Scientific Inc.) was used instead of FBS.

In vitro Migration Assay

RAW macrophages (1.0 x 10^5 cells) were seeded in 8 μm transwell inserts (BD Falcon), in DMEM containing 5% CSS, 1% P/S or 1000 nM GW2580. Inserts were placed in 24-well plates with 72 hrs conditioned media from Myc-CaP cells treated with 10 μM MDV3100 (MDV) or dimethyl sulfoxide (DMSO) vehicle incubated at 37°C for 6 hrs. After 6 hours, migrated cells were immediately fixed in 3% paraformaldehyde (PFA) stained with 4,6-diamidino-2-phenylindole (DAPI). At least 10 fields/well at 4x magnification were quantified using ImageJ Version 1.34s (NIH).

To block CSF-1-mediated migration we added GW2580 (1000 nM) to the top chamber containing the RAW cells. As a positive control for RAW macrophage migration, CSF-1 protein was added to the bottom chamber in DMEM, with 5% CSS and 1% P/S.

Real-time RT-PCR

Total cellular RNA was extracted with TRIzol Reagent. RNA was isolated according to the TRIzol procedure. Real-time quantitative reverse-transcribed polymerase chain reaction (RTPCR) was performed as previously described (18).

Co-Culture Assay

RAW (1.0×10^6 cells) were seeded in 4 μm transwell inserts in DMEM, with 10% FBS, and 1% P/S. Inserts were placed in 6 well plates containing Myc-CaP (2.5×10^5 cells) treated with MDV (10 μM) or vehicle (DMSO). Co-cultures were incubated for 48 hrs at 37°C. Following the incubation period cells were harvested with TRIzol Reagent and total cellular RNA was extracted as described above.

ELISA

CSF-1 levels in cell lysates and serum samples obtained at euthanasia were measured using enzyme-linked immunosorbent assay (ELISA). Cell lysates were prepared from Myc-CaP (2.5×10^5 cells) treated with vehicle (DMSO) or MDV (10 μM) for 48 hrs at 37°C. Following the incubation period cells were lysed in RIPA buffer (Upstate) containing proteinase inhibitor cocktail (Sigma), and centrifuged 5 min at 1,500 xg. ELISA was performed according to the instructions for the mouse CSF-1 ELISA Duoset Kit (R &D systems). Capture antibody (MAB416, R&D Systems, 2 μg/ml) was incubated on 96 well plates overnight at room temperature. Bovine serum albumin (1%) in phosphate buffered saline (PBS) was used for blocking. Sample incubation was performed according to the manufacturer's instructions, the plate was then incubated with detection antibody (BAF416, R&D Systems, 0.2 μg/ml). Optical

density of each well was determined immediately using a microplate reader set to 450 nm with a 570 nm subtraction. All standards and samples were assayed in duplicate.

In vivo Studies

FVB male mice (6-8 weeks old) were purchased from Taconic Farms, Inc. Myc-CaP cells (2×10^6 cells) were implanted subcutaneously above both shoulders. All animal experiments were approved by the Animal Research Committee of the University of California, Los Angeles. Mice were castrated when tumors reached 300-500 mm^3. Treatments were initiated the day after castration. For castration and GW2580 studies, mice were treated daily with control diluent (0.5% hydroxypropyl methylcellulose, Sigma-Aldrich; 0.1% Tween20 in distilled H_2O), 160 mg/kg GW2580 by oral gavage. For castration and PLX3397 studies, mice were fed daily chow containing PLX3397 or control chow formulated at an average dose per animal per day at 40 mg/kg. Tumor size was measured every 2-3 days by digital calipers as previously described (18). Mice were sacrificed and tissues were analyzed at the ethical tumor size limit of 1 cm in diameter. Tumor growth was monitored as above.

Immunohistochemistry

Tumor sections were harvested and fixed in 3% PFA overnight, then placed in 50% ethanol (EtOH) until paraffin embedding. Tumor sections (4 μm) were stained with F4/80 (1:500; Serotec), MMP-9 (1:1000; Abcam), CSF1R (1:200; Santa Cruz) CSF1R-Y723 (1:50; Santa Cruz). Stained samples were analyzed using the Nikon Eclipse 90i microscope and images were captured at 10x magnification. Images were processed using Photoshop CS software. Slides where scanned at the UCLA Translational Pathology Core Laboratory (TPCL). For

immunohistochemistry (IHC) and hematoxylin and eosin (H&E) staining slides were scanned using the Aperio wholeslide scanner and for immunohistofluorescence (IHF) staining slides were scanned using the Arial wholeslide scanner. Scanned slides were analyzed using the Definiens image analysis software.

Flow Cytometry

Tumor single cell suspensions were prepared for flow cytometry as previously described (19). After red blood cell (RBC) lysis (Sigma), single-cell suspensions were incubated for 30 minutes on ice with the following antibodies: CD11b-APC or CD11b-e450, Gr-1-PerCPCy5.5, Ly6C-FITC, F4/80-PE-Cy7 or F4/80-e450, MHCII-Alexa-700, and CD115 (CSF1R)-PE conjugated antibodies, 1:200 (eBioscience), followed by two washes with 2% FBS in PBS (FACS buffer). Cells were fixed in 3% PFA for 15 min at room temperature and washed two times with FACS buffer. Cell acquisition was done on a BD LSR-II flow cytometer (Beckman Coulter). Data were analyzed with FlowJo software (TreeStar) (19).

Statistical Analysis

Data are presented as mean plus or minus SEM. Statistical comparisons between groups were performed using the Student *t* test.

Results

Androgen blockade therapy increases the infiltration of tumor-associated macrophages. The implantable Myc-CaP murine prostate tumor is a useful model to investigate the role of TAMs in ABT of PCa for several reasons. First, the immunocompetent environment of this model enables the examination of both the adaptive and innate arms of the immune system in PCa progression (16). Second, the androgen signaling axis, including AR splice variants, plays a prominent role in the oncogenic progression of this model (20, 21). Furthermore, macrophages comprise a significant component of the tumor microenvironment in Myc-CaP tumors, as well as in the parental transgenic Hi-Myc spontaneous prostate cancer model (Figure 3.1a). For this study, the different tumor infiltrating myeloid cell (TIM) subsets were characterized in Myc-CaP tumors. Flow cytometric analysis revealed that TAMs ($F4/80^{+}CD11b^{+}$) are the predominant TIM population, constituting about 2-5% of viable cells in the tumor as compared to MDSCs ($CD11b^{+}Gr\text{-}1^{+}$) comprising only of 0.42% of viable cells (Figure 3.2a). Interestingly, in the Myc-CaP tumor model, the $F4/80^{+}$ TAMs uniformly expressed CSF1R (CD115, c-fms), with 97.7% concordant expression between these two markers (Figure 3.2b and Figure 3.1b). Since the $CSF1R^{+}$ population denotes an immune suppressive and protumorigenic myeloid cell population (22), and is also the putative targeted population of the small molecule CSF1R kinase inhibitors used here, the TAMs population will be defined in these studies as $CD11b^{+}CSF1R^{+}$. Immunofluorescent staining of Myc-CaP tumors revealed the prominent presence of $F4/80^{+}$ TAMs (Figure 3.2c) and these TAMs displayed extended reticular processes (Figure 3.2c).

Next, the impact of two modalities of ABT on TAM infiltration was examined. A significant increase in TAMs after AR blockade treatment with MDV3100 was observed by

immunohistochemistry, and flow cytometry (Figure 3.2c, d), as well as by qRT-PCR for F4/80 transcript from whole tumor (data not shown). This increase in TAMs was not limited to MDV3100 treatment, as androgen deprivation treatment (ADT) by surgical castration also caused a significant increase in the infiltration of CD11b+CSF1R+ TAMs. As shown in Figure 3.2e, the androgen-dependent Myc-CaP tumor responded to castration by a cessation of tumor growth for approximately 20 days. The content of TAMs peaked at 14 days after castration (mid point) and gradually declined thereafter (Figure 3.2f and Figure 3.1c). Since a significant increase of TAMs after ABT was observed, the induction of macrophage recruiting cytokines by this form of treatment was investigated.

ABT induces CSF-1 expression in prostate cancer cells. First, CSF-1 expression in the ABT-treated tumor was examined, as this cytokine is known to play a key role in recruiting macrophages. As shown in Figures 3.3a and 3.3b, a significant increase in CSF-1 mRNA in Myc-CaP tumor was observed after both MDV3100 treatment and surgical castration. In addition, CSF-1 protein was assessed in the sera of castrated mice and found to increase in a time-dependent manner from day 14 post-castration to day 36 post-castration (Figure 3.3c). To parse out the potential molecular crosstalk following ABT on the recruitment and function of TAMs, a cell culture system was used. Again, two different ABTs were employed, namely androgen deprivation using charcoal-striped serum (CSS) and AR blockade with MDV3100, on Myc-CaP tumor cells. Interestingly, both treatments significantly increased expression of CSF-1, and to a lesser extent IL-34, a novel CSF1R ligand, but not CCL-2 (MCP-1) or SDF-1 which were very lowly expressed (Figure 3.3d). The ability of ABT to induce CSF-1 expression is not restricted to the Myc-CaP model, and was also observed in LNCaP and LNCaP-C4-2 human

prostate cancer models (Figure 3.4a, b). The magnitude of secreted CSF-1 protein was also elevated after MDV3100 treatment *in vitro* (Figure 3.3e). Next, it was assessed whether or not the elevated CSF-1 was indeed functional and capable of inducing macrophage migration. As shown in Figure 3.3f, the migration of RAW264.7 (RAW) macrophage cell line was enhanced by conditioned media from Myc-CaP cells treated with MDV3100, compared to those treated with vehicle. Furthermore, treatment with a highly selective CSF1R inhibitor, GW2580 (19), abrogated the stimulatory effect of ABT-treated tumor conditioned media on RAW cells These results indicate that CSF-1 is a key cytokine produced following ABT that can recruit macrophages.

Paracrine influences of ABT promote the protumorigenic phenotype of macrophages. Extensive evidence suggests that tumor-derived factors educate macrophages to become the alternatively activated type, M2, that possess protumorigenic activities such as enhancing angiogenesis, tissue remodeling and immune suppression (19, 23). Treating Myc-CaP tumor cells alone with MDV3100 did not appreciably alter their expression of protumorigenic genes such as vascular endothelial growth factor A (*vegf-a*), matrix metalloproteinase 9 (*Mmp-9*) and arginase (*Arg-1*) (Figure 3.5a). However, it is clear that ABT can enhance the tumor cells' expression of M2-promoting cytokines such as IL-13 and IL-10, albeit another M2 cytokine IL-4 was unaltered (14) (Figure 3.5b). Next, a binary tumor cell-macrophage co-culture system was employed to assess the M2 phenotype of macrophages in context of ABT. Strikingly, a dramatic increase in the expression of VEGF-A, MMP-9 and Arg-1 (Figure 3.5c) and of M2 cytokines IL-10 and CSF-1, and a reduction in the pro-inflammatory M1 cytokine IL-12 (Figure 3.5d) were observed only in the MDV-treated tumor cell-macrophage co-cultures. These M2-polarizing

gene expression changes were not observed in ABT of macrophages alone (Figure 3.5d). The results of therapeutic trials in preclinical Myc-CaP tumor-bearing mice corroborated the ABT-induced paracrine influences on macrophages that were observed in cell cultures. For instance, the expression of VEGF-A, MMP-9 and Arg-1 genes (Figure 3.5e) and vascular density (Figure 3.5f) were increased after MDV3100 treatment in Myc-CaP tumors. Taken together, these findings indicate that ABT of prostate tumor cells elicits a paracrine crosstalk with TAMs that promotes their protumorigenic properties.

Blocking TAMs in combination with ADT improves therapeutic outcome. Next, the molecular crosstalk between tumor cells and TAMs was pursued in greater detail in a second therapeutic setting, namely ADT. The *in vitro* findings clearly pointed to CSF-1 being a critical cytokine involved in the recruitment and function of TAMs in ABT. Hence, a rational therapeutic strategy is to use a recently developed small molecule, the CSF1R kinase inhibitor PLX3397, to disrupt the protumorigenic influences of TAMs. This inhibitor was shown to be a potent inhibitor of CSF1R (cFMS) with IC50 of 20 nM and it is under active clinical investigation for several types of cancers, including CRPC (8). Specifically, the therapeutic impact of ADT was examined in combination with PLX3397. As these results and other reports have shown (Figure 3.2e, (16)), surgical castration clearly suppressed Myc-CaP tumor growth compared to sham surgery-treated (control) group (Figure 3.6a). In the castration only cohort, the growth rate of tumors recovered from approximately day 20 after surgery and onward, paralleled the emergence of CRPC in the clinical scenario. The addition of an oral regimen of the CSF1R inhibitor PLX3397 to castration resulted in a significant delay in the onset of CRPC (Figure 3.6a). Since the CSF-1/CSF1R signaling axis has been implicated in prostate cancer oncogenesis

(24), it was investigated whether the therapeutic effects of blocking this axis could be directed at the tumor cells. The Myc-CaP tumor cells express negligible levels of CSF1R but relatively high levels of CSF-1 (Figure 3.7a). The proliferation of Myc-CaP tumor cells was unaltered after effective knockdown of CSF-1 expression by shRNA or CSF1R blockade with GW2580 (Figure 3.6b-c). Since PLX3397 treatment alone did not suppress tumor growth (Figure 3.6a), these collective results are consistent with the assertion that the therapeutic effect of CSF1R blockade is tumor-extrinsic.

Detailed flow cytometric analysis of myeloid populations in the 4 treatment cohorts revealed that ADT induced a significant increase in intratumoral content of $CD11b^{+}CSF1R^{+}$ ($F4/80^{+}$) macrophages from an average of 4.15 +/- 0.47 to 6 .11 +/- 0.49 % of viable cells (n = 7) (Figure 3.6d). PLX3397 treatment resulted in a consistent and significant reduction of TAMs in both castration- and sham-treated tumors (Figure 3.6d). The effective blocking of $CSF1R^{+}$ TAM infiltration by PLX3397 is further supported by a decrease in CSF1R transcript levels in treated tumors and the diminution of CSF1R phosphorylation assessed by tumor histology (Figures 3.7b-c).

The impact of tumor-directed ABT can be transmitted systemically through circulating cytokines. As discussed previously, ADT on Myc-CaP tumor-bearing animals resulted in a significant increase of CSF-1 expression in the tumor and serum CSF-1 level (Figure 3.3b and c). The elevated serum CSF-1 can account for the observed significant increase in the circulating levels of $CD11b^{+}CSF1R^{+}$ ($Gr1^{+}$) myeloid cells in the peripheral blood after castration that was observed (Figure 3.8a). This population was decreased effectively by PLX3397 treatment (Figure 3.8a). Likewise, the systemic alterations of this myeloid population in response to therapy can also be observed in the spleen (Figure 3.8b). Further characterization showed that

TAMs in the castrated tumors are quite different from control tumors, as they displayed much lower levels of MHCII expression, indicative of an immunosuppressive M2-phenotye (Figure 3.6e) (25). This result led to further investigation of the therapeutic impact of PLX3397 on the protumorigenic M2 TAMs in castrated tumors.

CSF1R blockade abrogates the paracrine protumorigenic influences of TAMs induced by ADT. Parallel to the results of AR blockade therapy with MDV3100, surgical castration also induced the expression of MMP-9, VEGF-A, and Arg-1 mRNA in Myc-CaP tumors (Figure 3.9a). Moreover, CSF1R blockade treatment with PLX3397 resulted in a significant reduction of MMP-9, VEGF-A and to a lesser extent Arg-1 expression in the castrated tumors (Figure 3.9a). From these global gene expression analyses, it is not possible to discern the cellular origin of these protumorigenic influences. Hence, immunohistofluorescence (IHF) analyses were employed to investigate this issue. Corroborating with the prior results, ADT clearly increased the number of TAMs (Figures 3.6d and 3.9b, left panels). Furthermore, IHF analyses revealed that tumor cells expressed negligible level of MMP-9 and that it was the $F4/80^{+}$ macrophages that predominantly expressed MMP-9 (Figure 3.9b, right panels). Interestingly, the proportion of TAMs that expressed MMP-9 also increased significantly after castration (Figure 3.9b). PLX3397 treatment blocked both the recruitment and function TAMs as the number of TAMs and their expression of MMP-9 were greatly attenuated by the blockade of CSF1R (Figure 3.6d and 3.9b). The therapeutic effect of PLX3397 is likely attributed to its ability to inhibit CSF1R signaling, thus blocking the recruitment and the functions of the protumorigenic M2 TAMs in castrated tumors.

Discussion

Two recent studies suggested a potential negative impact of TAMs in ADT. Using the same Myc-CaP murine prostate cancer model, Ammirante and colleagues (16) demonstrated a castration induced influx of TAMs and other immune cells such as B cells, NK cells into the tumor. In a second study, Nonomura and colleagues demonstrated that higher levels of TAMs in tumor biopsy samples of PCa patients predicted a poor survival outcome after ADT (17). However, these studies did not examine the causal relationship between ADT and TAMs or what protumorigenic influences the TAMs could be contributing to treatment failure. Hence, in this study we dove deeper into the molecular signals emanating from inhibiting androgen signaling in tumors that could modulate the activity of macrophages. We observed that ABT using MDV3100 induced responsive prostate cancer cells to express cytokines, including CSF-1, IL-13 and IL-10, which are known to be critical in the recruitment and polarization of macrophages towards an alternatively-activated, protumorigenic state (26, 27). We went on to show that the M2 TAMs expressed elevated levels of the VEGF-A, MMP-9 and Arg-1 genes, which can promote treatment failure by enhancing tumoral angiogenesis, tissue-remodeling and immune suppression, respectively. In support of our hypothesis that TAMs are contributing to cancer progression after androgen signaling inhibition, we blocked the recruitment and function of TAMs through the CSF-1/ CSF1R axis. Extensive evidence supports that this axis is critical for the proliferation and function of the myeloid and macrophage lineages in particular (10, 28). Our data here, and in prior studies, suggests that in therapeutic settings, such as ABT, ADT or radiation therapy, tumor cells over-express CSF-1, which in turn promotes the protumorigenic activities of responsive $CSF1R^{+}$ macrophages (19, 29). Hence, the use of selective CSF1R kinase inhibitors, such as GW2580 and PLX3397, in combination with ADT was able to reverse the

treatment-induced increase in TAMs, leading to more effective and prolonged tumor growth suppression than ADT alone (Figure 3.6a). Figure 3.10 is a schematic representation of the proposed paracrine crosstalk between prostate tumor cells and TAMs induced by ABT and ADT that likely contribute to treatment failure.

It is a well-known phenomenon that dying/necrotic tumors have an increased inflammatory response. Dying tumor cells secrete cytokines that alert the immune system to respond as they would to a wound or injury (30). Macrophages are one of the first responders to a wound and have a important role in promoting angiogenesis and tissue remodeling (31). Macrophage cell involvement has been implicated in multiple aspects of cancer promotion and progression. Recent studies looking at macrophages have examined their involvement in resistance to various types of chemotherapies, including the anti-androgen bicalutamide. Macrophages were found to promote an antagonist to agonist conversion of bicalutamide by modulation of AR co-activators (32). However, the changes that occurred in PCa cells post anti-androgen treatment linking macrophage activity remained unknown. Moreover, the possible role of macrophages in conferring resistance to novel anti-androgen, MDV3100 or androgen depletion by surgical castration had not been explored.

Given that prostate cancer progression requires androgens for growth and survival, anti-androgen drugs that inhibit androgen receptor (AR) function are commonly used for the treatment of advanced prostate cancer. Although the majority of patients usually respond to anti-androgen therapies, many of them will eventually progress to CRPC. There are various mechanisms prostate cancer cells utilize after anti-androgen therapy for continuous growth; these include AR independent and AR-dependent pathways. In our studies, we found that, in the context of androgen inhibition, the macrophage phenotype changes from an M1 to an M2 state.

Macrophages were found to express higher levels of pro-tumorigenic/immune suppressive molecules such as MMP-9, VEGF-A, IL-10, Arg-1 and IGF-1 (data not shown). It is likely that some combination of the tumorigenic properties of these factors play a role in the promotion of resistance to ADT and ABT either by an extrinsic bypass mechanism or by a direct effect on AR regulation.

Various reports indicate growth factors aberrantly activate AR via PI3K/AKT pathways (33). In our system, we identified several growth factors whose levels correlated with TAM infiltration/modulation (Data not shown), suggesting a possible role for macrophages as a source of growth factors under androgen deprived conditions. Macrophages are a key source of angiogenic and matrix remodeling factors such as VEGFs and MMPs (34). We also found increased expression of angiogenic and matrix remodeling factors secreted from macrophages post ADT and ABT of PCa cells. Angiogenesis is considered a major indicator of poor survival in many tumors (35). Moreover, macrophage-mediated angiogenesis is thought to confer resistance to anti-angiogeneic therapies (7) Dr. Denardo and colleagues reported macrophage involvement in promoting angiogenesis in breast cancer models and show that inhibition of macrophage recruitment to tumors with PLX3397 in combination with paclitaxel improved the survival of mammary tumor bearing mice (8). Additionally, we found that macrophages increase expression of immune suppressive factors, such as Arg-1 and IL-10, that have been shown to suppress T-cell activity, as well increase the immune suppressive phenotype of macrophages (14). Thus, macrophages may be suppressing the adaptive anti-tumor T-cell response via Arg-1 and IL-10 expression. Further research is necessary to tease out the exact role of M2 macrophages in the onset of CRPC. There are novel immunotherapeutics emerging for PCa, such as Sipuleucel-T, which focus on activating the anti-tumoral T-cell response (36). Although

Sipuleucel-T treatment does result in increased overall survival in CRPC patients the effects are not permanent (37). Thus, it is imperative to further understand the interplay between PCa cells and the immune suppressive/tumor promoting properties of immune cells.

The results presented here is significant in that it anticipates a potential extrinsic mechanism of therapeutic resistance involving tumor infiltrating myeloid cells and investigates approaches to thwart this pro-tumorigenic mechanism. Given the promising efficacy and minimal side effects of the highly selective CSF1R inhibitors, they will likely be an important means towards the development of rational combination therapies that can extend the efficacy of conventional cancer therapeutics that target tumor-intrinsic growth pathways. In line with our findings, Plexxicon is currently pursuing a pilot study with PLX3397 on patients with advanced castration-resistant prostate cancer, bone metastasis and high circulating tumor cells with one of the key objectives to assess the anti-tumor effects of the compound (Clinicaltrial.gov identifier NCT01499043).

Figures

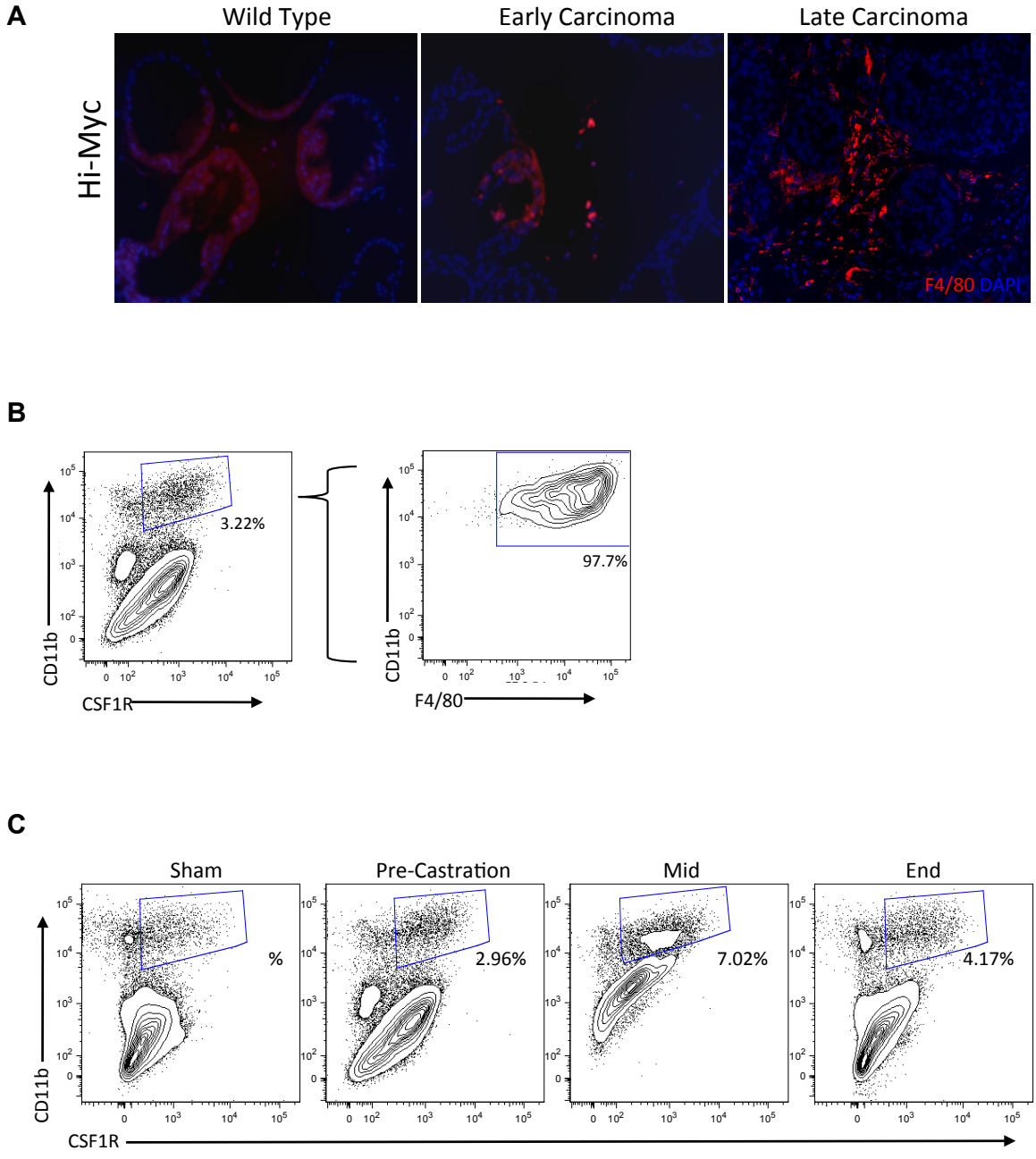
A
Wild Type
Early Carcinoma
Late Carcinoma
Hi-Myc
F4/80 DAPI
B
3.22%
97.7%
CD11b
CSF1R
F4/80
C
Sham
Pre-Castration
Mid
End
%
2.96%
7.02%
4.17%
CD11b
CSF1R

Figure 3.1: $CD11b^+CSF1R^+F4/80^+$ macrophages are the predominant myeloid population in Myc-CaP tumors. A) Hi-Myc transgenic mouse carcinomas IHF staining of F4/80 (red) macrophages and DAPI (blue). B) Representative flow cytometry plots of Myc-Cap subcutaneous tumors 300-500 mm^3 on male FVB mice showing overlap of $CD11b^+CSF1R^+$ with $CD11b^+F4/80^+$ macrophages. C) Representative flow cytometry plots of $CD11b^+CSF1R^+$ from Myc-CaP subcutaneous tumors at various time points starting with tumors 300-500 mm^3. Sham (14 days after sham surgery), pre-castration (day 0 not castrated), mid (day 14 post-castration), end (day 38 post-castration).

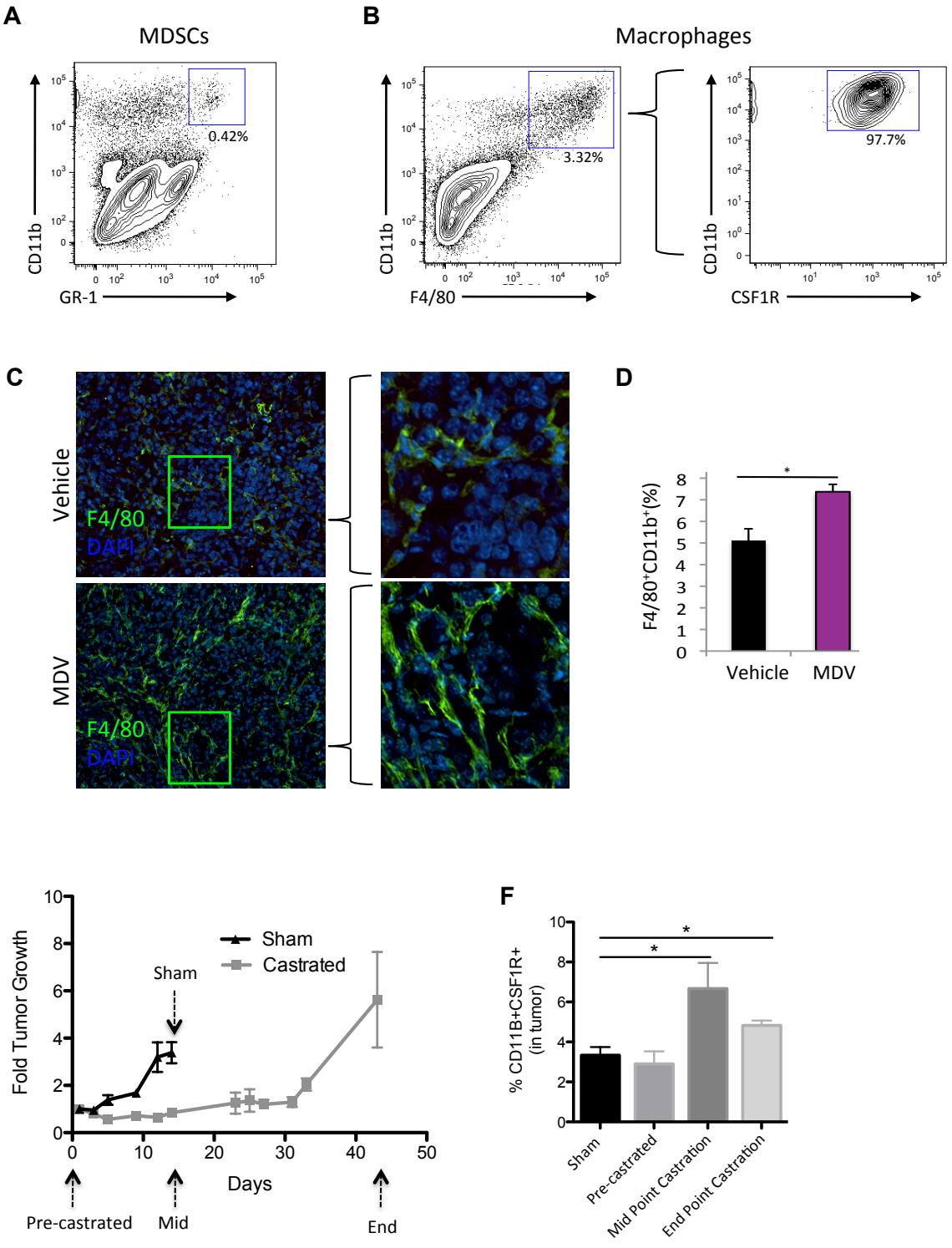
A
MDSCs
0.42%
CD11b
GR-1
B
Macrophages
3.32%
97.7%
CD11b
F4/80
CSF1R
C
Vehicle
MDV
F4/80
DAPI
D
F4/80+CD11b+(%)
Vehicle
MDV
E
Fold Tumor Growth
Sham
Castrated
Days
Pre-castrated
Mid
End
F
% CD11B+CSF1R+ (in tumor)
Sham
Pre-castrated
Mid Point Castration
End Point Castration

Figure 3.2: Macrophage infiltration in Myc-CaP tumors post ABT and ADT. A) Representative flow cytometry plots of Myc-CaP subcutaneous tumors on male FVB mice showing A) $CD11b^{+}GR\text{-}1^{+}$, MDSCs and B) overlap of $CD11b^{+}F4/80^{+}$ with $CD11b^{+}CSF1R^{+}$, macrophages. B) IHF staining of F4/80 (green) macrophages and DAPI (blue) from vehicle and MDV treated subcutaneously Myc-CaP tumors implanted in syngeneic FVB male mice. Mice were treated by daily oral gavage with vehicle or MDV (10 mg/kg) for 9 days. C) Quantification of $CD11b^{+}F4/80^{+}$ macrophages from B. Time course assessment of Myc-CaP tumor growth and macrophage infiltration post-castration. Myc-CaP cells were subcutaneously implanted in syngeneic FVB male mice. Mice were sham castrated or castrated when tumors reached 300-500 mm^3. E) Fold tumor growth F) Flow cytometry quantification of $CD11b^{+}CSF1R^{+}$ macrophages in Myc-CaP tumors from E. $*P < 0.05$. (n = 3-6 group).

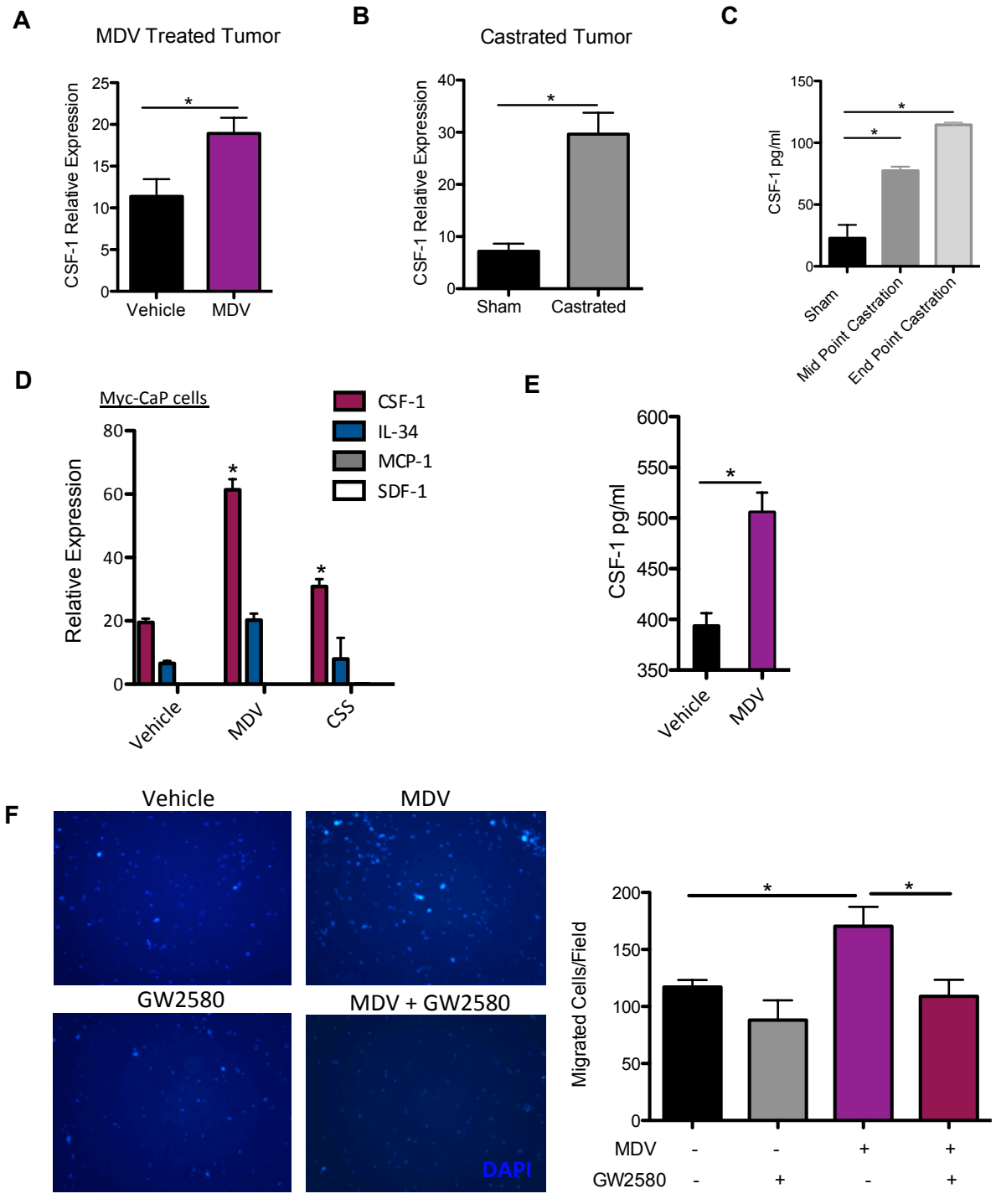

Figure 3.3: Anti-androgen treatment and androgen deprivation of PCa cells promotes TAM migration in a CSF-1 dependent manner. A) CSF-1 expression by RTPCR from vehicle

and MDV treated Myc-CaP tumors subcutaneously implanted in syngeneic FVB male mice. Mice were treated by daily oral gavage with vehicle, or MDV (10 mg/kg) for 9 days. B) CSF-1 expression by RTPCR from sham (day 14 after sham surgery) and castrated (day 36 post castration) Myc-CaP tumor bearing FVB mice. C) Sera CSF-1 protein analysis by ELISA from sham and castrated mice at sham (day 14 after sham surgery), mid point (day 14 after castration) and end point (day 38 after castration). D) RTPCR analysis of TAM recruiting cytokines after 48 hrs of MDV (10 μM) treatment of Myc-CaP cells. E) CSF-1 protein expression in Myc-Cap lysates after 48 hrs of MDV (10 μM) treatment. F) 6 hr migration assay using RAW264.7 murine macrophages and conditioned media from Myc-CaP cells treated with MDV (10 μM) or vehicle (DMSO) or RAW cells in vehicle and MDV conditioned media treated with 1 nM GW2580. DAPI staining of migrated RAW cells (left), migrated cell quantification of 10 fields/well at 4x magnification. *$P < 0.05$. (n = 3-6 group).

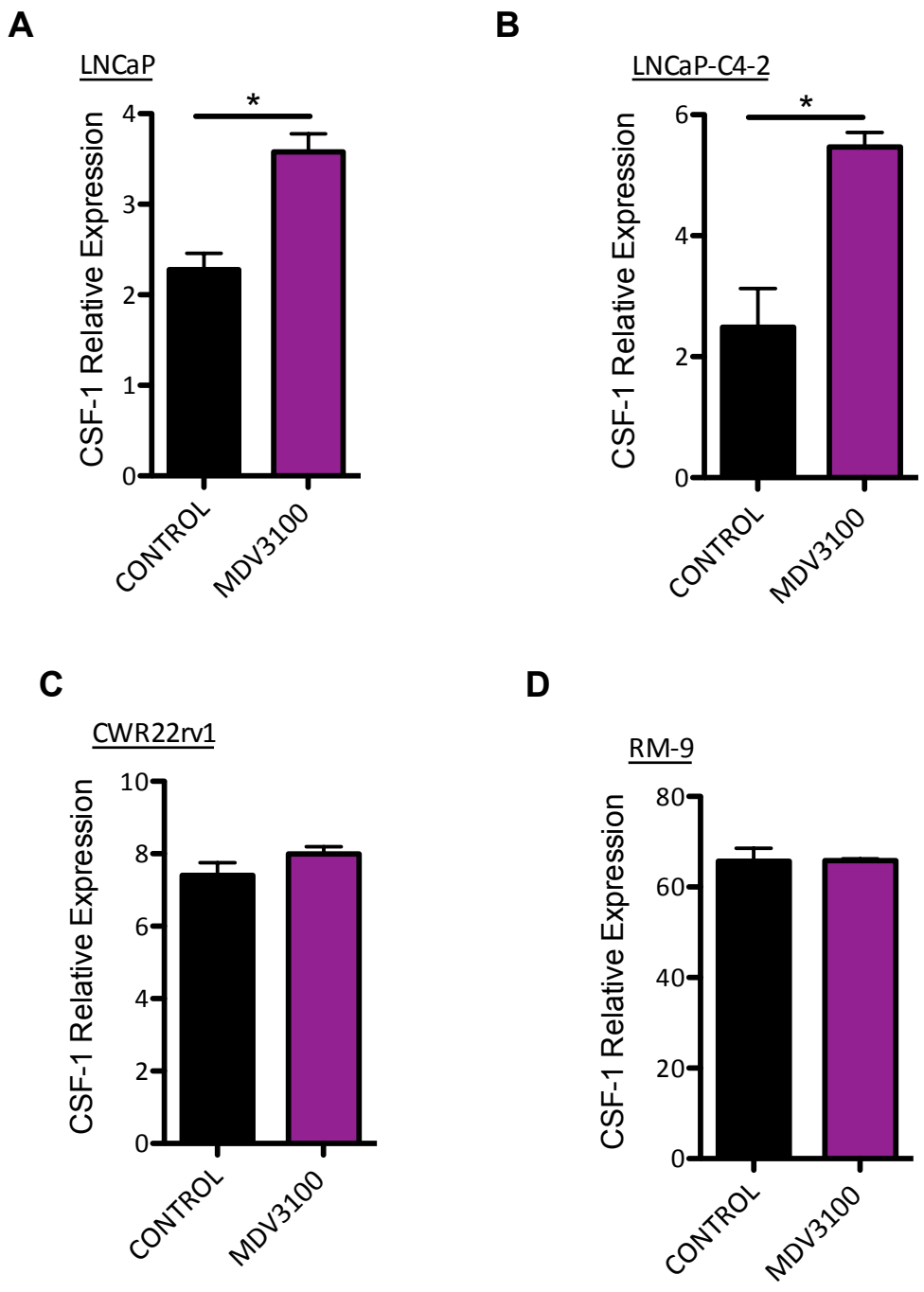

Figure 3.4: Anti-androgen treatment of PCa cells induces CSF-1 expression. RTPCR analysis of CSF-1 after 48 hrs of MDV (10 μM) treatment of A) LNCaP B) LNCaP-C4-2 C) CWR22rv1 D) RM-9. *$P < 0.05$. (n = 3).

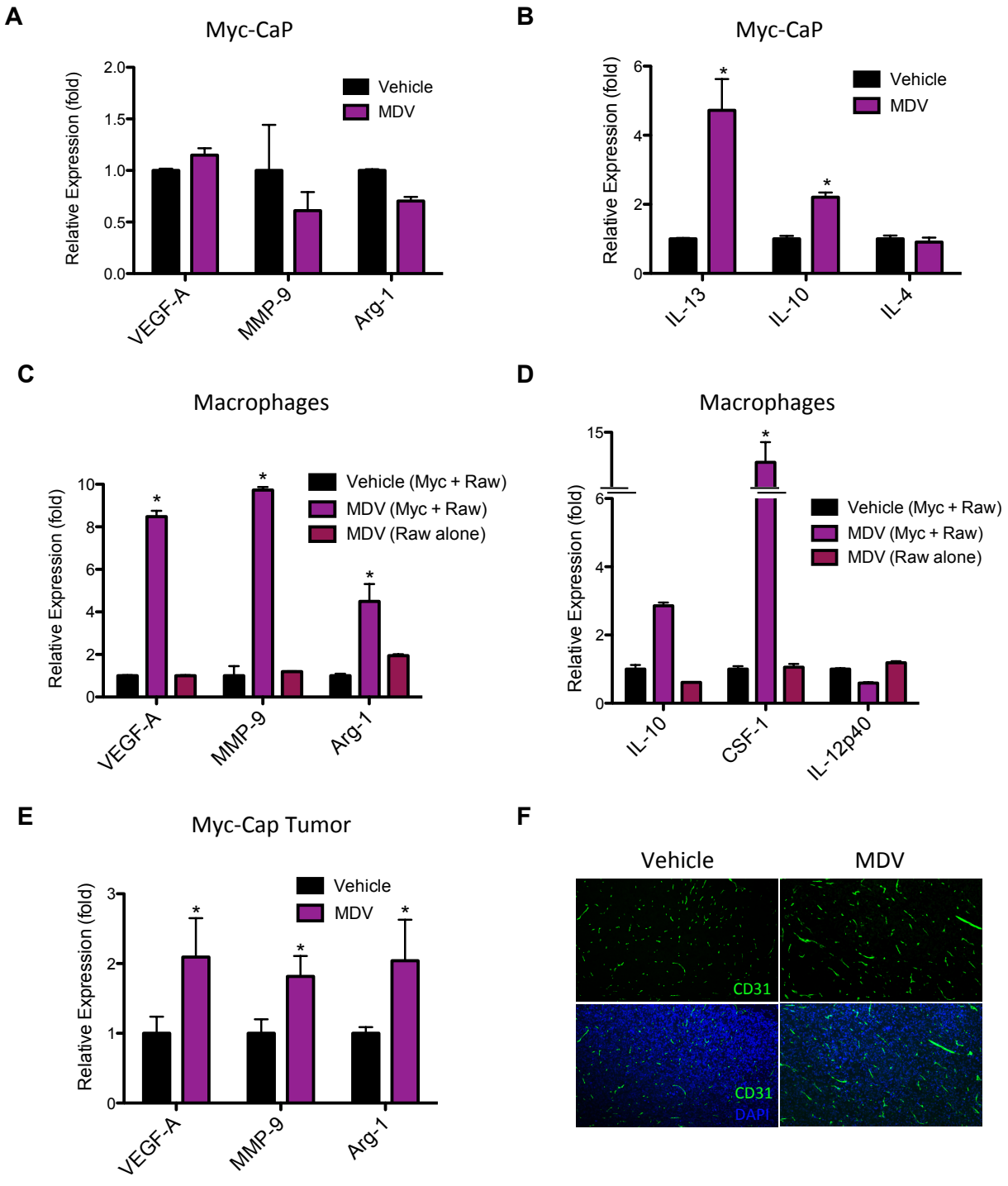

Figure 3.5: PCa cell induced alternative activation of macrophages after anti-androgen treatment. Co-culture assays of RAW264.7 macrophages and Myc-CaP cells treated with MDV

(10 μM) for 48 hrs. A-B) Transcript expression changes by RTPCR in Myc-CaP cells and C-D) in RAW264.7 cells. E) Transcript expression changes by RTPCR in MDV (10 mg/kg) treated Myc-CaP tumors. (n = 6-10/group). F) Representative images of CD31 blood vasculature (green), DAPI (blue) IHF staining of Myc-CaP tumors from MDV3100 (10 mg/kg) treated tumors. *$P < 0.05$.

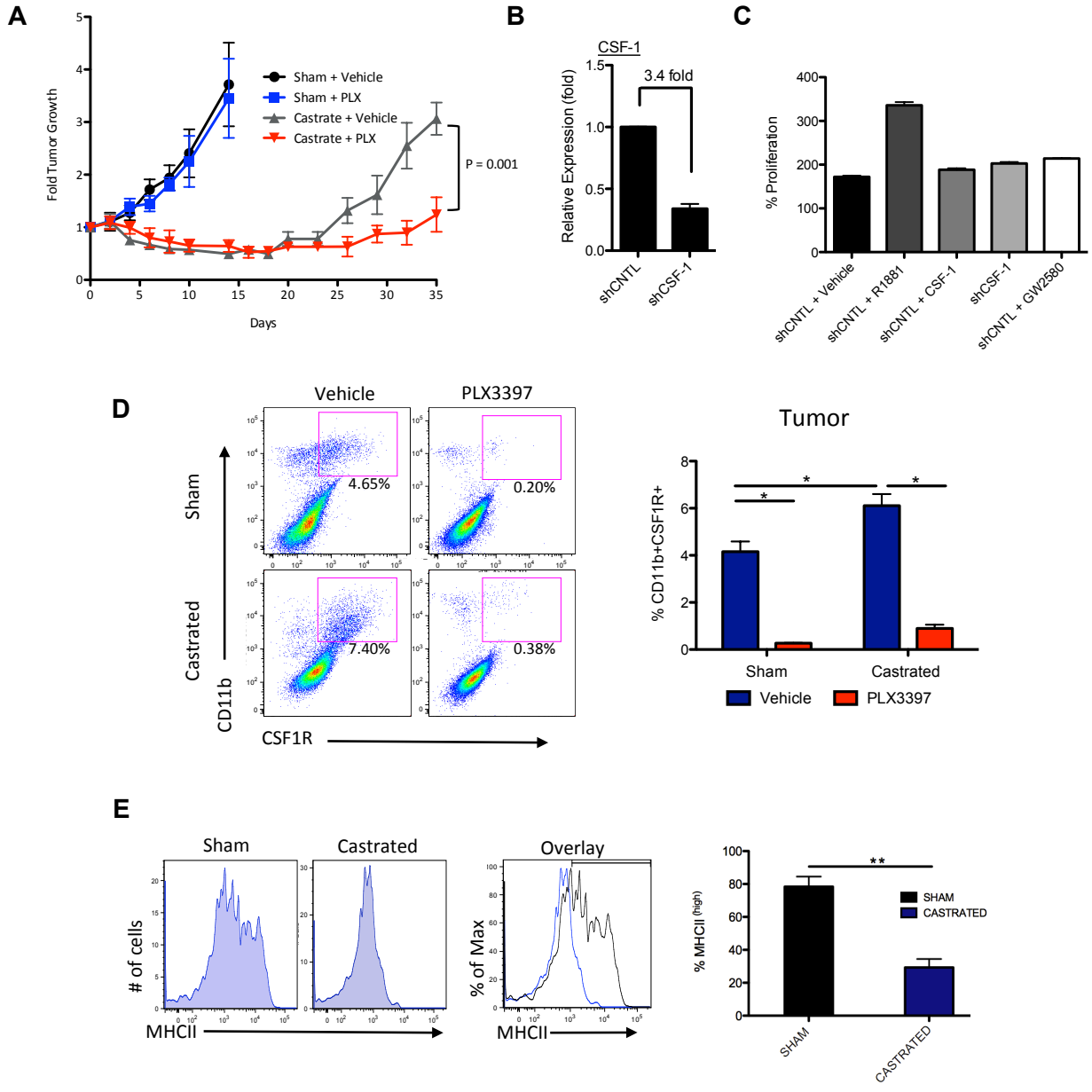

Figure 3.6: Delayed CRPC development from blockade of castration induced TAM infiltration. Myc-CaP cells were subcutaneously implanted in syngeneic FVB male mice. Mice were sham castrated or castrated when tumors reached 300-500 mm^3. Mice were fed with control chow or PLX3397 daily for 36 days. A) Fold tumor growth from each treatment group. B-C) Effects of CSF-1 inhibition on Myc-CaP proliferation were assessed by the CCK8 assay. Myc-

CaP cells transduced with a lentivirus shorthairpin control (SHCNTL) or SHCSF-1 followed by treatment with vehicle, 1 nM R1881 (synthetic androgen), recombinant 10 ng/ml CSF-1, 1 nM GW2580, or after shorthairpin knockdown of CSF-1. D) Representative flow cytometry plots of total $CD11B^{+}CSF1R^{+}$ TAMs in tumors and right, quantification of $CD11B^{+}CSF1R^{+}$ TAMs. E) Representative MHCII expression histograms of $CD11B^{+}CSF1R^{+}$ TAMs by flow from sham and castrated tumors (left), overlay of representative MHCII histograms (middle), quantification of high MHCII expression (right). $*P < 0.05$. (n = 6-10/group).

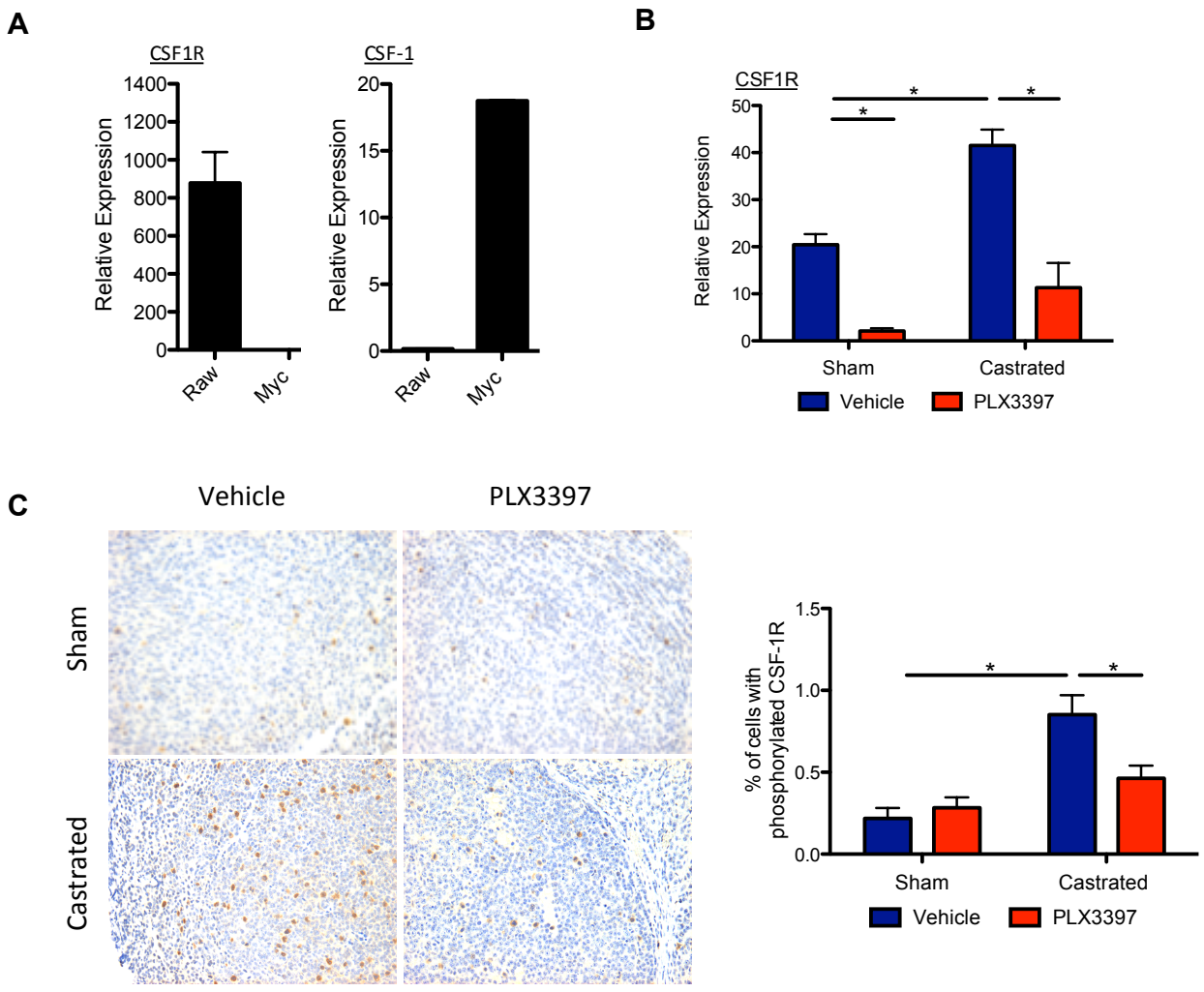

Figure 3.7: Characterization of CSF1R axis in Myc-CaP model and castration induced CSF1R activation in Myc-CaP tumors. RTPCR analysis of A) left, CSF-1 and right, CSF1R expression in RAW264.7 macrophages and Myc-CaP cells. *P < 0.05. (n = 3). Myc-CaP cells were subcutaneously implanted in syngeneic FVB male mice. Mice were sham castrated or castrated when tumors reached 300-500 mm^3. Mice were fed with control chow or PLX3397 daily for 36 days. Whole tumor RTPCR expression changes of B) CSF1R from each treatment group. C) Left, IHC staining of tumors in B for CSF1R-Tyr723. Right, Quantification of IHC staining CSF1R-Tyr723 in Myc-CaP tumors. *P < 0.05. (n = 6-10/group).

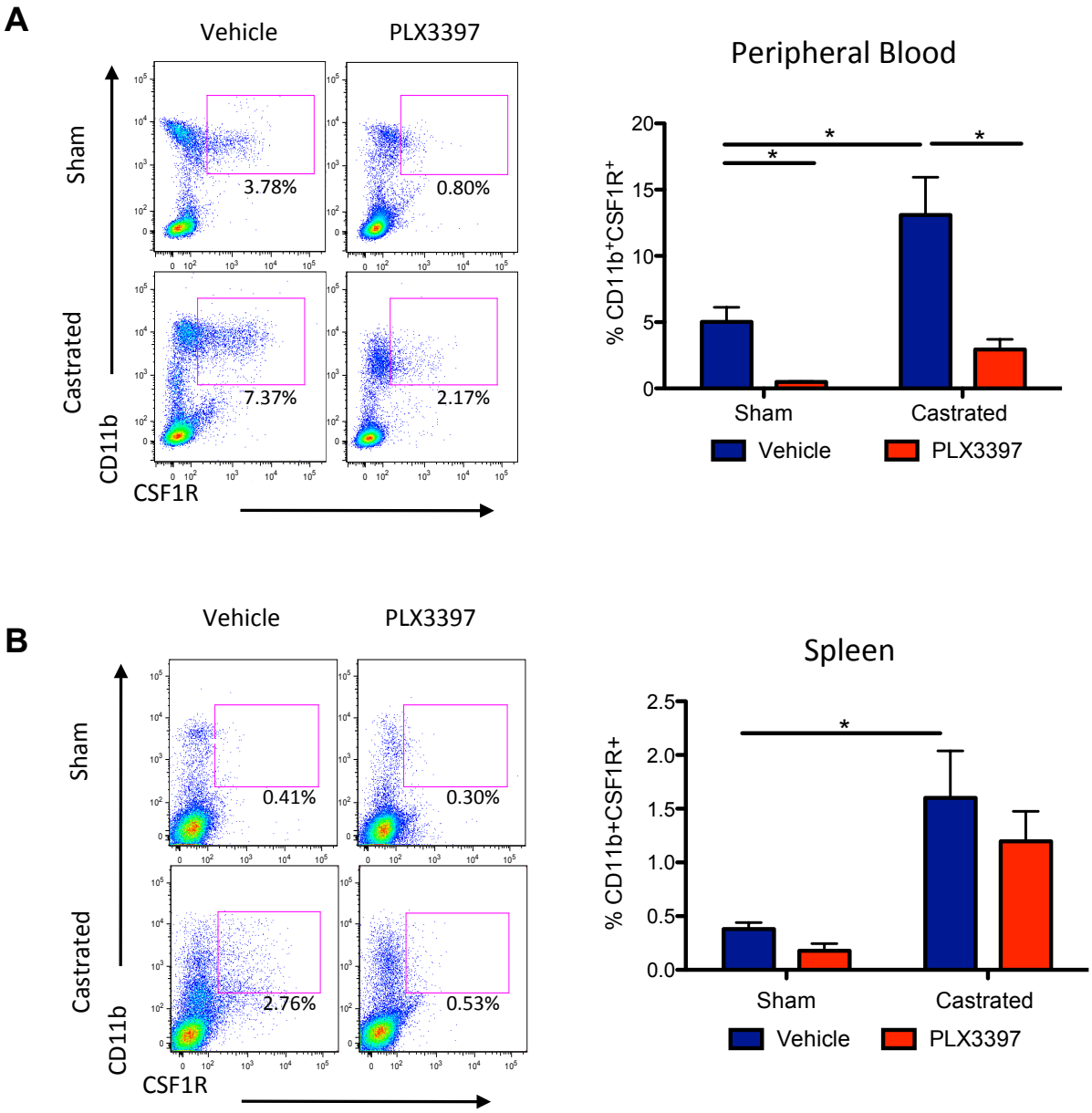

Figure 3.8: Systemic assessment of CD11b$^+$CSF1R$^+$ myeloid cells. Myc-CaP cells were subcutaneously implanted in syngeneic FVB male mice. Mice were sham castrated or castrated when tumors reached 300-500 mm^3. Mice were fed with control chow or PLX3397 daily for 36 days. A) Representative flow cytometry (left) plots of total CD11B$^+$CSF1R$^+$ myeloid cells and quantification (right) in peripheral blood and B) spleens. *P < 0.05. (n = 3-6/group).

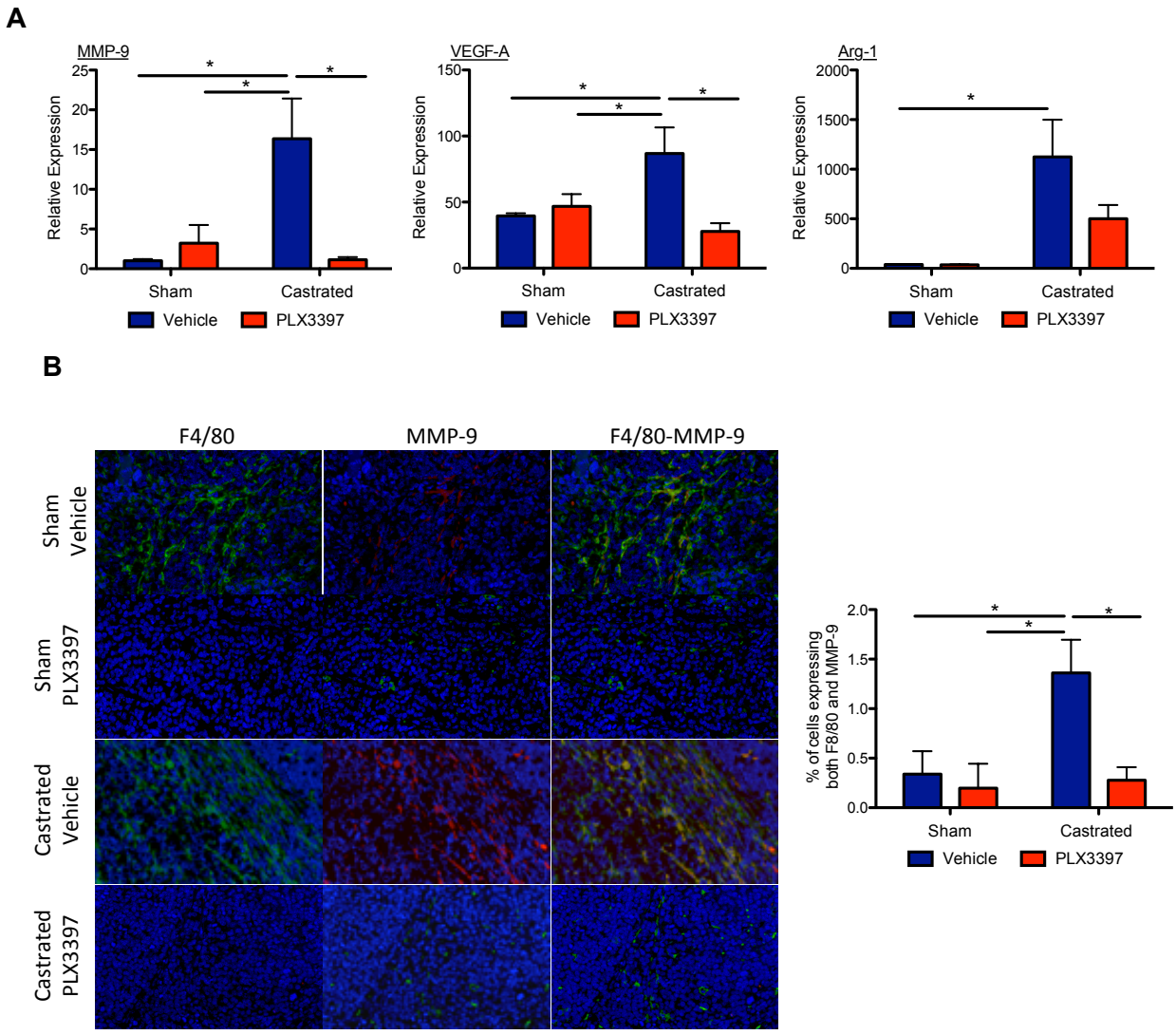

Figure 3.9: Modulation of changes in microenvironment factors with castration and PLX3397. Myc-CaP cells were subcutaneously implanted in syngeneic FVB male mice. Mice were sham castrated or castrated when tumors reached 300-500 mm^3. Mice were fed with control chow or PLX3397 daily for 36 days. Whole tumor RTPCR expression changes of A) Left to right, VEGF-A, MMP-9, and Arg-1 from each treatment group. B) IHF staining of representative Myc-CaP tumors from A showing images from F4/80 (green), MMP-9 (red) from each treatment group singly and overlaid (left), right, quantification of percent of cells expressing both F4/80

and MMP-9 (right). *P < 0.05. (n = 6-10/group).

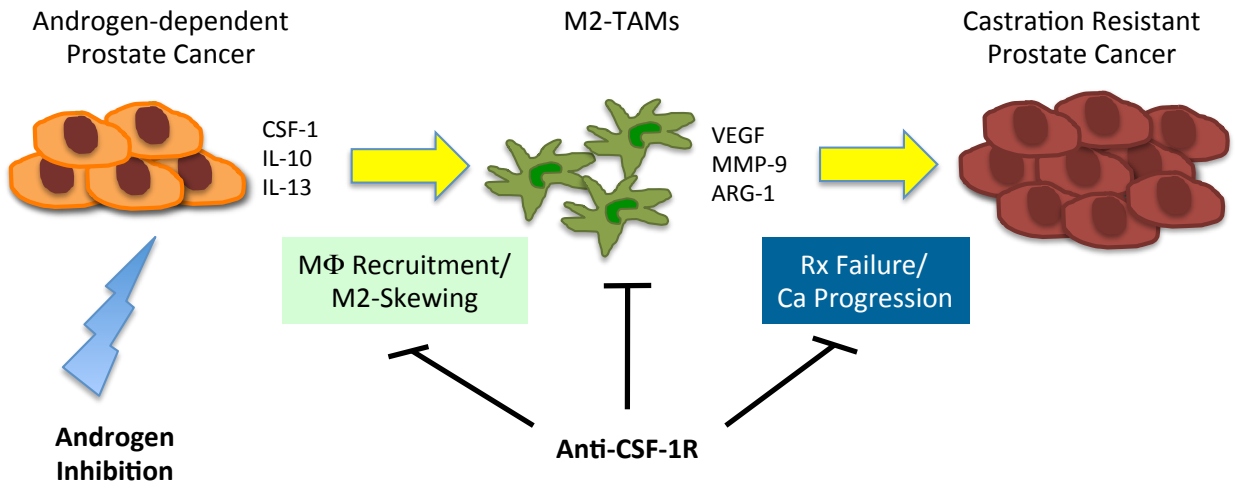

Figure 3.10: Model of androgen inhibition mediated recruitment and skewing of M2-macrophages and their effects on the onset of CRPC. Androgen deprivation by chemical or physical castration induces expression of macrophage recruiting cytokine CSF-1 as well as M2-skewing cytokines IL-10 and IL-13. M2-macrophages and their tumor promoting properties can be blocked using a CSF1R inhibitor, PLX3397 resulting in delayed onset of CRPC.

References

1. Huggins C, S.J.R., Hodges CV, *The effect of castration on advanced carcinoma of the prostate gland*. 1941.
2. Huggins, C., *Endocrine-induced regression of cancers*. 1967.
3. El-Amm, J. and J.B. Aragon-Ching, *The changing landscape in the treatment of metastatic castration-resistant prostate cancer*. Ther Adv Med Oncol. 5(1): p. 25-40.
4. Li, Y., et al., *Androgen receptor splice variants mediate enzalutamide resistance in castration-resistant prostate cancer cell lines*. 2012.
5. Tapio Visakorpi, E.H., Pasi Koivisto1, Minna Tanner1, Riitta Keinänen1, Christian Palmberg3, Aarno Palotie4, Teuvo Tammela3, Jorma Isola1 & Olli-P. Kallioniemi1, *In vivo amplification of the androgen receptor gene and progression of human prostate cancer*. Nature Genetics 1995. 9, 401 - 406.
6. Sun, Y., et al., *Treatment-induced damage to the tumor microenvironment promotes prostate cancer therapy resistance through WNT16B*. Nat Med. 18(9): p. 1359-68.
7. Loges, S., T. Schmidt, and P. Carmeliet, *Mechanisms of resistance to anti-angiogenic therapy and development of third-generation anti-angiogenic drug candidates*. Genes Cancer. 1(1): p. 12-25.
8. DeNardo, D.G., et al., *Leukocyte complexity predicts breast cancer survival and functionally regulates response to chemotherapy*. Cancer Discov. 1(1): p. 54-67.
9. Gordon, S., *Alternative activation of macrophages*. Nat Rev Immunol, 2003. 3(1): p. 23-35.
10. Hamilton, J.A., *Colony-stimulating factors in inflammation and autoimmunity*. Nat Rev Immunol, 2008. 8(7): p. 533-44.

11. Shih, J.-Y., *Tumor-Associated Macrophage: Its Role in Cancer Invasion and Metastasis*. Journal fo Cancer Molecules, 2006. 2(3): p. 101-106.

12. Talmadge, J.E., *Pathways mediating the expansion and immunosuppressive activity of myeloid-derived suppressor cells and their relevance to cancer therapy*. Clin Cancer Res, 2007. 13(18 Pt 1): p. 5243-8.

13. Pollard, J.W., *Tumour-educated macrophages promote tumour progression and metastasis*. Nat Rev Cancer, 2004. 4(1): p. 71-8.

14. Sica, A., et al., *Tumour-associated macrophages are a distinct M2 polarised population promoting tumour progression: potential targets of anti-cancer therapy*. Eur J Cancer, 2006. 42(6): p. 717-27.

15. Coussens, L.M. and Z. Werb, *Inflammation and cancer*. Nature, 2002. 420(6917): p. 860-7.

16. Ammirante, M., et al., *B-cell-derived lymphotoxin promotes castration-resistant prostate cancer*. Nature. 464(7286): p. 302-5.

17. Nonomura, N., et al., *Infiltration of tumour-associated macrophages in prostate biopsy specimens is predictive of disease progression after hormonal therapy for prostate cancer*. BJU Int.

18. Brakenhielm, E., et al., *Modulating metastasis by a lymphangiogenic switch in prostate cancer*. Int J Cancer, 2007. 121(10): p. 2153-61.

19. Priceman, S.J., et al., *Targeting distinct tumor-infiltrating myeloid cells by inhibiting CSF-1 receptor: combating tumor evasion of antiangiogenic therapy*. Blood. 115(7): p. 1461-71.

20. Ellwood-Yen, K., et al., *Myc-driven murine prostate cancer shares molecular features with human prostate tumors*. Cancer Cell, 2003. 4(3): p. 223–238.

21. Watson, P.A., et al., *Constitutively active androgen receptor splice variants expressed in castration-resistant prostate cancer require full-length androgen receptor*. Proc Natl Acad Sci U S A. 107(39): p. 16759-65.

22. Patsialou, A., et al., *Invasion of human breast cancer cells in vivo requires both paracrine and autocrine loops involving the colony-stimulating factor-1 receptor*. Cancer Res, 2009. 69(24): p. 9498-506.

23. Qian, B., et al., *A distinct macrophage population mediates metastatic breast cancer cell extravasation, establishment and growth*. PLoS One, 2009. 4(8): p. e6562.

24. Ide, H., et al., *Expression of colony-stimulating factor 1 receptor during prostate development and prostate cancer progression*. Proc Natl Acad Sci U S A, 2002. 99(22): p. 14404-9.

25. Benfan Wang, Q.L., Li Qin1, Siting Zhao1, Jinyan Wang1,4* and Xiaoping Chen1,2*, *Transition of tumor-associated macrophages from MHC class IIhi to MHC class IIlow mediates tumor progression in mice*. BMC Immunology 2011. 12:43.

26. Kambayashi, T., et al., *Potential involvement of IL-10 in suppressing tumor-associated macrophages. Colon-26-derived prostaglandin E2 inhibits TNF-alpha release via a mechanism involving IL-10*. J Immunol, 1995. 154(7): p. 3383-90.

27. Kim, J., et al., *IL-10 production in cutaneous basal and squamous cell carcinomas. A mechanism for evading the local T cell immune response*. J Immunol, 1995. 155(4): p. 2240-7.

28. Chitu, V. and E.R. Stanley, *Colony-stimulating factor-1 in immunity and inflammation*. Curr Opin Immunol, 2006. 18(1): p. 39-48.

29. Xu, J., et al., *Abrogating the protumorigenic influences of tumor-infiltrating myeloid cells byCSF1R signaling blockade improves the efficacy of radiotherapy in prostatecancer*. Cancer Res.

30. Hanahan, D. and R.A. Weinberg, *Hallmarks of cancer: the next generation*. Cell. 144(5): p. 646-74.

31. Van Ginderachter, J.A., *The wound healing chronicles*. Blood. 120(3): p. 499-500.

32. Zhu, P., et al., *Macrophage/cancer cell interactions mediate hormone resistance by a nuclear receptor derepression pathway*. Cell, 2006. 124(3): p. 615-29.

33. Marques, R.B., et al., *Bypass mechanisms of the androgen receptor pathway in therapy-resistant prostate cancer cell models*. PLoS One. 5(10): p. e13500.

34. Dirkx, A.E., et al., *Monocyte/macrophage infiltration in tumors: modulators of angiogenesis*. J Leukoc Biol, 2006. 80(6): p. 1183-96.

35. Pang, R.W. and R.T. Poon, *Clinical implications of angiogenesis in cancers*. Vasc Health Risk Manag, 2006. 2(2): p. 97-108.

36. Miller, A.M. and P. Pisa, *Tumor escape mechanisms in prostate cancer*. Cancer Immunol Immunother, 2007. 56(1): p. 81-7.

37. Lu, C., et al., *Immunotherapy for metastatic prostate cancer: where are we at with sipuleucel-T?* Expert Opin Biol Ther. 11(1): p. 99-108.

Chapter 4:

IGF1R Signaling in Castration-Resistant Prostate Cancer Induced by Tumor Associated Macrophage IGF-1 During Androgen Blockade Therapy

Abstract

Anti-apoptotic and mitogenic mechanisms are key factors in the progression of prostate cancer (PCa) toward castration-resistant prostate cancer (CRPC). Insulin like growth factor (IGF-1) has long been implicated in castration resistance. Concordantly, upregulation of IGF-1 expression and signaling are frequently observed in CRPC tumors. IGF-1 is thought to be primarily of stromal origin. Interestingly, macrophages have been shown to express IGF-1 when induced to an alternative activation state (M2) by the Th2 cytokines IL-4/IL-13. In the context of androgen blockade therapy (ABT), M2-macrophages as a source of IGF-1 and possibly a means of CRPC development has never been elucidated. Here, ABT-induced IL-13 expression in PCa cells is shown to increase both IGF-1 transcript and protein expression from co-cultured bone marrow derived macrophages (BMDM). Increased IGF-1 expression correlated with a ~5 fold increase in the downstream IGF1R target gene, *c-Fos*, in PCa cells. Moreover, IGF-1 expression was induced in PCa tumors following castration, then was reduced after macrophage depletion using the CSF1R inhibitor, PLX3397. This reduction in IGF-1 expression also correlated with a reduction of the Ki67 proliferation index of the tumors. Additionally, higher levels of IGF1R immunohistchemistry (IHC) staining were observed in castrated tumors. However, following macrophage depletion, p-ERK staining decreased, suggesting a reduction in the activation of IGFR signaling. Collectively, these findings are indicative of a novel paracrine stimulatory loop assisting in the growth of CRPC post-ABT, with PCa-produced Th2 cytokines recruiting and creating M2 macrophages that secrete IGF-1, which in turn, stimulates the growth of the PCa cells.

Introduction

Advances in the treatment of castration resistant prostate cancer (CRPC) have recently emerged, providing extended survival benefits to prostate cancer (PCa) patients; however, none of these approaches are curative and, will eventually fail (1). PCa remains the second leading cause of cancer related death in American men, accounting for 28% of male cancer related cases (2). Prostate cells require androgen signaling for growth and survival in normal and pathological conditions, thus androgen blockade therapy (ABT) is a mainstay treatment for advanced PCa (1). Additionally, with the discovery that a large portion of CRPC remains sensitive to androgen receptor (AR) signaling, innovative approaches to block this axis have emerged including Zitiga (abiraterone acetate), a CYP17 inhibitor, and MDV3100 (Enzalutamide, Xtandi or MDV), an AR competitive inhibitor with a triple inhibitory mechanism: blockade of ligand binding, AR nuclear translocation and DNA binding (3, 4).

Multiple lines of evidence suggest a significant involvement of the insulin-like growth factor 1 (IGF-1) axis in PCa progression and in mediating resistance to ABTs (5, 6). Androgen independent (AI) growth requires loss of the apoptotic response to ABT and activation of alternate cell survival pathways, as well as AR activation in the absence of ligand (7). Inhibition of the IGF-1 receptor (IGF1R) signaling in rodent models via antisense oligos, anti-IGF1R antibodies, and small molecule inhibitors are able to suppress PCa proliferation and growth both *in vivo* and *in vitro* (8). In the context of ABT, IGF-1 is thought to block the apoptotic effect of ABT on PCa, restoring proliferation in both AR-dependent and AR-independent mechanisms (9).

The IGF-1 axis is important for cell proliferation, apoptosis, and cell differentiation; thus,

it is very important for the growth and development of many normal tissues (8, 10). IGF1R is a transmembrane tyrosine kinase found overexpressed in many tumors, including melanoma, colon, kidney and prostate (11). IGF1R signaling in cancer is thought to protect cells from apoptosis, in particular when IGF1R is expressed at higher levels as is observed in many cancers (11). Upon ligand activation of IGF1R, downstream activation of signaling pathways commence, including the Ras/mitogen-activated protein kinase (MAPK)/extracellular signal-regulated kinases (ERK) and phosphatidylinositol 3'-kinase (PI3K)/AKT pathways (5, 11).

Prostate stromal cells are known to secrete IGF-1 and to be important for growth and development, as well as for neoplastic proliferation (8). The stromal cell population is comprised of fibroblasts, macrophages and endothelial cells (8, 12). Studies using murine bone marrow derived macrophages (BMDM) have shown that Th2 cytokines IL-4/IL-13 potently induce IGF-1 expression in a STAT6-dependent manner (13). In another study using a lung macrophage cell line and alveolar primary macrophages, exogenous IL-4 and IL-13 were shown to significantly increase IGF-1 expression (14). This study also showed that IGF-1 expression was over 2 times higher in tumor-educated macrophages versus naïve macrophages. In addition, media from tumor educated macrophages stimulated neoplastic proliferation in lung cancer cells, coinciding with increased phosphorylation of p-ERK 1/2 (14).

A large number of studies have shown macrophage activation by Th2 cytokines promote an alternative activation state, termed M2-macrophages. M2-macrophages are known to promote tumor progression in various cancers (15). Mechanisms by which M2-macrophages can promote cancer progression include: promoting angiogenensis by secreting angiogenic factors (VEGF-A), promoting growth and proliferation via production of growth factors (EGF, PDGF, and FGF),

matrix remodeling, and anti-tumor immune suppression (16).

The available data support the hypothesis that macrophages skewed to M2 by Th2 cytokines can be a source of IGF-1, and thus provide a possible CRPC AR bypass mechanism via IGF1Rs anti-apoptotic and proliferative capacities. Therefore, studies were undertaken to determine whether ABT treatment of PCa cells modulated the expression of IGF-1 in M2 macrophages. Here, we show that ABT treatment of PCa cells induced the expression of IL-13, which resulted in increased IGF-1 in BMDMs in co-culture. Additionally, tumors grown in castrated mice showed an increase in IGFR1 phosphorylation compared to tumors from mice that underwent a sham castration. Furthermore, increased IGF-1 expression in BMDMs correlated with increased expression of the downstream p-IGF1R/p-ERK target gene *c-Fos* (17) in PCa cells. Finally, blockade of tumor-associated macrophages (TAMs) recruitment *in vivo* using a CSF1R inhibitor, PLX3397, resulted in delayed onset of CRPC.

Materials and Methods

Cell Culture

Murine Myc-CaP cells (a kind gift from Dr. Charles Sawyers, Memorial Sloan Kettering New York), were cultured in Dulbecco modified Eagle medium (DMEM), containing 10% fetal bovine serum (FBS), 100 U/mL penicillin, and 100 μg/mL streptomycin (complete DMEM) at 37°C with 5% CO_2.

Real-time RT-PCR

Total cellular RNA was extracted with TRIzol Reagent. RNA was isolated according to the TRIzol procedure. Real-time quantitative reverse-transcribed polymerase chain reaction (RTPCR) was performed as previously described (18).

Co-Culture Assay

RAW (1.0 x 10^6 cells) were seeded in 4 μm transwell inserts in DMEM, with 10% FBS, and 1% P/S. Inserts were placed in 6 well plates containing Myc-CaP (2.5 x 10^5 cells) treated with MDV (10 μM) or dimethyl sulfoxide (DMSO, vehicle or veh). Co-cultures were incubated for 48 hrs at 37°C. Following the incubation period cells were harvested with TRIzol Reagent and total cellular RNA was extracted as described above.

ELISA

IGF-1 levels in cell lysates and serum samples were measured using enzyme-linked immunosorbent assay (ELISA). Cell lysates were prepared from Myc-CaP (2.5 x 10^5 cells) treated with DMSO (vehicle or veh) or MDV (10 μM) for 48 hrs at 37°C. Following the

incubation period, cells were lysed in RIPA buffer (Upstate) containing proteinase inhibitor cocktail (Sigma), centrifuged 5 min at 1,500 xg. ELISA was performed using the Mouse/Rat IGF-1 Quantikine Kit (R &D systems) according the manufacturer's instructions. Optical density of each well was determined immediately using a microplate reader set to 450 nm with a 570 nm subtraction. All standards and samples were assayed in duplicate.

In vivo Studies

FVB male mice (6-8 weeks old) were purchased from Taconic Farms, Inc. Myc-CaP cells (2 x 10^6 cells) were implanted subcutaneously above both shoulders. All animal experiments were approved by the Animal Research Committee of the University of California-Los Angeles. Mice were castrated when tumors reached 300-500 mm^3. Treatments were initiated the day after castration. For castration and PLX3397 studies, mice were fed daily chow containing PLX3397 or control chow formulated at an average dose per animal per day at 40 mg/kg. Tumor size was measured every 2-3 days by digital calipers as previously described (18). Mice were sacrificed and tissues were analyzed at the ethical tumor size limit of 1.5 cm in diameter.

Immunohistochemistry

Tumor sections were harvested and fixed in 3% paraformaldehyde (PFA) overnight, then placed in 50% ethanol (EtOH) until paraffin embedding. Tumor sections (4 μm) were stained with p-IGF1R (Tyr1161, 1:100; Santa Cruz), p-ERK (Thr202/Tyr204, 1:100; Santa Cruz), Ki67 (1:500, Vector Labs). Ki67 samples were analyzed using the Nikon Eclipse 90i microscope captured at 10x magnification and processed using Photoshop CS software. Five to six fields per slide at 10x magnification were quantified using ImageJ Version 1.34s (National Institute of

Health). The p-IGF1R and p-ERK slides where scanned at the UCLA Translational Pathology Core Laboratory (TPCL). For immunohistochemistry (IHC) and hematoxylin and eosin (H&E) staining slides were scanned using the Aperio wholeslide scanner.

Flow Cytometry

Tumor single cell suspensions were prepared for flow cytometry as previously described (19). After RBC lysis (Sigma), single-cell suspensions were incubated for 30 minutes on ice with the following antibodies: CD11b-e450, Gr-1- F4/80-PE-Cy7, and CD115 (CSF1R)-PE conjugated antibodies, 1:200 (eBioscience) followed by two washes wash with 2% FBS in PBS (FACS buffer). Cells were fixed in 3% PFA for 15 min at room temperature and washed twice with FACS buffer. Cell acquisition was done on a BD LSR-II flow cytometer (Beckman Coulter). Data was analyzed with FlowJo software (TreeStar).

Statistical Analysis

Data are presented as mean plus or minus SEM. Statistical comparisons between groups were performed using the Student *t* test.

Results

Androgen blockade therapy increases Th2 cytokine expression in PCa cells that induces IGF-1 expression in macrophages. A large amount of evidence suggests that prostate stroma play a large role in the progression of PCa to CRPC (9, 20, 21). Thus, the effects of ABT on myeloid subsets in the prostatic tumor microenvironment was studied using the syngeneic FVB murine prostate cancer model, Myc-CaP. The Myc-CaP model allows for PCa studies in an immune competent setting, allowing for myeloid cell analysis with the full complement of the immune system. Moreover, the Myc-CaP cell line is androgen-dependent which allows the study of the ABT effects both *in vivo* and *in vitro* (22).

Previous studies in our laboratory examining myeloid infiltrates in Myc-CaP tumors by flow cytometry showed that the predominant myeloid population is $CD11b^{+}F4/80^{+}CSF1R^{+}$ macrophages (~97% of total myeloid cells) comprising approximately 3-5% of the total tumor cell population. Moreover, we have previously shown that ABT induces the expression of the Th2 cytokines IL-13 and IL-10 but not IL-4. Additionally, co-culturing BMDMs with Myc-CaP cells treated with MDV3100 skewed macrophages to an M2 phenotype, displaying low MHCII levels, and high MMP-9, VEGF-A, and Arg-1 expression (data not shown). To corroborate our previous findings, Myc-CaP cells were treated with MDV3100 and changes in IL-13 expression were assessed. Figure 4.1 shows there was a 27 fold increase in IL-13 transcript expression in Myc-CaP cells after a 48 hr incubation with MDV3100 (10 μM).

Next, it was determined whether the increase in IL-13 expression in Myc-CaP cells correlated with increased IGF-1 expression in bone marrow-derived macrophages (BMDM). To this end, a transwell co-culture system combining ABT-treated Myc-CaP cells and BMDM for

48 hrs was employed. We found that BMDM cultured with Myc-CaP cells and MDV3100 had about a 2-fold increase in IGF-1 expression (Figure 4.2a). To further validate these findings, conditioned media from Myc-CaP cells cultured with MDV3100 for 48 hrs was used to stimulate BMDMs showing almost identical results as in the co-culture system (Figure 4.2b). When looking at IGF-1 transcript levels in Myc-CaP cells, no significant changes were found after MDV3100 treatment (Figure 4.2c).

In order to determine if the increase in IGF-1 transcript expression correlated with changes in IGF-1 protein levels, ELISA was performed. There was no detectable IGF-1 in Myc-CaP cells; however, IGF-1 levels in BMDM increased 2 fold after treatment with conditioned media from MDV3100 treated Myc-CaP cells (Figure 4.2d).

Next, we sought to determine if the increase in IGF-1 from BMDM resulted in increased expression of IGF1R target gene, c-Fos, which would suggest increased p-ERK signaling and activation of the downstream MAPK/ERK axis (23) in Myc-CaP cells. Using the co-culture system, a 25-fold increase in c-Fos expression was found in Myc-CaP cells when co-cultured with BMDM and MDV3100 (Figure 4.3).

To further validate these findings using another form of androgen blockade we employed surgical castration as a means of androgen deprivation. Levels of IGF1R activation were assessed by staining whole tumor sections for IGF1R-Tyr1161 (p-IGF1R) using immunohistochemistry (IHC). The preliminary studies comparing Myc-CaP tumors from sham surgery and castrated CRPC (38 days post castration) mice show there was a notable increase in p-IGF1R staining in CRPC tumors compared to sham (Figure 4.4). These results suggest that the IGF-1 induction in macrophages may lead to increased IGF1R activation in PCa cells.

Blocking TAMs reduces castration induced IGF-1 expression and improves therapeutic outcome. Next, the potential effects of macrophage secreted IGF-1 on Myc-CaP tumor growth and proliferation post-castration were assessed. To determine if the increase in IGF-1 expression in BMDM after co-culturing with ABT treated Myc-CaP coincided with IGF-1 changes in castrated tumors and whether IGF-1 levels could be modulated with macrophage depletion, the small molecule CSF1R inhibitor, PLX3397, was used. PLX3397 has been reported to be a potent CSF1R inhibitor, and has been shown to effectively deplete macrophages and other myeloid populations from breast and prostate tumors (24, 25). Moreover, PLX3397 efficacy is currently being investigated in patients with several ongoing clinical trials including CRPC (26). Flow cytometric analysis of Myc-CaP tumors revealed macrophage infiltration in the castrated tumors was a significant increase in macrophages (5.21 +/_ 0.41%) compared to the sham group (2.9 +/_ 0.66%) (Figure 4.5b). The increase in macrophage population was significantly reduced in the PLX3397 treated, castrated group (Figure 4.5b). Additionally, results showed that levels of IGF-1 transcript from castrated tumors were significantly increased in the CRPC tumors compared to the sham group. However, macrophage depletion by PLX3397 treatment resulted in decreased IGF-1 expression in the tumors from castrated mice (Figure 4.5c). More importantly, macrophage depletion in the castrated group showed a significant delay in the onset of CPRC (Figure 4.5a).

Next, we sought to determine if the delayed onset of CRPC in the PLX3397 treated group coincided with changes in proliferation as measured by the Ki67 proliferation marker. Using immunohistofluorescence (IHF) staining of paraffin-fixed tumor sections, we found that the castrated, untreated tumors had significantly higher levels of proliferation staining per nuclei

compared to the sham group. Furthermore, the castrated, macrophage-depleted group (PLX3397 treated) had significantly lower Ki67 levels than the castrated, untreated group (Figure 4.6a-b).

Lastly, to determine if reduced macrophage infiltration correlated with decreases in downstream signaling of IGF1R, ERK activation status was investigated in castrated, untreated and castrated, PLX3397 treated tumors. The preliminary findings using IHC staining for p-ERK (Thr202/Tyr204) suggested there were fewer p-ERK positive cells in the castrated plus PLX3397 tumors compared to castrated alone (Figure 4.7).

In summary, the combined preliminary results suggest that androgen inhibition of PCa induces TAM influx, as well as changes in their expression of anti-apoptotic and mitogenic factors such as IGF-1. Moreover, depletion of the macrophage tumor population by CSF1R blockade therapy with PLX3397 significantly decreased the tumor proliferation index and delayed the onset of CRPC.

Discussion

IGF1R signaling during androgen-independent growth of prostate cancer cells is thought to play a major role in resistance to ABT (5, 21). Stromal-derived factors promoting growth in both normal prostate and under pathological conditions is a well known phenomenon (8, 12, 27). Additionally, the involvement of stromal macrophages in cancer promotion and progression has recently received much attention due to the Th2 cytokines-induced, pro-tumorigenic role they can play in tumors (15, 16).

The results presented here suggest that TAMs, in the context of androgen signaling inhibition, promote growth of PCa via an IGF1R mechanism. We show that MDV3100 treatment of the murine PCa cell line, Myc-CaP, resulted in increased IL-13 expression, and that, there is a ~2-fold increase in IGF-1 expression in BMDMs following co-culturing experiments. We also show that the increase in IGF-1 from BMDMs correlates with increased expression of the downstream IGF1R target gene, *c-Fos*, in Myc-CaP cells. When comparing Myc-CaP tumors from sham surgery and castrated mice, we found there was an observable increase in phosphorylated IGF1R in the castrated tumors. Additional *in vivo* studies assaying ABT via castration of Myc-CaP tumor bearing mice demonstrated an increase in IGF-1 expression in castrated tumors and this increase was subsequently reduced after macrophage depletion using the CSF1R inhibitor, PLX3397. When examining at levels of phosphorylated ERK1/2 in castrated alone versus castrated and PLX3397 treated tumors, a decrease in p-ERK staining was measured by IHC. Moreover, the onset of CRPC in Myc-CaP tumors was significantly delayed with macrophage depletion. Lastly, the observed effects on tumor growth correlated with Ki67 proliferation index showing higher levels in castrated tumors and a significant decrease after macrophage depletion.

Tumor-educated macrophages have been shown to display tumor promoting phenotypes (28). Specifically, increased growth factor expression is observed from Th2 skewed macrophages, including increased IGF-1 after IL-4 and IL-13 stimulation (13, 14). Additionally, whether IL-13 is the sole factor inducing IGF-1 in BMDMs has not been determined. Although direct induction of IGF-1 expression by CSF-1 signaling in TAMs has not been reported to date, there are reports of CSF-1 inducing IGF-1 during the differentiation process of murine bone marrow cells (29). In previous studies using MDV3100 and Myc-CaP cells, we found that CSF-1 is also significantly increased (data not show). Thus, it is also possible that CSF-1 is another means of IGF-1 induction in TAMs, either singly or in concert with IL-13. Future studies including IL-13 blockade using neutralizing antibodies (30) or IL-4/IL-13 receptor antagonists are necessary, both alone and in combination with CSF-1R blockade (19), to determine the key mediators of IGF-1expression induction. In addition, further studies are is necessary to determine if the increased IL-13 transcript expression observed in Myc-CaP cells post-ABT translates to increased protein levels.

The downstream IGF1R target gene *c-Fos* used here as a readout of IGF1R activation is a direct target of the ERK signaling pathway (17). However, activation of the ERK signaling cascade is not restricted to IGF1R, but can be mediated by multiple receptor tyrosine kinases (RTKs) including VEGFR, CSF1R, EGFR, and FGFR (31, 32). Therefore, further studies are required to confirm the results presented here, such as inclusion of IGF1R inhibitors to identify the level of IGF1R involvement in increasing c-Fos transcription in Myc-CaP cells, or whether other RTKs are involved. Studies have shown that macrophage-secreted IGF-1 can increase the proliferation of neoplastic lung cells (14), thus, further testing is needed to determine whether BMDM IGF-1 can increase the proliferation of Myc-CaP cells in the context of ABT. The

increase in p-IGF1R IHC staining observed in castrated tumors compared to sham surgery also requires further analysis, such as concurrent staining of total IGF1R to determine whether the observed increase is, in fact, due to increased activation and not simply an artifact of increased receptor expression. In addition, IGF1R is expressed at high levels in macrophages (33); therefore, it is also possible that the increase in p-IGF1R staining observed is due to increased macrophage infiltration after castration, and not due to increased tumor cell activation (Figure 4.4).

To conclude, the possible effects of macrophage secreted IGF-1 are several fold. The IGF1R axis has been shown to be a key player in the progression of PCa to CRPC (5, 34). Here, we provide a novel mechanism of paracrine signaling between androgen-deprived PCa cells and macrophages that may, in part, provide an alternative to AR signaling for CRPC via macrophage secreted IGF-1. If these findings are correct, combinatorial approaches of ABT and CSF1R-mediated macrophage blockade may be a feasible strategy to improve the duration of novel PCa therapeutics.

Figures

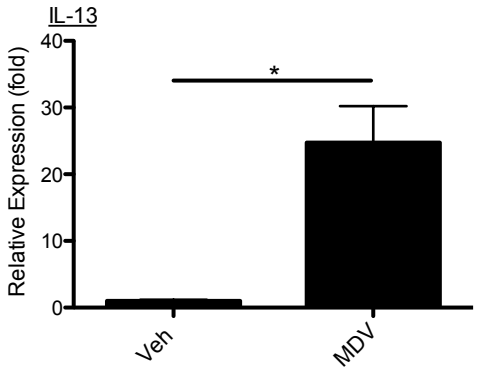

Figure 4.1: Th2 cytokine IL-13 induced expression in Myc-CaP cells after androgen blockade therapy. Assessment of IL-13 transcript changes in MDV (10 mg/kg) or DMSO (veh) treated Myc-CaP cells. Transcript expression changes were assessed by RTPCR from Myc-CaP cells cultured for 48 hrs. Data was normalized to actin. *$P < 0.05$ compared to control. ($n = 3$).

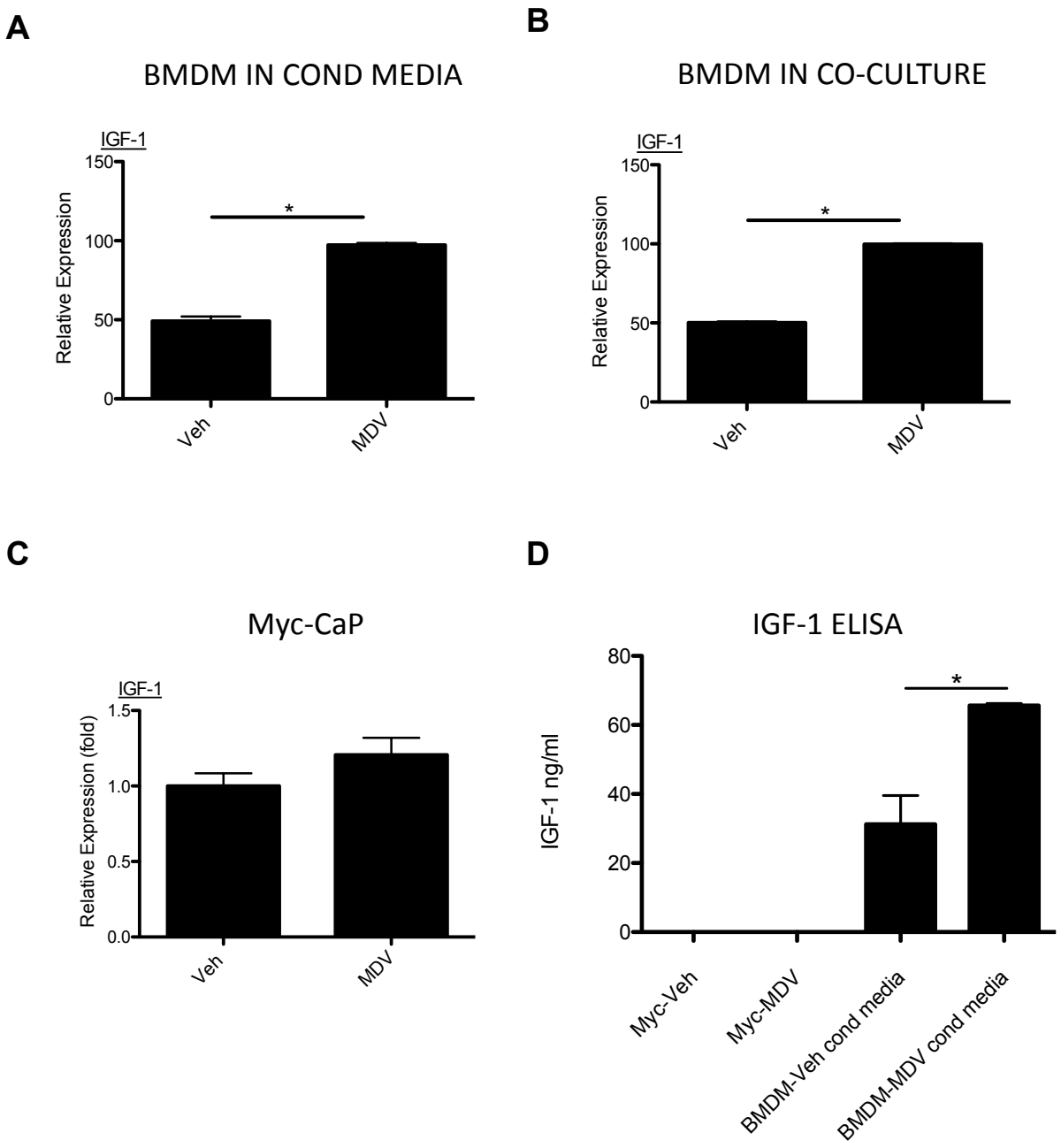

Figure 4.2: Macrophage secreted IGF-1 after androgen blockade treatment of Myc-CaP cells. Assessment of IGF-1 transcript expression changes in A) BMDM cultured in conditioned media from treated Myc-CaP cells (n = 4) or B) co-cultured with Myc-CaP cells with DMSO (veh) or MDV (10 μM or 20 μM, n = 2). C) IGF-1 transcript changes in Myc-CaP cells treated

with DMSO (Veh) or MDV (10 uM) D) IGF-1 ELISA of Myc-CaP and BMDM lysate. Myc-CaP cells were treated as in B and BMDM were cultured in conditioned media from Myc-CaP cells treated with DMSO or MDV 10 μM (n = 4).

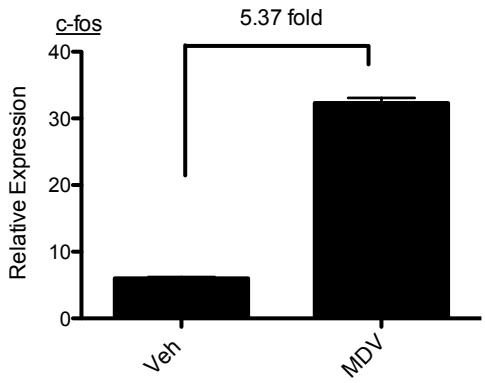

Figure 4.3: Myc-CaP and BMDM co-culture induced downstream IGF1R target c-Fos expression in Myc-CaP cells after anti-androgen treatment. Assessment of c-Fos transcript expression changes in Myc-CaP cells by RTPCR. BMDMs were co-cultured with Myc-CaP cells with DMSO (veh) or MDV (10 μM, n = 1).

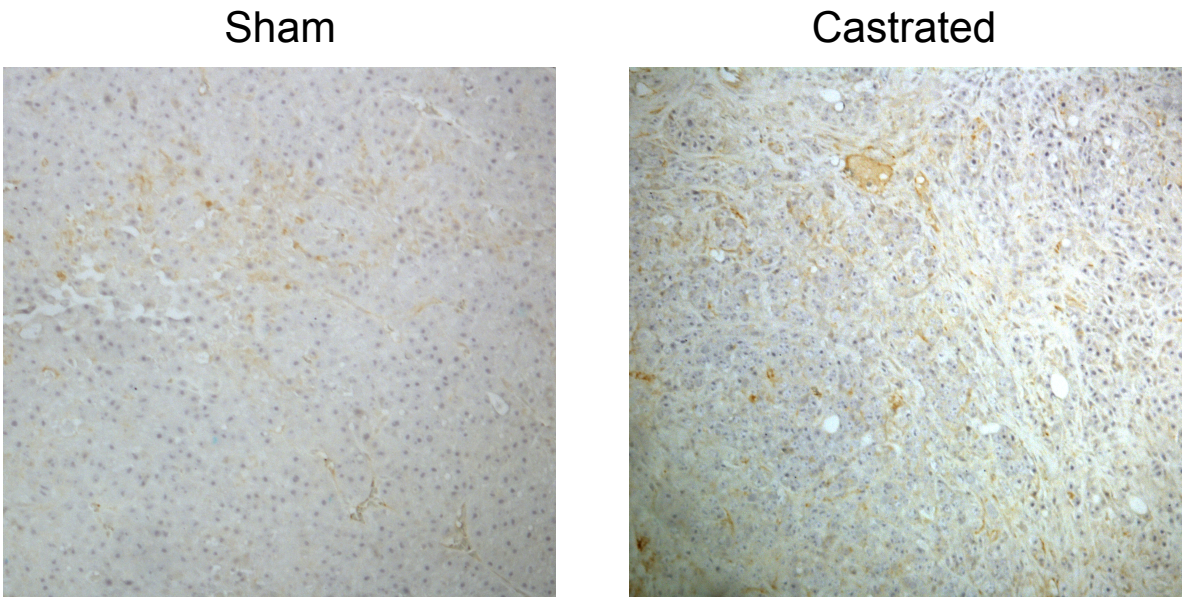

Figure 4.4: Castration induced IGF1R phosphorylation in Myc-CaP tumors. Myc-CaP cells were subcutaneously implanted in syngeneic FVB male mice. IHC staining for IGF1R-Tyr1161. Mice were sham castrated or castrated when tumors reached 300-500 mm^3. Tumors were harvest at day 14 for the sham group and day 38 for the castrated group (n = 1/group).

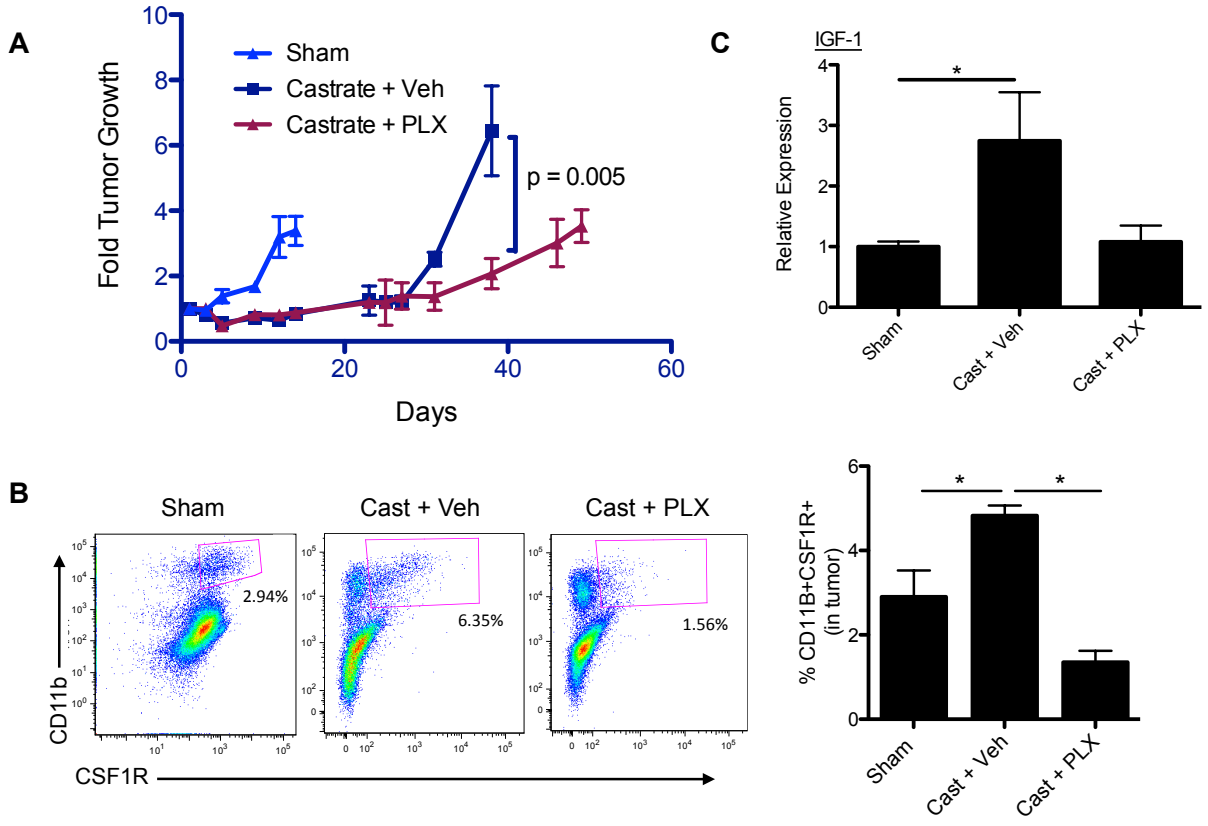

Figure 4.5: Delayed CRPC development from blockade of castration induced TAM infiltration. Myc-CaP cells were subcutaneously implanted in syngeneic FVB male mice. Mice were sham castrated or castrated when tumors reached 300-500 mm^3. Mice were fed with control chow or PLX3397 daily for 38 (castrated + veh) and 49 (castrated + PLX) days. A) Tumor growth from each treatment group. B) Representative flow cytometry plots of total $CD11B^+CSF1R^+$ TAMs in tumors. C) IGF-1 transcript expression from each group taken at day 38 (n = 6-10/group).

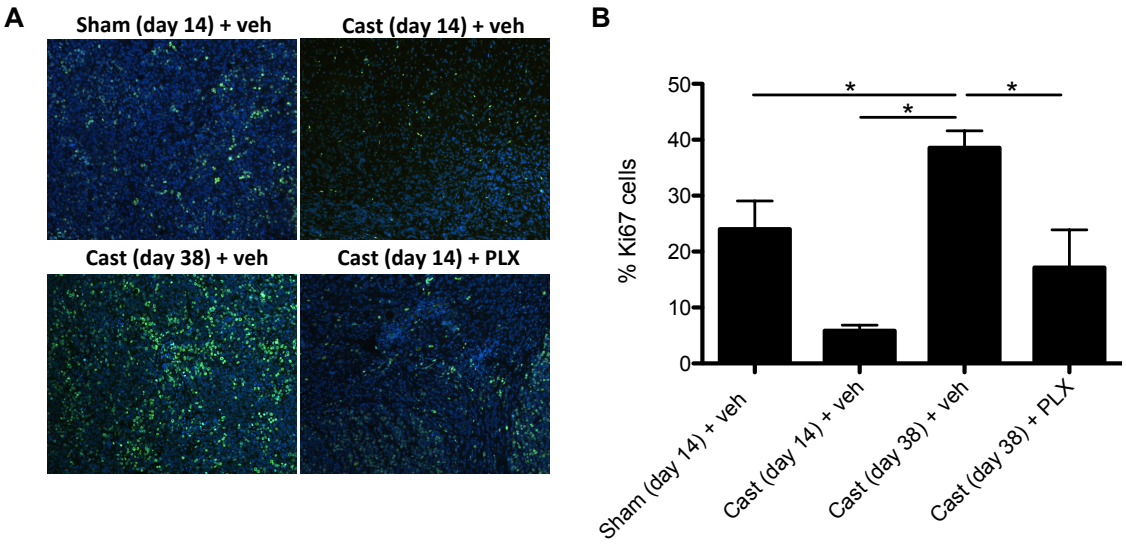

Figure 4.6: Blockade of TAM infiltration reduced Ki67 proliferation staining of Myc-CaP castrated tumors. Myc-CaP cells were subcutaneously implanted in syngeneic FVB male mice. Mice were sham castrated or castrated when tumors reached 300-500 mm^3. Mice were fed with control chow or PLX3397 daily for 38 days. A) Representative IHF staining of Myc-CaP tumors from sham tumors (day 14), day 14 post-castration, day 38 post-castration with or without treatment (Cast (day 38) + veh, Cast (day 38)+ PLX), Ki67 (green) and DAPI (blue). B) Quantification of Ki67 staining per group (total Ki67/total nuclei, n = 5).

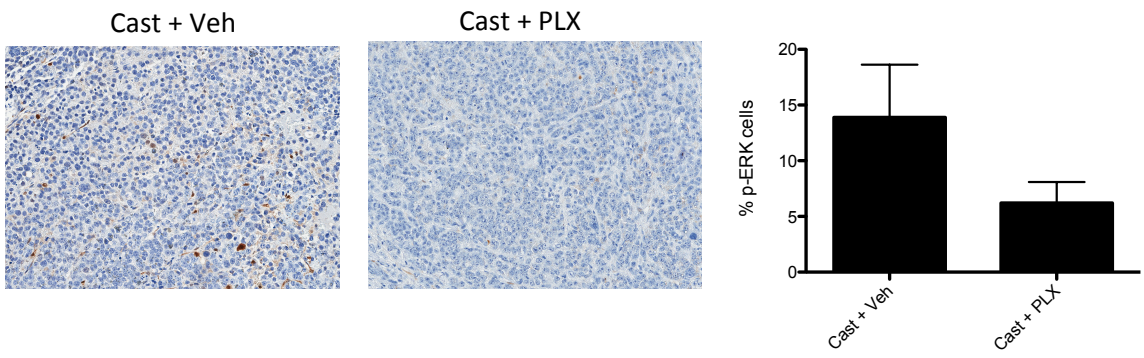

Figure 4.7: Macrophage depletion decreases p-ERK staining in CRPC tumors. Myc-CaP cells were subcutaneously implanted in syngeneic FVB male mice and treated as in Figure 4.6. IHC staining for ERK-Thr202/Tyr204 on day 38 tumors. (n = 3/group).

References

1. Harris, W.P., et al., *Androgen deprivation therapy: progress in understanding mechanisms of resistance and optimizing androgen depletion*. Nat Clin Pract Urol, 2009. 6(2): p. 76-85.
2. Siegel, R., D. Naishadham, and A. Jemal, *Cancer statistics, 2013*. CA Cancer J Clin. 63(1): p. 11-30.
3. El-Amm, J. and J.B. Aragon-Ching, *The changing landscape in the treatment of metastatic castration-resistant prostate cancer*. Ther Adv Med Oncol. 5(1): p. 25-40.
4. Fu, W., et al., *Progress of molecular targeted therapies for prostate cancers*. Biochim Biophys Acta. 1825(2): p. 140-52.
5. Krueckl, S.L., et al., *Increased insulin-like growth factor I receptor expression and signaling are components of androgen-independent progression in a lineage-derived prostate cancer progression model*. Cancer Res, 2004. 64(23): p. 8620-9.
6. Cale D Fahrenholtz, P.J.B., Kerry L Burnstein. *Targeting IGF-1R with ganitumab inhibits tumorigenesis and increases durability of response to androgen-deprivation therapy in VCaP prostate cancer xenografts*. 2013.
7. Gurumurthy, S., K.M. Vasudevan, and V.M. Rangnekar, *Regulation of apoptosis in prostate cancer*. Cancer Metastasis Rev, 2001. 20(3-4): p. 225-43.
8. Kawada, M., et al., *Insulin-like growth factor I secreted from prostate stromal cells mediates tumor-stromal cell interactions of prostate cancer*. Cancer Res, 2006. 66(8): p. 4419-25.

9. Wu, J.D., et al., *In vivo effects of the human type I insulin-like growth factor receptor antibody A12 on androgen-dependent and androgen-independent xenograft human prostate tumors*. Clin Cancer Res, 2005. 11(8): p. 3065-74.

10. Leo, S., C. Accettura, and V. Lorusso, *Castration-resistant prostate cancer: targeted therapies*. Chemotherapy. 57(2): p. 115-27.

11. Riedemann, J. and V.M. Macaulay, *IGF1R signalling and its inhibition*. Endocr Relat Cancer, 2006. 13 Suppl 1: p. S33-43.

12. Tuxhorn, J.A., et al., *Reactive stroma in human prostate cancer: induction of myofibroblast phenotype and extracellular matrix remodeling*. Clin Cancer Res, 2002. 8(9): p. 2912-23.

13. Wynes, M.W. and D.W. Riches, *Induction of macrophage insulin-like growth factor-I expression by the Th2 cytokines IL-4 and IL-13*. J Immunol, 2003. 171(7): p. 3550-9.

14. Fritz, J.M., L.D. Dwyer-Nield, and A.M. Malkinson, *Stimulation of neoplastic mouse lung cell proliferation by alveolar macrophage-derived, insulin-like growth factor-1 can be blocked by inhibiting MEK and PI3K activation*. Mol Cancer. 10: p. 76.

15. Porta, C., et al., *Cellular and molecular pathways linking inflammation and cancer*. Immunobiology, 2009. 214(9-10): p. 761-77.

16. Sica, A., et al., *Tumour-associated macrophages are a distinct M2 polarised population promoting tumour progression: potential targets of anti-cancer therapy*. Eur J Cancer, 2006. 42(6): p. 717-27.

17. Zhang, P.J., et al., *The inhibitory effects of NKX3.1 on IGF-1R expression and its signalling pathway in human prostatic carcinoma PC3 cells*. Asian J Androl. 14(3): p. 493-8.

18. Brakenhielm, E., et al., *Modulating metastasis by a lymphangiogenic switch in prostate cancer*. Int J Cancer, 2007. 121(10): p. 2153-61.

19. Priceman, S.J., et al., *Targeting distinct tumor-infiltrating myeloid cells by inhibiting CSF-1 receptor: combating tumor evasion of antiangiogenic therapy*. Blood. 115(7): p. 1461-71.

20. Niu, Y.N. and S.J. Xia, *Stroma-epithelium crosstalk in prostate cancer*. Asian J Androl, 2009. 11(1): p. 28-35.

21. Fahrenholtz, C.D., P.J. Beltran, and K.L. Burnstein, *Targeting IGF-IR with ganitumab inhibits tumorigenesis and increases durability of response to androgen-deprivation therapy in VCaP prostate cancer xenografts*. Mol Cancer Ther.

22. Ellwood-Yen, K., et al., *Myc-driven murine prostate cancer shares molecular features with human prostate tumors*. Cancer Cell, 2003. 4(3): p. 223–238.

23. Fulzele, K., et al., *Disruption of the insulin-like growth factor type 1 receptor in osteoblasts enhances insulin signaling and action*. J Biol Chem, 2007. 282(35): p. 25649-58.

24. DeNardo, D., et al., *Leukocyte complexity predicts breast cancer survival and functionally regulates response to chemotherapy*. Cancer Discovery, 2011. 1: p. 52-65.

25. Xu, J., et al., *Abrogating the protumorigenic influences of tumor-infiltrating myeloid cells byCSF1R signaling blockade improves the efficacy of radiotherapy in prostatecancer*. Cancer Res.

26. Plexxikon. *Pilot Study of PLX3397 in Patients With Advanced Castration-Resistant Prostate Cancer (CRPC)*. February 7, 2013 (updated); Available from: http://clinicaltrials.gov/ct2/show/NCT01499043.

27. Tuxhorn, J.A., G.E. Ayala, and D.R. Rowley, *Reactive stroma in prostate cancer progression*. J Urol, 2001. 166(6): p. 2472-83.

28. Pollard, J.W., *Tumour-educated macrophages promote tumour progression and metastasis*. Nat Rev Cancer, 2004. 4(1): p. 71-8.

29. Arkins, S., et al., *The colony-stimulating factors induce expression of insulin-like growth factor-I messenger ribonucleic acid during hematopoiesis*. Endocrinology, 1995. 136(3): p. 1153-60.

30. Nam, K.O., S.M. Shin, and H.W. Lee, *Cross-linking of 4-1BB up-regulates IL-13 expression in CD8(+) T lymphocytes*. Cytokine, 2006. 33(2): p. 87-94.

31. Dey, A., et al., *Colony-stimulating factor-1 receptor utilizes multiple signaling pathways to induce cyclin D2 expression*. Mol Biol Cell, 2000. 11(11): p. 3835-48.

32. Roberts, P.J. and C.J. Der, *Targeting the Raf-MEK-ERK mitogen-activated protein kinase cascade for the treatment of cancer*. Oncogene, 2007. 26(22): p. 3291-310.

33. Gow, D.J., D.P. Sester, and D.A. Hume, *CSF-1, IGF-1, and the control of postnatal growth and development*. J Leukoc Biol. 88(3): p. 475-81.

34. Nickerson, T., et al., *In vivo progression of LAPC-9 and LNCaP prostate cancer models to androgen independence is associated with increased expression of insulin-like growth factor I (IGF-I) and IGF-I receptor (IGF-IR)*. Cancer Res, 2001. 61(16): p. 6276-80.

Chapter 5:

Conclusions

Prostate cancer (PCa) remains a major cause of mortality in American men. It is predicted that in 2013, there will be 238,590 diagnoses and 29,720 deaths from this disease (1). In the last decade, many novel therapies for advanced PCa have emerged, targeting different mechanisms of progression. Given that the majority of PCa's are responsive to inhibition of androgen receptor (AR) signaling (2), many new therapies aim to target this axis in novel and innovative ways. MDV3100 (Enzalutamide) is a potent AR competitive inhibitor that was recently approved by the Food and Drug Administration (FDA) (3). abiraterone acetate (Zytiga) is a new CYP17 enzyme inhibitor that blocks the synthesis of androgen from precursors (4). Sipuleucel-T (Provenge), is a first-in-class, immunotherapeutic FDA-approved for the treatment of castration resistant prostate cancer (CRPC) (5). Sipuleucel-T functions by using a patient's own dendritic cells (antigen presenting cells, APCs), which are exposed to prostatic acid phosphatase (PAP). PAP is a tumor antigen present in 95% of PCa, thus the patient's APCs are primed to activate an anti-tumor T-cell response (5, 6). Sipuleucel-T has shown promising results in treating advanced PCa, although it does so with limited duration (5). Nevertheless, great strides in the field of cancer immunology were made with its FDA approval. Another promising immunothepeutic currently in clinical trails is PROSTVAC-VF, which employs a genetically modified virus engineered to express prostate specific antigen (PSA). The underlying mechanism of this system is that the immune system will be primed against prostate cancer cells expressing PSA (7). Improvements in radiotherapy (RT), a major frontline treatment option for PCa patients, have also gathered momentum. RT delivery has improved quite a bit with significant reductions in off-target effects, leading to damage of proximal tissues. Examples of such improvements are brachytherapy, were radiation seeds are implanted into the tumor, and focal delivery of external beam radiation therapy (EBRT) (8, 9). Despite the numerous advances in

PCa treatment options, recurrence of the disease, including resistance to these novel treatments, continues to result in significant mortality. Thus, a better understanding of the mechanisms underlying resistance to frontline treatments is crucial.

An emerging area of research in solid tumors is the involvement of the tumor microenvironment. Specifically, how immune cells can contribute to the tumor microenvironment, namely, how they operate to promote cancer progression. It is now well established that tumor vasculature is a major cause of metastasis is and the main cause of death from cancer. Tumor-infiltrating myeloid cells (TIMs) are key mediators of tumor neo-angiogenesis and have been shown to contribute to tumor resistance to anti-angiogenic agents (10-12). They can promote metastasis, suppress the anti-tumor immune response, and can promote growth by secreting growth factors (12-14). Studies that investigate modulation of TIMs in combination with the chemotherapeutic paclitaxol have highlighted the importance of TIMs in chemotherapy resistance in murine breast cancer models (15). It is therefore becoming clear that TIMs represent important therapeutic targets that may show anti-cancer effects and also improve overall efficacy of conventional therapies.

The studies described herein evaluate the contributions of TIMs to resistance to two frontline PCa treatments: RT and androgen blockade therapy (ADT) or androgen deprivation therapy (ABT). Using the RM-9 murine PCa model, we show that RT induces the recruitment of TIM subsets, including tumor associated macrophages (TAMs) and myeloid-derived suppressor cells (MDSCs), via colony stimulating factor-1 (CSF-1) induction in a ABL1-dependent mechanism. Moreover, blockade of TIM recruitment into tumors was potently achieved using CSF-1 receptor (CSF1R) inhibitors, GW2580 and PLX3397. More importantly, depletion of TIMs in combination with RT significantly delayed tumor recurrence.

Employing an androgen sensitive murine PCa model, Myc-CaP, we assessed the effects of ADT and ABT on TIM recruitment and function. We found that the predominant TIM subset was TAMs in this model. Treatment with MDV3100 and castration induced CSF-1 expression both in PCa cells and systemically in mouse sera. Additionally, MDV3100 induced paracrine communication between PCa cells and bone marrow-derived macrophages (BMDMs), resulting in promotion of a pro-tumorigenic phenotype in BMDM. ABT and ADT induced the expression of matrix remodeling, angiogenic, and immune suppressive factors MMP-9, VEGF-A and ARG-1 in TAMs. The most notable finding being that blockade of TAMs using PLX3397 showed a significant delay in the onset of CRPC.

Further dissections of potential AR signaling bypass mechanisms in CRPC resistance conferred by TAMs suggest a possible role of insulin like growth factor -1 (IGF-1). We found that PCa cells treated with MDV3100 *in vitro* showed an increase in the Th2 cytokine IL-13. Co-culture studies combining Myc-CaP cells and BMDMs showed the increase in IL-13 correlated with increased IGF-1 expression in BMDM and downstream IGF-1 receptor (IGF1R) target gene, c-Fos, in Myc-CaP cells. Furthermore, blockade of TAMs in the tumor microenvironment with PLX3397 both delayed the onset of CRPC and decreased tumor proliferation, as determined by Ki67 staining.

Future studies include sorting TIM populations before and after RT and androgen inhibition in an effort to explore other possible tumor promoting mechanisms as well as functionally validate the results obtained herein. Additional studies are warranted to fully understand the role of the TAM-dependent IGF-1 axis, such as the direct impact of the secreted IGF-1 on tumor cell proliferation during androgen blockade. cDNA microarrays will help shed light on the changes in gene expression profiles of TIMs during the progression of PCa towards

therapeutic resistance. Determining the role of these TIMs on T-cell proliferation and cytotoxic activity will be important to determine their likely contribution to anti-tumor immune-suppression. Metastasis is the major cause of death due to cancer thus additional studies should include assessment of the functional role of TIM secreted MMP-9, a key factor implicated in metastatic spread (16). Likewise, the relationship between increased MMP-9 expression in TIMs and changes in other genes involved in metastasis, including loss E-cadherin (16) in tumors will be invaluable to determine the possible contribution of TIMs in cancer dissemination. Another important area to examine is the relationship between CSF-1/CSF1R signaling in TIMs and the changes in M2 tumorigenic factors shown here and whether blockade of this axis is simply blocking tumor recruitment or also their proliferation and gene expression patterns. It is very likely that TIMs tumor promoting activities vary between treatment settings thus a better understanding of the precise mechanisms involved in each setting is essential for designing better anti-tumor combinatorial treatment approaches as well developing TIM directed treatments that modulate their functions against cancer cells.

The success of an anti-cancer agent or therapy depends largely on understanding the molecular pathways that govern the requirements of the target for tumor growth. Because most anti-cancer treatments eventually fail and tumor burden continues, researchers are actively pursuing an improved understanding of the mechanisms involved in therapeutic resistance in an effort to prolong the efficacy of such therapies and possibly design novel combinatorial approaches for the treatment of cancer. For example, failure to Sipuleucel-T treatment has stressed how much remains to be ascertained about the full complement of the immune system in anti-cancer vaccine research, such as the interplay of innate immune cells like TIMs and their immune suppressive properties potentially inhibiting the function of primed APCs against PCa.

Furthermore, RT is thought to result in increased exposure of tumor antigens to the immune system (17); however, it is possible that the immune suppressive properties of TIMs may be blocking the anti-tumor cytotoxic abilities of T-cells.

Multiple mechanisms are implicated in CRPC development after androgen ablation or AR blockade, such as IL-6 mediated activation of STAT3 signaling, which leads to aberrant activation of AR (18). Secretion of IL-6 cytokine by TIM subsets has been reported (19); therefore, it may be possible for TIMs to activate AR via STAT3 in an androgen-depleted environment.

In 2010, Dr. Ammirante and colleagues reported that physical castration of mice bearing murine PCa tumors showed increased inflammatory cytokine expression and influx of inflammatory cells, including B-cells, natural killer (NK) cells, and macrophages. This study focused primarily on B-cells, and identified B-cell derived lymphotoxin as a key factor in the emergence of CRPC. The results showed lymphotoxin was able to promote resistance to both castration and anti-androgen, flutamide tumor suppression via IKK-α activation in PCa cells (20). This study revealed for the first time the importance of inflammatory cells, specifically B-cells, as possible contributors to CRPC development. These results underscore the importance of determining the possible contribution of other inflammatory cells, such as TIMs is on the evolution of CRPC. B-cells have been reported to secrete the anti-inflammatory cytokine IL-10 and promote an M2 protumorigenic phenotype (21). Therefore, the mechanisms of B-cells and TIMs in CRPC progression are likely not mutually exclusive and may be intertwined. Thus, further studies are necessary to decipher the mechanisms connecting immune infiltrates and their involvement in CRPC.

Our work clearly demonstrates the importance of TIMs in the prostatic microenvironment and their importance in resistance to major frontline PCa treatments. Moreover, it underscores the importance of the CSF1R axis in mediating TIM recruitment and ultimately its activity in various contexts of PCa therapy. However, further research is necessary to fully understand the precise mechanisms behind TIMs contributions on resistance to RT and androgen inhibition. These studies demonstrate the diversity of TIM functions and abilities in various anti-cancer settings and further emphasize the importance of understanding these complex pathways in order to develop improved therapeutic strategies.

References

1. Siegel, R., D. Naishadham, and A. Jemal, *Cancer statistics, 2013*. CA Cancer J Clin. 63(1): p. 11-30.
2. Harris, W.P., et al., *Androgen deprivation therapy: progress in understanding mechanisms of resistance and optimizing androgen depletion*. Nat Clin Pract Urol, 2009. 6(2): p. 76-85.
3. Tran, C., et al., *Development of a second-generation antiandrogen for treatment of advanced prostate cancer*. Science, 2009. 324(5928): p. 787-90.
4. El-Amm, J. and J.B. Aragon-Ching, *The changing landscape in the treatment of metastatic castration-resistant prostate cancer*. Ther Adv Med Oncol. 5(1): p. 25-40.
5. Arlen, P.M., *Prostate cancer immunotherapy: the role for sipuleucel-T and other immunologic approaches*. Oncology (Williston Park). 25(3): p. 261-2.
6. Cheever, M.A. and C. Higano, *PROVENGE (Sipuleucel-T) in Prostate Cancer: The First FDA Approved Therapeutic Cancer Vaccine*. Clin Cancer Res.
7. Madan, R.A., et al., *Prostvac-VF: a vector-based vaccine targeting PSA in prostate cancer*. Expert Opin Investig Drugs, 2009. 18(7): p. 1001-11.
8. Agarwal, P.K., et al., *Treatment failure after primary and salvage therapy for prostate cancer: likelihood, patterns of care, and outcomes*. Cancer, 2008. 112(2): p. 307-14.
9. Crook, J., *The role of brachytherapy in the definitive management of prostate cancer*. Cancer Radiother. 15(3): p. 230-7.
10. Loges, S., T. Schmidt, and P. Carmeliet, *Mechanisms of resistance to anti-angiogenic therapy and development of third-generation anti-angiogenic drug candidates*. Genes Cancer. 1(1): p. 12-25.

11. Shojaei, F., et al., *Tumor refractoriness to anti-VEGF treatment is mediated by CD11b+Gr1+ myeloid cells*. Nat Biotechnol, 2007. 25(8): p. 911-20.

12. Priceman, S.J., et al., *Targeting distinct tumor-infiltrating myeloid cells by inhibiting CSF-1 receptor: combating tumor evasion of antiangiogenic therapy*. Blood. 115(7): p. 1461-71.

13. Umemura, N., et al., *Tumor-infiltrating myeloid-derived suppressor cells are pleiotropic-inflamed monocytes/macrophages that bear M1- and M2-type characteristics*. J Leukoc Biol, 2008. 83(5): p. 1136-44.

14. Gabrilovich, D.I. and S. Nagaraj, *Myeloid-derived suppressor cells as regulators of the immune system*. Nat Rev Immunol, 2009. 9(3): p. 162-74.

15. DeNardo, D., et al., *Leukocyte complexity predicts breast cancer survival and functionally regulates response to chemotherapy*. Cancer Discovery, 2011. 1: p. 52-65.

16. Shih, J.-Y., *Tumor-Associated Macrophage: Its Role in Cancer Invasion and Metastasis*. Journal fo Cancer Molecules, 2006. 2(3): p. 101-106.

17. Formenti, S.C. and S. Demaria, *Combining radiotherapy and cancer immunotherapy: a paradigm shift*. J Natl Cancer Inst. 105(4): p. 256-65.

18. Chen, T., L.H. Wang, and W.L. Farrar, *Interleukin 6 activates androgen receptor-mediated gene expression through a signal transducer and activator of transcription 3-dependent pathway in LNCaP prostate cancer cells*. Cancer Res, 2000. 60(8): p. 2132-5.

19. Schmid, M.C. and J.A. Varner, *Myeloid cells in the tumor microenvironment: modulation of tumor angiogenesis and tumor inflammation*. J Oncol. 2010: p. 201026.

20. Ammirante, M., et al., *B-cell-derived lymphotoxin promotes castration-resistant prostate cancer*. Nature. 464(7286): p. 302-5.

21. Wong, S.C., et al., *Macrophage polarization to a unique phenotype driven by B cells*. Eur J Immunol, 2010. 40(8): p. 2296-307.